



**HAL**  
open science

# Pathophysiology and imaging of early memory impairment in multiple sclerosis

Vincent Planche

► **To cite this version:**

Vincent Planche. Pathophysiology and imaging of early memory impairment in multiple sclerosis. Neurons and Cognition [q-bio.NC]. Université de Bordeaux, 2016. English. NNT : 2016BORD0392 . tel-01552296v2

**HAL Id: tel-01552296**

**<https://theses.hal.science/tel-01552296v2>**

Submitted on 3 Jul 2017

**HAL** is a multi-disciplinary open access archive for the deposit and dissemination of scientific research documents, whether they are published or not. The documents may come from teaching and research institutions in France or abroad, or from public or private research centers.

L'archive ouverte pluridisciplinaire **HAL**, est destinée au dépôt et à la diffusion de documents scientifiques de niveau recherche, publiés ou non, émanant des établissements d'enseignement et de recherche français ou étrangers, des laboratoires publics ou privés.

Ecole doctorale des sciences de la vie et de la santé, spécialité neurosciences



Thèse présentée pour obtenir le grade de

**DOCTEUR DE  
L'UNIVERSITÉ DE BORDEAUX**

Ecole doctorale des sciences de la vie et de la santé, spécialité neurosciences

Soutenue publiquement le 16 décembre 2016

par

**Vincent Planche, né le 22 mai 1986 à Clermont-Ferrand**

**PATHOPHYSIOLOGY AND IMAGING OF EARLY MEMORY  
IMPAIRMENT IN MULTIPLE SCLEROSIS**

**Sous la direction de Monsieur le Professeur Thomas Tourdias**

**Jury :**

**Monsieur le Professeur Sridar Narayanan, *Mc Gill University, Montreal.***

**Président**

**Monsieur le Professeur Pierre Clavelou, *Université Clermont Auvergne.***

**Rapporteur**

**Monsieur le Professeur Charles R.G. Guttmann, *Harvard University, Boston.***

**Rapporteur**

**Monsieur le Professeur Stéphane Kremer, *Université de Strasbourg.***

**Examineur**

**Monsieur le Docteur Romain Marignier, *Université de Lyon.***

**Examineur**

**Madame le Docteur Agnès Nadjar, *Université de Bordeaux.***

**Examinatrice**



## **Titre : Physiopathologie et imagerie des troubles mnésiques précoces dans la sclérose en plaques**

**Résumé :** Les troubles mnésiques sont fréquents dans la sclérose en plaques (SEP) mais leurs substrats anatomique et biologique sont mal connus. L'objectif de cette thèse translationnelle était de comprendre les mécanismes physiopathologiques des troubles mnésiques à la phase précoce de la SEP, avec pour perspective de trouver de nouvelles cibles thérapeutiques et de définir de nouveaux marqueurs d'imagerie. Nous avons réalisé une analyse neuropsychologique et IRM de patients atteints de forme précoce de SEP et nous avons étudié des souris à la phase précoce d'une encéphalomyélite auto-immune expérimentale (EAE, le modèle animal de la SEP) avec une combinaison d'expériences comportementales, d'IRM, histologiques, électrophysiologiques et pharmacologiques. Nous avons démontré que l'atteinte hippocampique était précoce dans l'histoire de la maladie et qu'elle était corrélée au déclin mnésique des patients atteints de SEP. Nous avons identifié chez les souris EAE que la structure et la fonction du gyrus denté étaient plus vulnérables que les autres sous-champs de l'hippocampe au stade précoce de la maladie et nous avons transposé cette découverte à la pathologie humaine en démontrant une perte des capacités de *pattern separation* chez des patients atteints de forme précoce de SEP. Du point de vue mécanistique, nous avons démontré que l'activation microgliale précoce était responsable de l'atteinte du gyrus denté et des troubles mnésiques dans l'EAE et que cette cascade physiopathologique pouvait être prévenue grâce à un traitement par minocycline. Du point de vue de l'imagerie, nous avons également démontré que l'atteinte microstructurale de l'hippocampe ainsi que la neurodégénérescence précoce du gyrus denté pouvaient être étudiées *in vivo* en tenseur de diffusion (DTI). Nous travaillons à la mise en place de méthode encore plus spécifique par l'imagerie de densité neuritique et d'orientation/dispersion (NODDI). Nos résultats relient l'atteinte mnésique précoce de la SEP à une neurodégénérescence sélective du gyrus denté. Ce processus physiopathologique peut être prévenu en inhibant l'activation microgliale chez les souris EAE et peut être étudié *in vivo* grâce au DTI chez la souris comme chez l'homme, offrant d'évidentes perspectives cliniques dans la prise en charge des patients atteints de SEP.

**Mots clés :** Mémoire épisodique, hippocampe, gyrus denté, microglie, sclérose en plaques, encéphalomyélite auto-immune expérimentale, IRM, imagerie par tenseur de diffusion



## **Title: Pathophysiology and imaging of early memory impairment in multiple sclerosis**

**Abstract:** Memory impairment is frequent in multiple sclerosis (MS) but its anatomical and biological substrates are poorly understood. The objective of this translational thesis was to understand the pathophysiological mechanisms of early memory impairment in MS, to find new potential therapeutic targets and to define new imaging biomarkers related to memory impairment. We used neuropsychological and MRI experiments in patients with early MS and we explored experimental autoimmune encephalomyelitis (EAE) mice (a mouse model of MS) at the early stage of the disease with a combination of behavioral, *in vivo* MRI, histological, electrophysiological and pharmacological approaches. In patients with MS, we demonstrated that hippocampal damage occurs early during the course of the disease and that it correlates with memory impairment. In EAE-mice, we identified that dentate gyrus structure and function are more vulnerable than other hippocampal subfields at the early stage of the disease and we translated this finding back to humans by demonstrating loss of pattern separation performances in patients with early MS. From a mechanistic point of view, we demonstrated that early microglial activation causes dentate gyrus disruption and memory impairment in EAE-mice and that this pathophysiological cascade can be prevented with minocycline. From the imaging point of view, we demonstrated that hippocampal microstructural damage and early dentate gyrus degeneration can be monitored *in vivo* with diffusion tensor imaging (DTI). We are currently developing more specific imaging approaches with optimization of the Neurite Orientation Dispersion and Density Imaging (NODDI) to assess hippocampal subfields. Our results link early memory impairment in MS to a selective disruption of the dentate gyrus. We were able to prevent this neurodegenerative process with microglial inhibitors in EAE-mice and to capture these features non-invasively with DTI in both humans and rodents, paving the way toward new clinical perspectives in MS.

**Keywords :** Episodic memory, hippocampus, dentate gyrus, microglia, multiple sclerosis, experimental-autoimmune encephalomyelitis, MRI, diffusion tensor imaging



## Acknowledgements

---

Au Professeur Thomas Tourdias,

*Tu m'as fait l'honneur de diriger ce travail. Merci pour toute l'énergie que tu as dépensée à me guider, à m'encadrer et à me raisonner. Merci d'avoir si largement participé à la réalisation des expériences présentées ici. Merci pour ta disponibilité et pour toutes nos discussions. Merci de m'avoir transmis ton enthousiasme, ta passion pour l'imagerie et ta vision translationnelle de la recherche. J'ai une admiration sans limite pour ton parcours et ta clairvoyance.*

To Professor Sridar Narayanan,

*Thank you very much for accepting to preside the thesis jury. Thank you for taking the time to make the journey to join us in Bordeaux from Montreal. It is a great honour to present my results in front of an international expert of brain imaging in the field of multiple sclerosis.*

Au Professeur Pierre Clavelou,

*Merci Monsieur d'avoir accepté d'être l'un des rapporteurs de cette thèse. Merci d'être présent à Bordeaux en ce jour si particulier pour vous. Merci surtout pour votre écoute et pour m'avoir guidé vers Bordeaux pour la réalisation de cette thèse. Merci enfin pour votre enseignement clinique et pour m'avoir transmis votre intérêt pour l'étude de la sclérose en plaques.*

Au Docteur Agnès Nadjar, au Professeur Charles Guttmann, au Professeur Stéphane Kremer et au Docteur Romain Marignier,

*Vous me faites l'honneur de juger mon travail au regard de vos expertises respectives. Je vous remercie de votre présence aujourd'hui.*

Aux membres du Neurocentre Magendie (Inserm U1215).

A Stéphane Oliet *pour m'avoir accueilli avec tant de sympathie au sein de son équipe; merci pour nos discussions et ton regard critique sur notre travail.* A Aude Panatier *pour m'avoir encadré durant toutes mes manip d'électrophysiologie; merci surtout pour ta disponibilité et ta gentillesse; merci aussi de m'avoir montré le chemin de la rigueur scientifique, j'ai beaucoup appris à ton contact.* A Nadège Dubourdieu *pour ton aide indispensable au quotidien (même le dimanche); merci aussi pour ton rire inimitable, pour les madeleines Bijou, pour le café, pour les surnoms viriles...* A Aline Desmedt *pour notre collaboration et nos discussions; merci infiniment de nous avoir initiés au monde merveilleux du comportement animal.* A Eva Ducourneau *pour ton aide indispensable dans la réalisation de la manip la plus importante de cette thèse; merci pour ces séances de chirurgie en musique, merci pour ton humour et ta disponibilité.* A Amandine Crombé *pour ton travail acharné à faire tourner ce maudit NODDI; merci surtout pour ton sens critique et ta curiosité. Et merci à tous ceux que je n'ai pas cités et qui m'ont accompagné durant ces 3 années (oui oui, même toi Aurélie!).*

Aux équipes hospitalières du Professeur Bruno Brochet et du Professeur Vincent Dousset

A Monsieur Brochet *de m'avoir si judicieusement dirigé vers Thomas Tourdias afin de réaliser cette thèse; merci aussi à vous et à Aurélie Ruet pour nous avoir permis de travailler sur vos cohortes de patients; merci enfin à vous deux pour tous nos échanges et discussions.* A Mathilde Deloire *pour ta gentillesse, ta disponibilité et ta réactivité.* A Julie Charré-Morin *pour avoir pris le temps de me suivre dans cette drôle d'initiative de tester le pattern separation chez des patients souffrants de SEP.* A Monsieur Dousset *pour nos discussions, pour votre soutien, et pour votre regard critique sur notre travail.*

Aux membres du Centre de Résonance Magnétique des Systèmes Biologiques (CNRS 5536).

A Bassem Hiba *pour nous avoir concocté toutes ces bonnes séquences de diffusion et à Gérard « MacGyver » Raffard pour ta bonne humeur, ton ingéniosité et ta disponibilité.*

A l'École de l'Inserm-Liliane Bettencourt

A Jean-Claude Chottard et Philippe Ascher *pour avoir créé cette belle aventure et l'avoir fait si bien grandir, avec toute l'équipe administrative; merci infiniment pour votre soutien et vos conseils. A toutes les rencontres faites à l'École : Jessica, Nathan, Philippe, Thomas, Baptiste, Olivier, Fabien, Charline&Stéphanie, Naïl; merci pour cette incroyable école de février, pour nos échanges et nos randos.*

A tous ceux qui m'ont transmis très tôt le virus de la recherche.

A Odile Boespflug-Tanguy, *vous resterez pour moi toujours un modèle.* A Catherine Vaurs-Barrière; *merci de m'avoir montré pour la première fois le chemin de la paillasse.* A Marc Peschanski, Anselme Perrier et Laetitia Aubry *pour avoir fait de mon passage à i-Stem un moment si riche.* A Xavier Moisset, *pour m'avoir montré le chemin de la thèse pendant l'internet; merci aussi et surtout pour ta confiance et ton amitié.*

A mes amis

A mes amis d'enfance, Edouard, Adrien, JR, Thomas&Thomas, Mathieu&Mathieu, Anthony, François, Pierre-Alexandre, Vincent, Olivier, Pénélope, Stéphanie, Aurélie, Chachou et Camille; *nous avons grandi ensemble et ça compte énormément, malgré les distances.* A Nicolas et Guillaume, *les deux faces d'une même pièce, je vous adore.* A mes compagnons de P1, Antoine, Nico&Nico et Vincent. A la dream team de l'externat, Pierre, JB, Thibaut&Marine, Hugo, Raïko, Ben, Pablo, François&Aline, Camille, Eugénie, Julie&Djoule, Clément, Romain, Mathieu, Berthy et Cruchot; *c'est grâce à vous que tout s'est passé si vite et si bien.* A mes plus belles rencontres des années d'internat, Thibaud, Audrey, Xavier, Jenni, Jason&Claire, Eve, et Marion; *merci pour votre folie du quotidien.* Aux bordelais, Alex&Mumu, Albane&Louis, François, Oliv, Florian, Marion, Thomas&Elisa et Amandine; *merci d'avoir rendu ses années de thèse si joyeuses.*

A ma famille

*A mes parents, pour leur amour, leur tendresse, leur éducation et leur fierté. A mes grands-parents, pour leur curiosité, leurs attentions, et leur soutien pendant ces longues années d'études. A ma sœur, pour notre complicité, nos échanges et nos fou-rires. A Alex et Nina, pour le plaisir de vous avoir vu arriver parmi nous.*

A Amandine

*Sans toi, cette thèse ne serait pas. Merci pour tout, absolument tout. Merci surtout de m'avoir fait comprendre que «la vie est semée de ces miracles que peuvent toujours espérer les personnes qui aiment<sup>#</sup> ». J'espère suffisamment grandir pour avoir un jour ta vision du monde.*

<sup>#</sup>Marcel Proust, *A la recherche du temps perdu*

## Table of contents

---

**Presentation of the candidate** **p.13**

**Glossary** **p.17**

**Chapter 1: Introduction** **p.19**

1. Physiology of episodic memory
2. Multiple sclerosis and clinically isolated syndrome
3. Cognitive impairment in multiple sclerosis
4. Memory impairment and hippocampal pathology in multiple sclerosis
5. Experimental autoimmune encephalomyelitis
6. Technical approaches to explore hippocampus in humans and rodents
7. Aims of the thesis
8. Thesis outline

**Chapter 2: Early hippocampal degeneration in patients with multiple sclerosis** **p.39**

1. Summary page
2. Article 1: "Hippocampal microstructural damage correlates with memory impairment in clinically isolated syndrome suggestive of multiple sclerosis"

**Chapter 3: Early dentate gyrus disruption in experimental multiple sclerosis** **p.63**

1. Summary page
2. Article 2: "Selective dentate gyrus disruption causes memory impairment at the early stage of experimental multiple sclerosis"

**Chapter 4: Loss of pattern separation performances in patients with early multiple sclerosis**

**p.117**

1. Summary page
2. Article 3: "Decreased pattern separation performances suggest dentate gyrus dysfunction in patients with early multiple sclerosis"

**Chapter 5: Conclusion, limitations and perspectives**

**p.135**

1. Bullet points summary of the thesis
2. Limitations of the work
3. Future directions in clinical research:
  - a. Hippocampal subfields analyses in patients with MS
  - b. Clinical trials: Preventing memory impairment in multiple sclerosis with minocycline
4. Future directions in fundamental research:
  - a. Explaining early selective dentate gyrus disruption in multiple sclerosis: the complement hypothesis
  - b. Toward more specific *in vivo* marker of the dentate gyrus vulnerability
4. General conclusion

## Presentation of the candidate

---

Vincent Planche

Born on May the 22<sup>th</sup>, 1986 in Clermont-Ferrand, France

29 route des Puys, 63870 Orcines

planche.vincent@gmail.com

+33(0)6.84.97.93.98



### Personal statement

I'm a student of the Inserm MD-PhD program (Ecole de l'Inserm) since 2006, which means that I run in parallel training in medicine (Neurology), and training as a scientist (Neurosciences). This career provides the unique opportunity to be involved in bridging the gap between basic research and clinical practice. In this context, I have a strong interest in the pathophysiology and imaging of cognitive decline in inflammatory and neurodegenerative diseases.

### Education and internship

- From 2013 to present: **PhD student in Neurosciences** at Bordeaux University. Neurocentre Magendie, INSERM U1215.
- From 2011 to present: **Medical internship specializing in Neurology** in Clermont-Ferrand University hospital (Neurology Resident).
- From 2007 to 2008: **Genetic Research Master's degree** at Paris University. Institut des cellules Souches pour le Traitement et l'Etude des maladies Monogéniques (I-Stem), Inserm/UEVE 861.
- From 2006 to present: French Inserm **MD-PhD program** (Ecole de l'Inserm - Liliane Bettencourt)

### Diploma

- **PhD thesis** expected to be defended in December 16<sup>th</sup>, 2016. Subject: "Pathophysiology and imaging of early memory impairment in multiple sclerosis".
- **MD thesis** expected to be defended in April 2017. Subject: "MRI predictors of cognitive decline after subthalamic stimulation in Parkinson's Disease".
- 2013: **Academic degree in Neurology**: "Inflammatory and demyelinating diseases of the central nervous system" (Diplome Inter-Universitaire, Université d'Auvergne)

- 2011 : **Resident entrance examination** (concours d'internat en médecine)
- 2008: **Genetic Research Master's degree**. Subject: "Stem cell therapy in Huntington's Disease".
- 2004: **Baccalaureate** specialized in Physics. Mention Très Bien.

### Grants and work contract

- From May 2017 to May 2018: Post-doctoral fellowship and research grant (77000 euros) was obtained from **ARSEP** Foundation (French association for research on multiple sclerosis).
- From 2014 to 2015: Grant from **Inserm** (French National Institute of Health) for a second year of PhD in Neurosciences, fully dedicated to research (**Contrat d'Accueil Inserm**)
- From 2013 to 2014: Grant from **Clermont-Ferrand University Hospital** for a first year of PhD in Neurosciences, fully dedicated to research (**Année Recherche**)

### Publications

- Planche V, Panatier A, Hiba B, Ducourneau EG, Raffard G, Cassagno N, Brochet B, Dousset V, Desmedt A, Oliet SH, Tourdias T. *Selective dentate gyrus disruption causes early memory impairment in experimental multiple sclerosis*. Brain Behav Immun, 2016 Nov 12. doi:10.1016/j.bbi.2016.11.010. (IF=5,874)
- Planche V, Ruet A, Coupé P, Lamargue-Hamel D, Deloire, M, Pereira B, Manjon JV, Munsch F, Moscufo N, Meier DS, Guttman CRG, Dousset V, Brochet B, Tourdias T. *Hippocampal microstructural damage correlates with memory impairment in clinically isolated syndrome suggestive of multiple sclerosis*. Mult Scler. 2016 Oct 25. doi:10.1177/1352458516675750. (IF=4,671)
- Moroso A, Ruet A, Lamargue-Hamel D, Munsch F, Deloire M, Coupé P, Ouallet JC, Planche V, Moscufo N, Meier DS, Tourdias T, Guttman CRG, Dousset V, Brochet B. *Posterior lobules of the cerebellum and information processing speed at various stages of multiple sclerosis*. J Neurol Neurosurg Psychiatry. 2016 Oct 27. doi:10.1136/jnnp-2016-313867. (IF=6,807)
- Moisset X, Ruet A, Brochet B, Planche V, Jaffeux P, Gilleron V, Ong N, Clavelou P. *Who Performs Lumbar Puncture, How Many Do They Perform, How and Why? A Retrospective Study of 6,594 Cases*. Eur Neurol. 2016 Jun 24;76(1-2):8-11. (IF=1,403)
- Planche V, Gibelin M, Cregut D, Pereira B, Clavelou P. *Cognitive impairment in a population-based study of patients with multiple sclerosis: differences between late relapsing-remitting, secondary progressive and primary progressive multiple sclerosis*. Eur J Neurol. 2016 Feb;23(2):282-9. (IF=3,956)

- Planche V, Dousset V, Ouallet JC, Tourdias T. *An unusual case of CSF leak following post-traumatic rupture of a sacral meningeal cyst*. Cephalalgia. 2015 Oct;35(12):1130-2. (IF=6,052)
- Planche V, Marques A, Ulla M, Ruivard M, Durif F. *Intravenous immunoglobulin and rituximab for cerebellar ataxia with glutamic acid decarboxylase autoantibodies*. Cerebellum. 2014 Jun;13(3):318-22. (IF=2,429)
- Planche V, Chassin O, Leduc L, Regnier W, Kelly A, Colamarino R. *Sturge-Weber syndrome with late onset hemiplegic migraine-like attacks and progressive unilateral cerebral atrophy*. Cephalalgia. 2014 Jan;34(1):73-7 (IF=6,052)
- Combes P\*, Planche V\*, Eymard-Pierre E, Sarret C, Rodriguez D, Boespflug-Tanguy O, Vaurs-Barriere C. *Relevance of SOX17 variants for hypomyelinating leukodystrophies and congenital anomalies of the kidney and urinary tract (CAKUT)*. Ann Hum Genet. 2012 May;76(3):261-7. \* both authors contributed equally to this work. (IF=1,889)

## **Communications to congress**

### **Oral communications:**

- Planche V, Ruet A, Coupé P, Lamargue-Hamel D, Deloire, M, Pereira B, Manjon JV, Munsch F, Moscufo N, Meier DS, Guttmann CRG, Dousset V, Brochet B, Tourdias T. *Hippocampal microstructural damage and memory impairment in clinically isolated syndrome suggestive of multiple sclerosis*. Days of Novelties in Clinical Research (JNRC), Paris, France, January 21<sup>st</sup>-22<sup>nd</sup> 2016 [in French]
- Planche V, Panatier A, Hiba B, Ducourneau EG, Raffard G, Cassagno N, Brochet B, Dousset V, Desmedt A, Olié SH, Tourdias T. *Microglial activation causes selective dentate gyrus disruption and memory impairment in experimental multiple sclerosis*. Neurology Residents Annual Meeting (JNIN), Paris, France, November 20<sup>th</sup>-21<sup>st</sup> 2015 [in French]
- Planche V, Panatier A, Hiba B, Ducourneau EG, Raffard G, Cassagno N, Brochet B, Dousset V, Desmedt A, Olié SH, Tourdias T. *Vulnerability of dentate gyrus to microglial activation leads to early memory impairment in a model of multiple sclerosis*. European Committee for Treatment and Research in Multiple Sclerosis (ECTRIMS), Barcelona, Spain, October 7<sup>th</sup>-10<sup>th</sup> 2015 [in English]

### **Posters presentations:**

- Planche V, Ruet A, Coupé P, Lamargue-Hamel D, Deloire, M, Pereira B, Manjon JV, Munsch F, Moscufo N, Meier DS, Guttmann CRG, Dousset V, Brochet B, Tourdias T. *Hippocampal microstructural damage and memory impairment in clinically isolated syndrome suggestive of multiple sclerosis*. Journées de Neurologies en Langue Française (JNLF), Nantes, April 5<sup>th</sup>-8<sup>th</sup> 2016

- Planche V, Ruet A, Coupé P, Lamargue-Hamel D, Deloire, M, Pereira B, Manjon JV, Munsch F, Moscufo N, Meier DS, Guttmann CRG, Dousset V, Brochet B, Tourdias T. *Hippocampal microstructural damage and memory impairment in clinically isolated syndrome* European Committee for Treatment and Research in Multiple Sclerosis (ECTRIMS), Barcelona, Spain, October 7<sup>th</sup>-10<sup>th</sup> 2015
- Planche V, Panatier A, Hiba B, Raffard G, Cassagno N, Brochet B, Dousset V, Desmedt A, Olié SH, Tourdias T. *Microglial activation causes selective dentate gyrus disruption and memory impairment in experimental multiple sclerosis*. 2<sup>nd</sup> International Bordeaux Neurocampus - Brain Conferences (GliSyn), 1<sup>st</sup>-2<sup>nd</sup> October, Bordeaux, France.
- Planche V, Panatier A, Hiba B, Raffard G, Cassagno N, Brochet B, Dousset V, Desmedt A, Olié SH, Tourdias T. *Diffusion tensor imaging identifies early dentate gyrus vulnerability in a memory-impaired mouse model of multiple sclerosis*. Annual meeting of the students to the health and life sciences Doctoral School (EDSVS), Arcachon, France, April 16<sup>th</sup> 2015
- Planche V, Gibelin M, Cregut D, Dumont E, Pereira B, Clavelou P. *Cognitive impairment in secondary-progressive, primary-progressive, and late relapsing-remitting multiple sclerosis : quantitative but not qualitative differences*. European Committee for Treatment and Research in Multiple Sclerosis (ECTRIMS), Copenhagen, Denmark, October 2<sup>nd</sup>-5<sup>th</sup> 2013

### Awards

- Best poster presentation from the French Society of Multiple Sclerosis, JNLF, Nantes, April 5<sup>th</sup>-8<sup>th</sup> 2016 (1000 euros): *Hippocampal microstructural damage and memory impairment in clinically isolated syndrome suggestive of multiple sclerosis*
- Best oral presentation from the French Academy of Neurology teachers, JNIN, Paris, November 20<sup>th</sup>-21<sup>st</sup> 2015 (500 euros): *Microglial activation causes selective dentate gyrus disruption and memory impairment in experimental multiple sclerosis*.
- Best poster presentation during Annual meeting of the students to the health and life sciences Doctoral School (EDSVS), Arcachon, France, April 16<sup>th</sup> 2015 (150 euros): *Diffusion tensor imaging identifies early dentate gyrus vulnerability in a memory-impaired mouse model of multiple sclerosis*

### Other institutional activities

- From 2011 to 2013: Elected member of the **Scientific committee of Auvergne University**
- From 2012 to 2013: Residents' delegate in the **Medical committee of Clermont-Ferrand University hospital**.

## Glossary

---

AD = Axial Diffusivity

AMPA = Acide  $\alpha$ -amino-3-hydroxy-5-methyl-4-isoxazolepropionic

BDI = Beck Depression Inventory

BVMT = Brief Visuospatial Memory Test

CA = Cornu Ammonis

CFA: Complete Freund's Adjuvant

CIS = Clinically Isolated Syndrome

CNS = Central Nervous System

CSCT = Computerized Speed Cognitive Test

CVLT: California Verbal Learning Test

DG = Dentate Gyrus

d.p.i = days post-injection

DTI = Diffusion Tensor Imaging

DWI = Diffusion Weighted Images

EBV = Epstein-Barr virus

EC = Entorhinal Cortex

d.p.i = days post-injection

DTI = Diffusion Tensor Imaging

DWI = Diffusion Weighted Images

EAE = Experimental Autoimmune Encephalomyelitis

FA = Fractional Anisotropy

FLAIR = Fluid-Attenuated Inversion-Recovery

fEPSP = field Excitatory PostSynaptic Potential

GFAP = Glial Fibrillary Acidic Protein

HFS = High Frequency Stimulation

HLA = Human Leukocyte Antigen

Iba1 = Ionized calcium binding adaptor molecule 1: microglia-calcium binding protein

IFN= Interferon

IL-1 $\beta$  = Interleukin-1 $\beta$

IPS = Information Processing Speed  
LTP = Long Term Potentiation  
LTD = Long Term Depression  
MBP = Myelin Basic protein  
MD = Mean Diffusivity  
MINO = Minocycline  
ML = Molecular Layer (of the dentate gyrus)  
MOG = Myelin Oligodendrocyte Glycoprotein  
MPP = Medial Perforant Pathway  
MRI = Magnetic Resonance Imaging  
MS = Multiple Sclerosis  
MST = Mnemonic similarity test  
NHV = Normalized Hippocampal Volume  
NIH = National Institute of Health  
NMDA = N-Methyl-D-Aspartate  
PBS = Phosphate Buffer Saline  
PFA = Paraformaldehyde  
PPMS = Primary Progressive Multiple Sclerosis  
PwCIS = Person with CIS  
PweMS = Person with early MS  
PwMS = Person with MS  
RRMS = Relapsing-Remitting Multiple Sclerosis  
SDMT = Symbol Digit Modalities Test  
SPMS = Secondary-Progressive Multiple Sclerosis  
SR = Stratum Radiatum (of CA1)  
SRT = Selective Reminding Test  
ROC = Receiver Operating Characteristic  
95%CI = 95% Confidence Interval

## Introduction

## Chapter 1: Introduction

### 1. Physiology of episodic memory

**Learning and memory** are adaptive systems that allow acquiring, retaining and recalling distinct experiences. From the computational point of view, memory can also be defined as “the panoply of changes in the activity or connectivity of neural systems that are triggered by stimuli or brain states and then persist over a duration longer than the triggering events”<sup>1</sup>. Distinct subtypes of memories have been defined (Fig. 1), referring to different neuropsychological, anatomical and biological substrates. Short term memory (working memory) is opposed to long term memory regarding persistence in time (tens of seconds vs decades)<sup>1</sup>. Declarative (explicit) memory refers to the conscious awareness of previous experiences and concepts whereas procedural (implicit) memory is automatically retrieved. Episodic memory gathers life’s experiences whereas semantic memory refers to the acquisition of factual knowledges<sup>2</sup>.

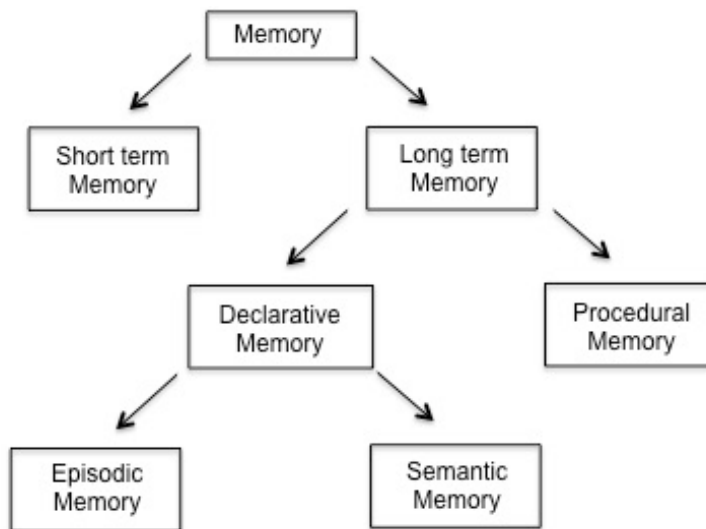


*Fig. 1: Schematic classification of the different types of memory.*

**Episodic memory** has been first defined by Turing in 1973 and refers to memory of specific personal experiences or the conscious ability “to travel back in time”<sup>3</sup>. The episodic memory theory postulates that information about specific events is linked to spatial, temporal, and other situational contexts in which the events occurred (“where”, “when” and “what”). Based on this operational definition, demonstrations that animals can remember events associated to a particular context provided compelling evidence that core properties of episodic memory are also present in nonhumans and depends on a fundamental neural circuit that is similar across mammalian species<sup>4</sup>. In this thesis we are going to focus on this memory subtype considering that the biological substrates of episodic memory formation and dysfunction can be studied in both human and rodents.

The role of the **hippocampus** in episodic memory and more generally in declarative memory is widely accepted in humans since the famous description of the patient H.M., who underwent bilateral surgical resection of the medial temporal lobes (1957)<sup>5</sup>. The hippocampus, located within the medial temporal lobe, is composed of the dentate gyrus, the cornu ammonis (CA, with subdivisions from C1 to CA4) and the subiculum. It receives connections from the primary sensory areas of the cortex, as well as from associative areas and the rhinal and entorhinal cortices. Since the hippocampus receives multimodal information from different brain structures, it is important to note that the encoding of this information requires the recruitment of attention not only for optimal encoding of memory but also for subsequent retrieval<sup>6</sup>.

The “classical” **corticohippocampal circuit** is the well described glutamatergic trisynaptic pathway in which entorhinal cells send excitatory projections through the perforant path to granular neurons of the dentate gyrus whose mossy fiber projections excite CA3 pyramidal neurons which in turn excite CA1 pyramidal neurons through the Schaffer collateral (Fig. 2)<sup>7</sup>. Information leaves the hippocampus through CA1 projections, the main output pathway, to the entorhinal cortex or other neocortical areas. The other major set of outputs of the hippocampus projects via the fimbria/fornix system to the anterior nucleus of the thalamus (both directly and via the mammillary bodies), which in turn projects to the cingulate cortex<sup>8</sup>.

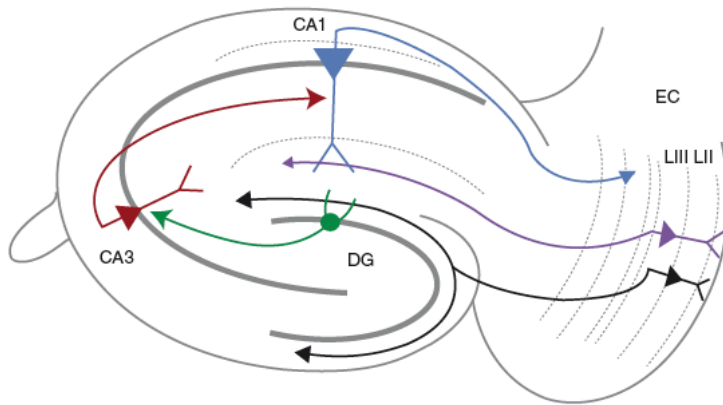


*Fig. 2: The classical corticohippocampal glutamatergic circuit in rodents. DG = dentate gyrus; CA = Cornu Ammonis; EC = Entorhinal Cortex; LII/III = Layer II/III of the EC. The trisynaptic pathway: black represents the perforant path; green represents the mossy fibers; red represents the Schaffer collateral and blue represent the output pathway. Note also a monosynaptic path from EC to distal CA1 (purple). (Adapted from Basu and Siegelbaum, Cold Spring Harb Perspect Biol, 2015)*

The hippocampus is considered as the crucial anatomical structure implicated in acquisition and recall of new episodic memories whereas long term storage and consolidation would also involve neocortical structures<sup>8</sup>. From the computational point of view, the hippocampus is then involved in two distinct mechanisms linked to encoding and retrieval, named “pattern separation” and “pattern completion”. **Pattern separation** is the ability to establish independent and non-overlapping new memories (uncorrelated or “orthogonalized” memory representations). At the same time, an important property of the cortico-hippocampal system is to complete a whole memory when just a partial cue for retrieval is provided: this concept is named pattern completion<sup>8</sup>. Electrophysiological, gene knock-out and behavioral experiments in rodents<sup>9,10</sup> and functional magnetic resonance imaging (fMRI) studies in humans<sup>11,12</sup> have demonstrated that the **dentate gyrus** enables the hippocampus to remove redundancy from the inputs, producing a more sparse and categorized set of outputs (pattern separation) whereas an auto-association or “attractor” process in CA3 mediates pattern completion.

Putative biological substrates of long term/episodic memory in the trisynaptic hippocampal loop are persistent **changes in synaptic structure and strength**. Mainly, long term potentiation (LTP) has been first described by Bliss and Lomo in 1973<sup>13</sup>. They found that high-frequency electrical stimulation of the perforant path inputs to the hippocampus resulted in an increase

in the strength of the dentate gyrus stimulated synapses that lasted for many days. LTP has been further described as an N-methyl-D-aspartate (NMDA) receptor dependent synaptic plasticity mechanism that enhanced trafficking of AMPA receptors to the postsynaptic element of dentate gyrus or CA1 neurons, resulting in a strengthened response to the next excitatory potential. Then, LTP provides a plausible biochemical mechanism for encoding new declarative memories in the hippocampus<sup>6</sup>. Furthermore, it has been recently demonstrated that LTP formation also requires glial cells through the astrocytic release of gliotransmitters such as D-serine or glycine<sup>14</sup>.

“[Episodic] memory is the glue that holds our mental life together. Without its unifying power, our [...] life would be broken into as many fragments as there are seconds in the day. Our life would be empty and meaningless” wrote Kandel et al.<sup>6</sup>. Unfortunately, episodic memory is thought to be more vulnerable than the other memory systems to neuronal dysfunction<sup>3</sup>. Then, struggling against **disorders that affect episodic memory** is of particular importance. Alzheimer’s disease is the archetypal neurodegenerative pathology that impairs memory performance in the elderly. Other brain pathology, such as multiple sclerosis, can alter episodic memory in young adults.

## 2. Multiple sclerosis and clinically isolated syndrome

**Multiple sclerosis** (MS) is an inflammatory, demyelinating and neurodegenerative disease of the central nervous system (CNS)<sup>15</sup>. It usually affects young adults during their third decade and women are more prone to develop the disease (2.3/1 female-to-male ratio)<sup>16</sup>. More than 2.5 million people worldwide are affected and the prevalence in France is around 95 per 100000<sup>17</sup>. The exact etiology of the disease is currently unknown although genetic and environmental risk factors have been identified, such as HLA genotype, EBV infection, low sunlight, vitamin D deficiency, salty diet and smoking<sup>15</sup>. It is usually accepted that a dysimmune response is initiated in the periphery, with increased migration of autoreactive lymphocytes across the blood–brain barrier. As lymphocytes and macrophages accumulate, pro-inflammatory cytokines (IL-1 $\beta$ , TNF- $\alpha$ ...) amplify the immune response through recruitment of naive microglia. At least one part of infiltrating T-lymphocytes are directed against myelin antigens and will trigger acute demyelinating lesions. Areas of demyelination coexist with diffuse axonal and neuronal degeneration<sup>15</sup>.

The early phase of MS is usually characterized by inflammatory relapses (also called attacks or exacerbations) and remissions (relapsing-remitting MS, RRMS) due to demyelination and remyelination processes. The later phase is characterized by progressive disability and neurodegeneration<sup>15,18</sup> (secondary-progressive MS, SPMS). Primary-progressive multiple sclerosis (PPMS) is characterized by steady worsening of neurologic functioning, without any distinct relapses or periods of remission (Fig. 3).

According to consensual definition based on clinical and/or imaging criteria, MS is defined by the dissemination in time and space of the demyelinating lesions<sup>19,20</sup>. **Clinically isolated syndrome** describes the first clinical episode with features suggestive of MS (Fig. 3). Then, clinically isolated syndrome (CIS) is a disease that could be MS, but has yet to fulfill criteria of dissemination in time. The long term risk to develop MS after CIS is around 60-80% when demyelinating lesions are present on the first MRI scan<sup>21</sup>.

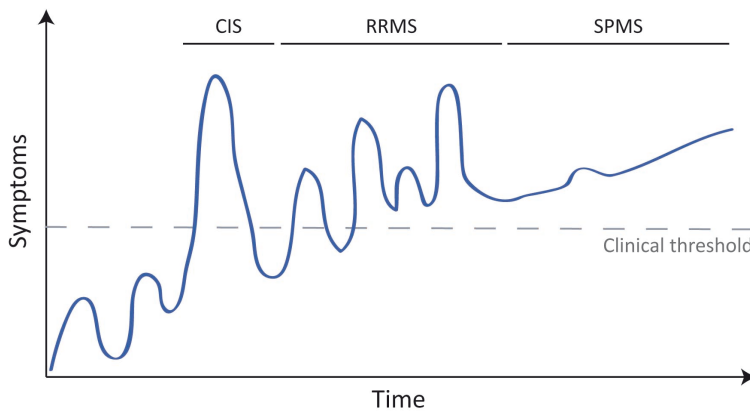


*Fig. 3: The clinical course of multiple sclerosis. CIS: Clinically Isolated Syndrome; RRMS: Relapsing-Remitting Multiple Sclerosis; SPMS: Secondary progressive Multiple Sclerosis (the primary progressive form of the disease (PPMS) is not depicted here).*

During the course of MS, relapses are consensually treated with high-dose methylprednisolone to rapidly relieve symptoms. However, corticosteroid treatments have no significant impact on long-term disability and don't prevent future relapses. Then, patients with RRMS are usually treated with **disease modifying treatments** with immunomodulatory or immunosuppressive characteristics that decrease relapse-rate and accumulation of disability.

There are currently nine approved treatments in RRMS with various degrees of effectiveness and side effects: interferon- $\beta$  (IFN- $\beta$ ), glatiramer acetate, mitoxantrone, natalizumab, fingolimod, teriflunomide, dimethyl fumarate, alemtuzumab and daclizumab. IFN- $\beta$  and glatiramer-acetate are also indicated in people with CIS to delay the conversion to MS<sup>22</sup>.

### 3. Cognitive impairment in multiple sclerosis

For many years, clinicians and scientists have been mainly focused on motor, sensitive, visual and cerebellar symptoms of MS. However, we now know that cognitive impairment is another manifestation of MS that affects 40-90% of patients with MS, depending on the clinical course of the disease<sup>23,24,25</sup> (Fig. 4). The impact of cognitive decline on quality of life and vocational status is major for affected patients who are young adults<sup>26</sup>. Then, the research on this particular topic is growing up since the 90's<sup>27</sup>.

Cognitive impairment associated with MS is classically defined (rightly or wrongly) as a subcortical dementia because it affects information processing speed, attention, working memory, episodic memory and executive functions whereas "cortical features" such as aphasia, apraxia and agnosia are usually absent<sup>28</sup> (Fig. 4). Cognitive decline can occur very early during the course of the disease, from the stage of CIS<sup>29</sup> and even prior to all other physical symptoms (radiologically isolated syndrome; *i.e* incidental findings of MRI abnormalities suggestive of MS in patients undergoing MRI for unrelated indications such as head trauma or headache)<sup>30</sup>. The most frequently affected cognitive domains in MS are **information processing speed and episodic memory**. Slowing of information processing speed is usually explained by disconnection<sup>31</sup>, demyelinating lesion-load<sup>32</sup>, diffuse brain damage and/or grey matter atrophy<sup>33</sup>. Memory impairment is thought to be rather explained by a more focal pathological process involving the hippocampus<sup>34,35</sup>. From the neuropsychological point of view, verbal memory impairment in MS would be due to deficient acquisition, while visual memory impairment would be attributable to deficits in acquisition and storage<sup>36,37</sup>.

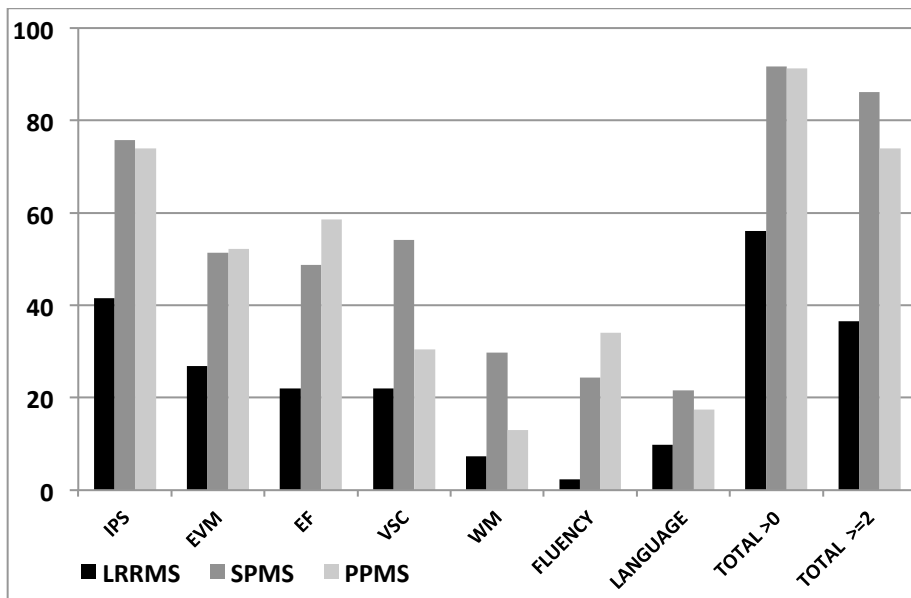
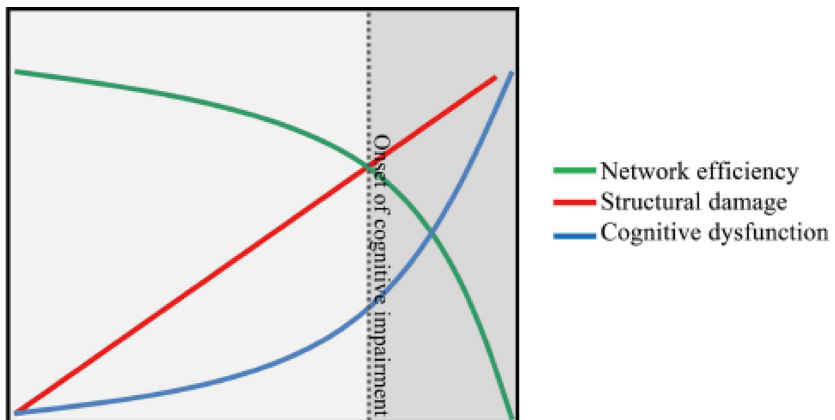


Fig. 4: Cognitive impairment in the three subtypes of MS. Percentage of impaired patients for each cognitive domain and percentage of patients with at least one or two impaired cognitive domain(s). LRRMS, Late Relapsing-Remitting Multiple Sclerosis; SPMS, Secondary Progressive Multiple Sclerosis; PPMS, Primary Progressive Multiple Sclerosis; IPS, information processing speed; EVM, episodic verbal memory; WM, working memory; EF, executive functions; VSC, visuospatial construction. (Adapted from Planche et al. *Eur J Neurol*, 2015)

#### 4. Memory impairment and hippocampal pathology in multiple sclerosis

The first evidence to claim that hippocampal damage can contribute to the episodic memory deficit observed in patients with MS came in 2008 when Sicotte and colleagues correlated **hippocampal atrophy** measured on MRI to memory decline<sup>34</sup>. Furthermore, they identified that hippocampal volume loss was in excess of global brain atrophy which suggests that the hippocampus can be particularly vulnerable to MS. In line with these results, post-mortem histological studies confirmed that hippocampi can be extensively demyelinated during MS<sup>35</sup> and that proteins and microRNA essential for axonal transport, synaptic plasticity and glutamate homeostasis were altered in demyelinated hippocampi, but not in demyelinated motor cortices from MS brains<sup>38,39</sup>. Altogether, such MRI and post-mortem histological studies suggest that the hippocampus could be more vulnerable to neurodegenerative processes than other cortical structures during the course of MS.

Some authors argue that it's not sufficient to look solely at global hippocampal atrophy to understand and diagnose early stages of neurodegenerative diseases affecting memory<sup>40</sup>. Then, it seems crucial to **pinpoint the vulnerability of distinct hippocampal subfields** (subiculum, dentate gyrus, CA3 and CA1) because they are very different in their morphological, molecular, electrophysiological and functional profiles<sup>41</sup>. In this context, human MRI data from people with MS suggest that some hippocampal regions could indeed be more affected than others<sup>34,42,43,44</sup>. However, these studies provide controversial results that may come from measurements performed at different stages and with different methodology to measure atrophy, pinpointing either CA3/dentate gyrus or CA1 subfields as the main locus of alterations.



*Figure 5: A hypothesis of network collapse as a cause for developing cognitive impairment in MS. In early stages of MS, structural damage is low, leaving network efficiency relatively high. As the structural damage accumulates overtime, network efficiency levels drop, inducing a network collapse after a critical threshold is exceeded. After this, the network is unable to function normally and cognitive impairment develops. (Adapted from Schoonheim et al., Front Neurol, 2015)*

On top of structural alterations of the hippocampus, several studies have highlighted that hippocampal **functional connectivity** was modified in the memory network of patients with MS, especially the connections with parahippocampal areas, the anterior cingulate gyrus, and the prefrontal cortex<sup>45,46</sup>. Current thought about brain functional reorganization in MS postulate that compensatory mechanisms occur early during the course of the disease but are

finally overtaken by structural damage later on<sup>47</sup> (Fig. 5). However, this “dynamic” theory is facing several discrepancies from one cross-sectional study to another and needs to be demonstrated in future longitudinal follow-up of patients.

Several pharmacological agents or memory rehabilitation programs have been proposed to treat or prevent memory impairment in MS but evidences of effectiveness are very limited<sup>48</sup>. Some studies evaluating behavioral treatments for impairment in learning and memory have demonstrated some objective improvement but they suffer from several methodological problems and they often lack long-term follow-up. Furthermore, they need ecologically valid outcome assessments<sup>49</sup> (*i.e.* corresponding to “everyday life” abilities) that are usually not used. Symptomatic drug treatments such as anticholinesterase inhibitors<sup>50</sup>, L-amphetamine<sup>51</sup> or memantine<sup>52</sup> are inefficient to treat or prevent memory decline. Because they decrease brain inflammation and irreversible axonal damage, disease modifying therapies could have the potential to prevent cognitive impairment in people with MS. However, cognitive outcomes were under-evaluated in clinical trials (and only as secondary end-points or in ancillary studies) and conclusions remain largely inconsistent, even if IFN- $\beta$  could have a significant beneficial effect on tests of information processing and learning/memory<sup>53,54</sup>. Then, there is still **no uncontroversial treatment to cure or prevent memory impairment in MS**.

More specific biological targets associated with memory impairment need to be identified to develop specific therapeutic strategies. Especially, the MS community needs to understand what happens before hippocampal atrophy that is likely a late stage with irreversible damages. However, MRI studies based on measurement of hippocampal atrophy and post-mortem histological studies are the main sources of understanding but are both inherently biased toward the chronic stage of the disease. Because these early pathophysiological mechanisms are not assessable with noninvasive techniques in humans, an alternative way to address this question is to use experimental autoimmune encephalomyelitis, the most widely accepted animal model of MS (below and Box 1).

## 5. Experimental autoimmune encephalomyelitis

As for many neurological diseases, MS is unique to humans and there is no spontaneous disease of other species to provide translatable insights into the human disorder. Experimental autoimmune encephalomyelitis (EAE) is a family of disease models discovered fortuitously a century ago after vaccination against rabies virus. Indeed, the vaccinating inoculum was prepared from brain or spinal cord tissue coming from animals, and some patients developed an allergic encephalomyelitis or “Pasteur encephalomyelitis” after injection. These observations were reproduced and further characterized in non-human primates and rodents: myelin antigens injected with adjuvant can induce specific T-cell activation and central demyelination, mimicking MS pathophysiology and symptoms<sup>55,56</sup>.

From then, EAE has largely contributed to our understanding of interactions between central nervous system and immune system, neuroinflammation, blood-brain barrier disruption, demyelination, remyelination and has helped to develop new drugs<sup>57</sup>. For instance, EAE-research identified the central role of alpha4-beta1 integrins in leukocyte entry into the central nervous system<sup>58</sup>. Antibodies against this adhesion molecule prevent the development of EAE and the direct transposition of these findings to humans leads to the commercialization of natalizumab, one of the most effective therapies in MS to date. Furthermore, by allowing direct MRI-histological correlations, EAE models are used to validate new MRI technics in order to characterize new imaging biomarkers for MS diagnosis and monitoring and to guide drug development<sup>59,60</sup>.

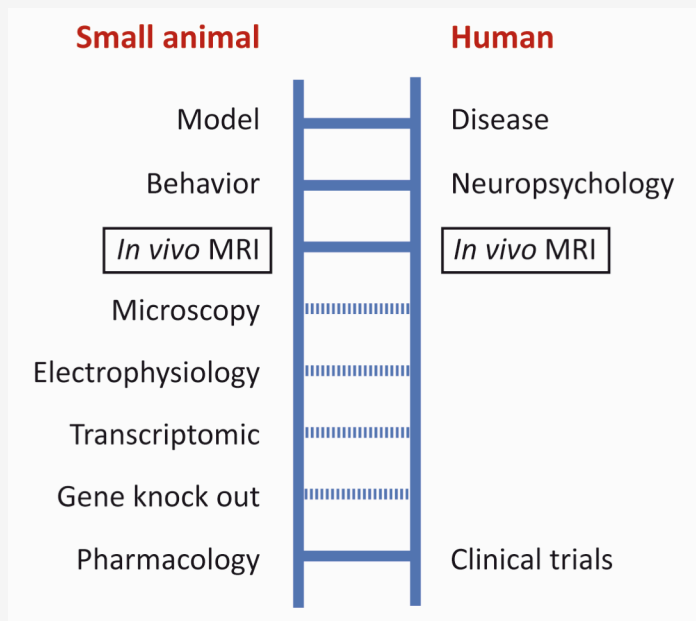
EAE models have been used essentially to develop new immunomodulatory drugs to target the immune-specific and demyelinating aspect of MS. However, recent works suggest that EAE models can also be used in order to understand the neurodegenerative processes associated with MS, including within hippocampus<sup>61</sup>.

### Box1. Translational research: from bench to bedside

The US National Institute of Health (NIH) defined translational research as “the process of applying discoveries generated during research in the laboratory, and in preclinical studies, to the development of trials and studies in humans” and as “a continuum in which research findings are moved from the researcher’s bench to the patient’s bedside and community”<sup>1</sup>.

This thesis has been thought as a translational project in order to understand early memory impairment in MS. Several experiments were conducted with EAE, the animal model of MS to decipher molecular, cellular and functional mechanisms leading to hippocampal disruption at the early stage of the disease. A part of these experiments were reproduced in humans to extrapolate the whole pathophysiological process to the human pathology and to define perspective for future clinical trials.

In such a strategy, *in vivo* imaging is an important methodological approach. Indeed, the same non-invasive imaging methods can be applied in humans and rodents. If a similar imaging pattern can be observed in humans and rodents, we postulate that it would be a strong argument to believe that in-depth characterization of mechanisms elucidated in rodents (with technics non applicable in humans such as microscopy, electrophysiology, transcriptomic, gene knock out...) holds also true in humans.



1. Rubio DM et al., Defining translational research: implications for training. Acad Med. 2010

## 6. Technical approaches to explore hippocampus in humans and rodents

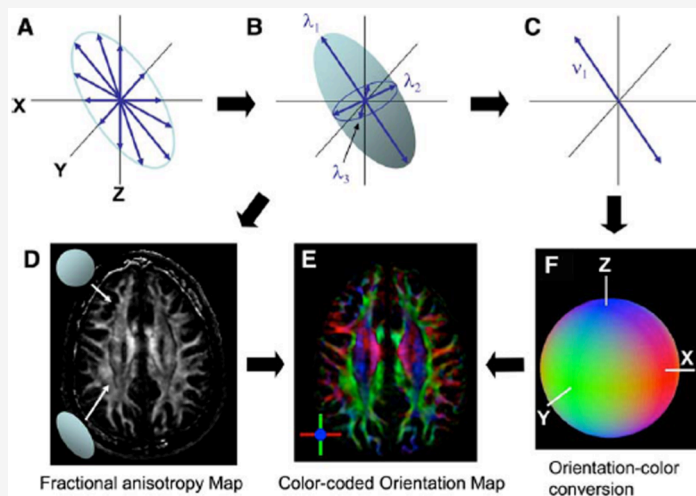
In humans, the function of the hippocampus can be assessed with neuropsychological tests of episodic memory. The tests classically used in clinical practice can assess encoding, storage and retrieval of verbal or visuospatial materials. Some new behavioral tasks designed to tax pattern separation or pattern completion are currently introduced for research purposes but outside the context of MS so far (aging, Alzheimer's disease). However, all these tests are hippocampal-dependent but not purely hippocampal-specific. The structure of the hippocampus at the early stage of the MS can be assessed *in vivo* using morphological MRI and more advanced quantitative MRI methods such as diffusion tensor imaging (DTI, Box2). Functional MRI (fMRI) can also be used to assess hippocampal function *in vivo* through the observation of neuro-vascular coupling in the whole hippocampus but this technic fails to properly identify hippocampal subfields.

In rodents, several behavioral experiments are available to assess hippocampal-based episodic spatial memory such as the Morris water maze, contextual fear conditioning, object recognition, and also pattern separation and completion<sup>62</sup>. MRI technics similar to the ones used in humans can be applied in rodent, using specific magnets (small bore, high magnetic field). Furthermore, animals can be sacrificed after imaging in order to perform MRI-histological correlations or *ex vivo* imaging<sup>63</sup>. Histological or transcriptional analyses (after laser-microdissection) can be performed in each region of interest within the hippocampus, along the hippocampal long axis or in different hippocampal subfields. It is also possible to use invasive technics such as *in vivo* or *ex vivo* electrophysiological recordings or genetically engineered mice to perform *knock-out* or optogenetics experiments<sup>64</sup>. Systemic or intra-hippocampal injections of pharmacological agents interfering with hippocampal functions can be performed to address mechanistic issues<sup>65</sup>.

## Box 2: Diffusion tensor imaging (DTI)

Diffusion tensor imaging (DTI) is an MRI technic first described in 1994 in order to determine *in vivo* the displacements of water molecules in tissues and fiber track orientation<sup>1</sup>. Since then, DTI has been extensively used to evaluate large myelinated fibers and structural connectivity of the brain in several neurological disorders, including MS. Thanks to recent advances in biophysics, it is now possible to achieve high-resolution DTI at a submillimeter resolution and to assess neuritic damages in the gray matter<sup>2</sup>.

DTI uses the water motion as a probe to infer the neuroanatomy. By applying gradients, it is possible to quantify the extent of microscopic water diffusion along several directions of a sphere on a pixel-by-pixel basis *in vivo*. When water motion is random (brownian motion, as in the cerebrospinal fluid), the diffusion is called “isotropic”. When water motion is constrained or hindered in one axis by neurites, membranes or cell infiltrates, the diffusion is called “anisotropic”. One of the most widely used metrics of diffusion MRI is mean diffusivity (MD) that quantifies the amount of diffusion and fractional anisotropy (FA), scaled from 0 (isotropic) to 1 (anisotropic), that quantifies the relative degree of anisotropy (directionality) in a voxel<sup>3</sup>. Any modifications of the microscopic structure of the tissue can induce modifications of water diffusion properties.



*The principle of DTI and contrast generation from diffusion measurements along multiple axes (A). The shape and the orientation of a “diffusion ellipsoid” is estimated (B). An anisotropy map (D) can be created from the shape, in which dark regions are isotropic (spherical) and bright regions are anisotropic (elongated): quantitative metric going from 0 to 1. From the estimated ellipsoid (B), the orientation of the longest axis can be found (C), which is assumed to represent the local fiber orientation. This orientation information is converted to a color (F) at each pixel. By combining the intensity of the anisotropy map (D) and color (F), a color-coded orientation map is created (E). (Adapted from Mori et al., Neuron, 2006)*

1. Basser PJ et al., MR Diffusion Tensor Spectroscopy and Imaging. Biophys J. 1994
2. Yassa MA., Searching for Novel Biomarkers Using High Resolution Diffusion Tensor Imaging. J Alzheimers Dis. 2011
3. Mori S & Zhang J., Principles of diffusion tensor imaging and its applications to basic neuroscience research. Neuron. 2006

## 7. Aims of the thesis

The general objective of this translational thesis was to tackle some pathophysiological mechanisms of early memory impairment in MS, to define new imaging biomarkers related to memory impairment and ultimately to find new potential therapeutic targets. All the approaches are focused at the early stage of the disease considering that early modifications are the ones that should be targeted in the future (early treatments and prevention). To achieve this goal we used a translational multidisciplinary approach by:

- Using advanced MRI technics and neuropsychological testing in persons with CIS and early MS.
- Using several complementary experiments on EAE-mice including: behavioral experiments, advanced MRI technics, transcriptomics, histology, neuromorphology, electrophysiology and pharmacology.

## 8. Thesis outline

In **chapter 2**, we investigated the early anatomical substrate of memory impairment in MS, prior to atrophy. By quantifying diffusion of water molecules within the whole hippocampus with DTI in persons with clinically isolated syndrome, we found a correlation between hippocampal microstructural damage and memory impairment at this early stage of the disease. Furthermore, hippocampal DTI discriminates between memory-impaired and memory-preserved patients with a good accuracy.

In **chapter 3**, we aimed at exploring in details the histological substrate of the DTI alterations within the hippocampus and also at investigating whether the hippocampal subfields could be differentially affected. We demonstrated in EAE-mice that synaptic dysfunction and dendritic degeneration, both driven by microglial activation, were encountered within the hippocampus at the early stage of the disease. Importantly such alterations of structure and function were mainly observed within the dentate gyrus that was therefore more vulnerable than other hippocampal subfields to early microglial activation. This early neurodegenerative process responsible for memory impairment could be prevented after inhibition of microglial activation with minocycline. This selective neurodegenerative process could also be monitored *in vivo* with DTI at a very high resolution to resolve each hippocampal subfields individually.

In **chapter 4**, we aimed at translating back our findings from EAE-mice to patients with early MS. In other words, we hypothesized that alterations measured within the whole hippocampus of patients (chapter 2) could be mainly driven by dentate gyrus vulnerability as demonstrated in EAE mice (chapter 3). Because it is still challenging to quantify diffusion MRI within each subfield in patients (very long acquisition time in EAE), we used a neuropsychological approach by testing the patients with cutting edge cognitive tests more specifically related to the integrity of the dentate gyrus. We demonstrated that pattern separation performances (a crucial feature of episodic memory supported by the dentate gyrus) are decreased in patients with early MS compared to healthy controls. This loss of pattern separation performances was observed while slowing of information processing speed and “classical” visuospatial episodic memory impairment were not found, suggesting that loss of pattern separation precedes the other deficit in early MS. This neuropsychological result suggests that the early dentate gyrus dysfunction demonstrated in EAE-mice holds also true during the course of MS in patients.

In **chapter 5**, we discuss the limitations and the perspectives of this work and we present some preliminary results and ongoing projects.

## References

1. Chaudhuri R, Fiete I. Computational principles of memory. *Nat Neurosci*. 2016;19:394–403.
2. Tulving E, Markowitsch HJ. Episodic and declarative memory: role of the hippocampus. *Hippocampus*. 1998;8:198–204.
3. Tulving E. Episodic memory: from mind to brain. *Annu Rev Psychol*. 2002;53:1–25.
4. Allen TA, Fortin NJ. The evolution of episodic memory. *Proc Natl Acad Sci U S A*. 2013;110 Suppl 2:10379–10386.
5. Scoville WB, Milner B. Loss of recent memory after bilateral hippocampal lesions. *J Neurol Neurosurg Psychiatry*. 1957;20:11–21.
6. Kandel ER, Dudai Y, Mayford MR. The molecular and systems biology of memory. *Cell*. 2014;157:163–186.
7. Basu J, Siegelbaum SA. The Corticohippocampal Circuit, Synaptic Plasticity, and Memory. *Cold Spring Harb Perspect Biol*. 2015;7.
8. Kesner RP, Rolls ET. A computational theory of hippocampal function, and tests of the theory: new developments. *Neurosci Biobehav Rev*. 2015;48:92–147.
9. McHugh TJ, Jones MW, Quinn JJ, et al. Dentate gyrus NMDA receptors mediate rapid pattern separation in the hippocampal network. *Science*. 2007;317:94–99.
10. Neunuebel JP, Knierim JJ. CA3 retrieves coherent representations from degraded input: direct evidence for CA3 pattern completion and dentate gyrus pattern separation. *Neuron*. 2014;81:416–427.
11. Bakker A, Kirwan CB, Miller M, Stark CEL. Pattern separation in the human hippocampal CA3 and dentate gyrus. *Science*. 2008;319:1640–1642.
12. Berron D, Schütze H, Maass A, et al. Strong Evidence for Pattern Separation in Human Dentate Gyrus. *J Neurosci*. 2016;36:7569–7579.
13. Bliss TV, Lomo T. Long-lasting potentiation of synaptic transmission in the dentate area of the anaesthetized rabbit following stimulation of the perforant path. *J Physiol*. 1973;232:331–356.
14. Henneberger C, Papouin T, Oliet SHR, Rusakov DA. Long-term potentiation depends on release of D-serine from astrocytes. *Nature*. 2010;463:232–236.
15. Compston A, Coles A. Multiple sclerosis. *Lancet*. 2008;372:1502–1517.
16. Kalincik T, Vivek V, Jokubaitis V, et al. Sex as a determinant of relapse incidence and progressive course of multiple sclerosis. *Brain*. 2013;136:3609–3617.
17. Fromont A, Biquet C, Sauleau EA, et al. Geographic variations of multiple sclerosis in France. *Brain*. 2010;133:1889–1899.
18. Hemmer B, Kerschensteiner M, Korn T. Role of the innate and adaptive immune responses in the course of multiple sclerosis. *Lancet Neurol*.

2015;14:406–419.

19. Polman CH, Reingold SC, Edan G, et al. Diagnostic criteria for multiple sclerosis: 2005 revisions to the “McDonald Criteria.” *Ann Neurol*. 2005;58:840–846.

20. Polman CH, Reingold SC, Banwell B, et al. Diagnostic criteria for multiple sclerosis: 2010 revisions to the McDonald criteria. *Ann Neurol*. 2011;69:292–302.

21. Miller DH, Chard DT, Ciccarelli O. Clinically isolated syndromes. *Lancet Neurol*. 2012;11:157–169.

22. Ciccarelli O, Thompson A. Multiple sclerosis in 2015: Managing the complexity of multiple sclerosis. *Nat Rev Neurol*. 2016;12:70–72.

23. Planche V, Gibelin M, Cregut D, Pereira B, Clavelou P. Cognitive impairment in a population-based study of patients with multiple sclerosis: differences between late relapsing-remitting, secondary progressive and primary progressive multiple sclerosis. *Eur J Neurol*. 2016;23(2):282-9

24. Rocca MA, Amato MP, De Stefano N, et al. Clinical and imaging assessment of cognitive dysfunction in multiple sclerosis. *Lancet Neurol*. 2015;14:302–317.

25. Chiaravalloti ND, DeLuca J. Cognitive impairment in multiple sclerosis. *Lancet Neurol*. 2008;7:1139–1151.

26. Ruet A, Deloire M, Hamel D, Ouallet J-C, Petry K, Brochet B. Cognitive impairment, health-related quality of life and vocational status at early stages of multiple sclerosis: a 7-year longitudinal study. *J Neurol*. 2013;260:776–784.

27. Rao SM, Leo GJ, Bernardin L,

Unverzagt F. Cognitive dysfunction in multiple sclerosis. I. Frequency, patterns, and prediction. *Neurology*. 1991;41:685–691.

28. DeLuca GC, Yates RL, Beale H, Morrow SA. Cognitive impairment in multiple sclerosis: clinical, radiologic and pathologic insights. *Brain Pathol*. 2015;25:79–98.

29. Feuillet L, Reuter F, Audoin B, et al. Early cognitive impairment in patients with clinically isolated syndrome suggestive of multiple sclerosis. *Mult Scler*. 2007;13:124–127.

30. Lebrun C, Blanc F, Brassat D, Zephir H, de Seze J, CFSEP. Cognitive function in radiologically isolated syndrome. *Mult Scler*. 2010;16:919–925.

31. Dineen RA, Vilisaar J, Hlinka J, et al. Disconnection as a mechanism for cognitive dysfunction in multiple sclerosis. *Brain*. 2009;132:239–249.

32. Deloire MSA, Salort E, Bonnet M, et al. Cognitive impairment as marker of diffuse brain abnormalities in early relapsing remitting multiple sclerosis. *J Neurol Neurosurg Psychiatry*. 2005;76:519–526.

33. Deloire MSA, Ruet A, Hamel D, Bonnet M, Dousset V, Brochet B. MRI predictors of cognitive outcome in early multiple sclerosis. *Neurology*. 2011;76:1161–1167.

34. Sicotte NL, Kern KC, Giesser BS, et al. Regional hippocampal atrophy in multiple sclerosis. *Brain*. 2008;131:1134–1141.

35. Papadopoulos D, Dukes S, Patel R, Nicholas R, Vora A, Reynolds R. Substantial

- archaeocortical atrophy and neuronal loss in multiple sclerosis. *Brain Pathol.* 2009;19:238–253.
36. DeLuca J, Gaudino EA, Diamond BJ, Christodoulou C, Engel RA. Acquisition and storage deficits in multiple sclerosis. *J Clin Exp Neuropsychol.* 1998;20:376–390.
37. Olivares T, Nieto A, Sánchez MP, Wollmann T, Hernández MA, Barroso J. Pattern of neuropsychological impairment in the early phase of relapsing-remitting multiple sclerosis. *Mult Scler.* 2005;11:191–197.
38. Dutta R, Chang A, Doud MK, et al. Demyelination causes synaptic alterations in hippocampi from multiple sclerosis patients. *Ann Neurol.* 2011;69:445–454.
39. Dutta R, Chomyk AM, Chang A, et al. Hippocampal demyelination and memory dysfunction are associated with increased levels of the neuronal microRNA miR-124 and reduced AMPA receptors. *Ann Neurol.* 2013;73:637–645.
40. Maruszak A, Thuret S. Why looking at the whole hippocampus is not enough—a critical role for anteroposterior axis, subfield and activation analyses to enhance predictive value of hippocampal changes for Alzheimer’s disease diagnosis. *Front Cell Neurosci.* 2014;8:95.
41. Small SA. Isolating pathogenic mechanisms embedded within the hippocampal circuit through regional vulnerability. *Neuron.* 2014;84:32–39.
42. Gold SM, Kern KC, O’Connor M-F, et al. Smaller cornu ammonis 2-3/dentate gyrus volumes and elevated cortisol in multiple sclerosis patients with depressive symptoms. *Biol Psychiatry.* 2010;68:553–559.
43. Longoni G, Rocca MA, Pagani E, et al. Deficits in memory and visuospatial learning correlate with regional hippocampal atrophy in MS. *Brain Struct Funct.* 2015;220:435–444.
44. Rocca MA, Longoni G, Pagani E, et al. In vivo evidence of hippocampal dentate gyrus expansion in multiple sclerosis. *Hum Brain Mapp.* 2015;36:4702–4713.
45. Hulst HE, Schoonheim MM, Roosendaal SD, et al. Functional adaptive changes within the hippocampal memory system of patients with multiple sclerosis. *Hum Brain Mapp.* 2012;33:2268–2280.
46. Roosendaal SD, Hulst HE, Vrenken H, et al. Structural and functional hippocampal changes in multiple sclerosis patients with intact memory function. *Radiology.* 2010;255:595–604.
47. Schoonheim MM, Meijer KA, Geurts JGG. Network collapse and cognitive impairment in multiple sclerosis. *Front Neurol.* 2015;6:82.
48. Amato MP, Langdon D, Montalban X, et al. Treatment of cognitive impairment in multiple sclerosis: position paper. *J Neurol.* 2013;260:1452–1468.
49. das Nair R, Martin K-J, Lincoln NB. Memory rehabilitation for people with multiple sclerosis. *Cochrane Database Syst Rev.* 2016;3:CD008754.
50. Krupp LB, Christodoulou C, Melville P, et al. Multicenter randomized clinical trial of donepezil for memory impairment in multiple sclerosis. *Neurology.* 2011;76:1500–1507.

51. Benedict RHB, Munschauer F, Zarevics P, et al. Effects of l-amphetamine sulfate on cognitive function in multiple sclerosis patients. *J Neurol.* 2008;255:848–852.
52. Peyro Saint Paul L, Creveuil C, Heinzlef O, et al. Efficacy and safety profile of memantine in patients with cognitive impairment in multiple sclerosis: A randomized, placebo-controlled study. *J Neurol Sci.* 2016;363:69–76.
53. Fischer JS, Priore RL, Jacobs LD, et al. Neuropsychological effects of interferon beta-1a in relapsing multiple sclerosis. Multiple Sclerosis Collaborative Research Group. *Ann Neurol.* 2000;48:885–892.
54. Patti F, Amato MP, Bastianello S, et al. Effects of immunomodulatory treatment with subcutaneous interferon beta-1a on cognitive decline in mildly disabled patients with relapsing-remitting multiple sclerosis. *Mult Scler.* 2010;16:68–77.
55. Horaud F. La sécurité virale des produits biologiques : aspects historiques et conceptuels. *Virologie.* 1997;1:365–372.
56. Ransohoff RM. Animal models of multiple sclerosis: the good, the bad and the bottom line. *Nat Neurosci.* 2012;15:1074–1077.
57. 't Hart BA, Gran B, Weissert R. EAE: imperfect but useful models of multiple sclerosis. *Trends Mol Med.* 2011;17:119–125.
58. Yednock TA, Cannon C, Fritz LC, Sanchez-Madrid F, Steinman L, Karin N. Prevention of experimental autoimmune encephalomyelitis by antibodies against alpha 4 beta 1 integrin. *Nature.* 1992;356:63–66.
59. Budde MD, Kim JH, Liang H-F, Russell JH, Cross AH, Song S-K. Axonal injury detected by in vivo diffusion tensor imaging correlates with neurological disability in a mouse model of multiple sclerosis. *NMR Biomed.* 2008;21:589–597.
60. Nathoo N, Yong VW, Dunn JF. Using magnetic resonance imaging in animal models to guide drug development in multiple sclerosis. *Mult Scler.* 2014;20:3–11.
61. Ziehn MO, Avedisian AA, Tiwari-Woodruff S, Voskuhl RR. Hippocampal CA1 atrophy and synaptic loss during experimental autoimmune encephalomyelitis, EAE. *Lab Invest.* 2010;90:774–786.
62. Sharma S, Rakoczy S, Brown-Borg H. Assessment of spatial memory in mice. *Life Sci.* 2010;87:521–536.
63. Laitinen T, Sierra A, Pitkänen A, Gröhn O. Diffusion tensor MRI of axonal plasticity in the rat hippocampus. *NeuroImage.* 2010;51:521–530.
64. Strange BA, Witter MP, Lein ES, Moser EI. Functional organization of the hippocampal longitudinal axis. *Nat Rev Neurosci.* 2014;15:655–669.
65. Kaouane N, Porte Y, Vallée M, et al. Glucocorticoids can induce PTSD-like memory impairments in mice. *Science.* 2012;335:1510–1513.

**Early hippocampal degeneration  
in patients with multiple sclerosis**

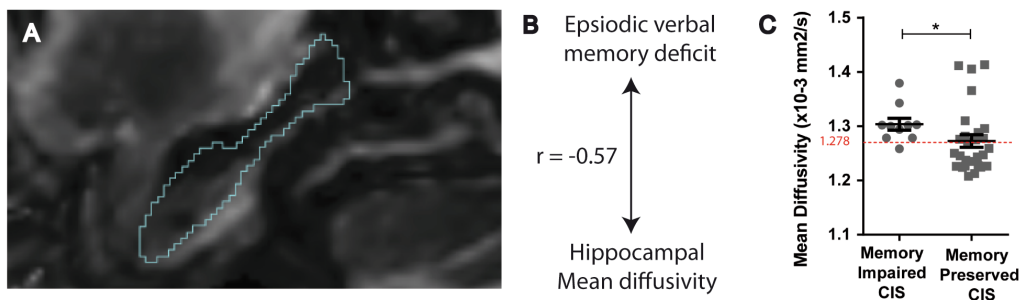


## Chapter 2: Early hippocampal degeneration in patients with multiple sclerosis

### 1. Summary page

**Rationale:** Memory impairment is frequent and occurs early in multiple sclerosis (MS). However, hippocampal damage related to memory performances have never been reported at the early stage of the disease, prior to atrophy. We aimed at demonstrating that hippocampal microstructural damage are present from the first demyelinating event suggestive of multiple sclerosis (clinically isolated syndrome, CIS) and that it is correlated with memory decline while there is still no atrophy.

**Summary of the methods:** We measured hippocampal volume and diffusion tensor imaging (DTI) metrics within the whole hippocampus of persons with CIS (PwCIS) to look for correlations with episodic memory scores and to test their ability to discriminate between memory-impaired and memory-preserved PwCIS. A group of healthy subjects and a group of persons with MS (PwMS) were used as negative and positive controls, respectively.



*Summary Figure: DTI alterations within the hippocampus (A) correlates with episodic memory performance (B) and discriminates persons with CIS according to their memory status (C).*

**Main results:** Hippocampal microstructural alterations measured by DTI appeared to be already present in the early stages of MS (PwCIS) while no significant hippocampal or global brain atrophy compared to healthy controls was evident. Such hippocampal microstructural

alterations were strongly correlated with early deficit in episodic memory, independently of age, gender, depression and T2-lesion load. Furthermore, hippocampal mean diffusivity discriminated memory-impaired from memory-preserved PwCIS.

**Comments:** This study argues for a very early neuropathological process occurring within the hippocampus during the course of MS that participates to memory impairment. The histopathological substrates of these early DTI alterations are not understood but could be investigated by using animal models of MS. Furthermore, the ability of DTI to discriminate between memory-impaired and memory-preserved PwCIS provides encouraging evidence for using DTI as a biomarker in future clinical trials targeting neuroprotection in PwCIS and PwMS.

## 2. Article

### **Hippocampal microstructural damage correlates with memory impairment in clinically isolated syndrome suggestive of multiple sclerosis**

Vincent Planche<sup>1,2,3</sup>, Aurélie Ruet<sup>1,2,4</sup>, Pierrick Coupé<sup>5</sup>, Delphine Lamargue-Hamel<sup>1,2</sup>, Mathilde Deloire<sup>4</sup>, Bruno Pereira<sup>3</sup>, José V. Manjon<sup>6</sup>, Fanny Munsch<sup>1,2</sup>, Nicola Moscufo<sup>7</sup>, Dominik S. Meier<sup>7</sup>, Charles R.G. Guttmann<sup>1,7</sup>, Vincent Dousset<sup>1,2,4</sup>, Bruno Brochet<sup>1,2,4,\*</sup>, Thomas Tourdias<sup>1,2,4,\*</sup>

<sup>1</sup> Univ. Bordeaux, F-33000 Bordeaux, France;

<sup>2</sup> Inserm U1215 - Neurocentre Magendie, F-33000 Bordeaux, France

<sup>3</sup> CHU de Clermont-Ferrand, F-63000 Clermont-Ferrand, France;

<sup>4</sup> CHU de Bordeaux, F-33000 Bordeaux, France;

<sup>5</sup> Laboratoire Bordelais de Recherche en Informatique, UMR CNRS 5800, F-33405 Talence, France;

<sup>6</sup> Univ. Politécnica de Valencia, 46022 Valencia, Spain

<sup>7</sup> Brigham and Women's Hospital, Harvard Medical School, Boston, MA, United States.

\* BB and TT share co-seniorship of this study

***Mult Scler. (2016) doi:10.1177/1352458516675750.***

## **Abstract**

**Objective:** We investigated whether diffusion tensor imaging (DTI) could reveal early hippocampal damage, and clinically relevant correlates of memory impairment in persons with clinically isolated syndrome (CIS) suggestive of multiple sclerosis (MS).

**Methods:** 37 persons with CIS, 32 with MS and 36 controls prospectively included from 2011 to 2014 were tested for cognitive performances and scanned with 3T-MRI to assess volumetric and DTI changes within the hippocampus, whole brain volume, and T2-lesion load.

**Results:** While there was no hippocampal atrophy in the CIS group, hippocampal fractional anisotropy (FA) was significantly decreased compared to controls. Decrease in hippocampal FA together with increased mean diffusivity (MD) was even more prominent in MS patients. In CIS, hippocampal MD was correlated with episodic verbal memory performance ( $r=-0.57$ ,  $p=0.0002$  and  $OR=0.058$  (95%CI=0.0057-0.59),  $p=0.016$  adjusted for age, gender, depression and T2-lesion load), but not with cognitive tasks unrelated to hippocampal functions. Hippocampal MD was the only variable discriminating memory-impaired from memory-preserved persons with CIS (AUC=0.77; sensitivity 90.0%; specificity 70.3%; PPV 52,9%; NPV 95,0%).

**Conclusion:** DTI alterations within the hippocampus might reflect early neurodegenerative processes that are correlated with episodic memory performance, discriminating persons with CIS according to their memory status.

## Introduction

Cognitive impairment is frequent in multiple sclerosis (MS)<sup>1,2</sup> and strongly impacts quality of life and vocational status<sup>3</sup>. The two most frequently affected domains are information processing speed (IPS) and episodic memory<sup>1</sup>. While IPS impairment is usually explained by disconnections due to demyelinating lesions and diffuse brain damage<sup>4</sup>, several groups have reported that memory impairment could be more specifically related to hippocampal atrophy<sup>5,6,7,8</sup>.

Significant memory impairment is already present at the stage of clinically isolated syndrome (CIS)<sup>9,10</sup>, the first clinical episode suggestive of MS. However, hippocampal damage is typically not detected at this early stage of MS because atrophy is not yet observed or still confined to few locations such as the thalamus or the striatum<sup>11,12,13,14</sup>. To the best of our knowledge, only one study has reported hippocampal atrophy in a CIS group with high T2-lesion load<sup>15</sup>. Therefore, there is a need for imaging biomarkers more sensitive than atrophy, especially at the stage of CIS, which could reflect clinically relevant hippocampal alterations to help the development and validation of future neuroprotective strategies.

Diffusion tensor imaging (DTI) has been efficiently used to reveal widespread white matter damages from the stage of CIS<sup>16</sup> but less consistently within grey matter<sup>17,18</sup>. Specifically, there is no report of altered DTI within the hippocampus of persons with CIS and no strong imaging correlate of memory impairment at this stage. Outside the field of MS, DTI has revealed subtle and early hippocampal alterations in Alzheimer's disease<sup>19</sup>, but it's currently unknown whether this technique can also be sensitive enough to capture clinically relevant modifications at the very early stage of MS.

In this study, we hypothesized that microstructural damage contributing to early memory impairment could occur in the hippocampus at the stage of CIS and that it might be measurable with DTI while there is no hippocampal atrophy. To test this hypothesis, we measured hippocampal volume and DTI metrics within the hippocampus of persons with CIS (PwCIS) to look for correlations with episodic memory scores and to test their ability to discriminate between memory-impaired and memory-preserved PwCIS. A group of healthy subjects and a group of persons with MS (PwMS) were used as negative and positive controls, respectively.

## **Methods**

### ***Participants***

All subjects were prospectively enrolled from 2011 to 2014 at our MS center. Written informed consent was obtained prior to participation.

The main population of interest consisted of thirty-seven persons with CIS (PwCIS) enrolled prospectively after approval by the local institutional ethics review board (NCT01865357) between 2 to 6 months after a first clinical event compatible with a demyelinating inflammatory syndrome. At least two clinically silent lesions with 3 mm minimum diameter were needed for inclusion. One had to be cerebral (ovoid or periventricular), while the other could be located in spine or brain. Exclusion criteria: contraindications to MRI, presence of other neurologic, psychiatric or systemic diseases, steroid treatment within one month, starting or stopping antidepressants or anxiolytic treatments within 2 months of MRI and neuropsychological examination.

We pooled these data with data from a MS study (NCT01207856) to analyze patients with long lasting disease as a positive control. Thirty-two persons with MS (PwMS) diagnosed according to the 2005-revised McDonald criteria<sup>20</sup> were included (27 relapsing-remitting, 3 secondary progressive and 2 primary progressive form of MS). Exclusion criteria were dementia (Mini Mental State Examination <27), other neurologic or psychiatric disorders, drug or alcohol abuse, relapse and/or steroid treatment within 2 months, or severe depression (Beck Depression Inventory >27).

A total of seventy-six healthy control (HC) subjects, included as negative controls, were free of neurologic, psychiatric, or systemic diseases, and drug or alcohol abuse. Fifty-four subjects were tightly matched for age, sex and educational level to PwCIS, to calculate cognitive z-score (see below). The twenty-two additional subjects were matched for age, sex and educational level to PwMS.

### ***Neuropsychological testing***

All patients and controls performed the Symbol Digit Modalities Test (SDMT) to assess IPS and the forward digit span subtest of the WAIS-III to assess attention/working memory. In order to assess hippocampal functions (verbal learning and recall), PwCIS and matched controls performed the Selective Reminding Test (SRT) while PwMS and matched controls performed

the California Verbal Learning Test (CVLT). Indeed, the SRT was frequently used in previous studies of CIS<sup>9,10</sup> and is part of the brief repeatable battery of neuropsychological testing<sup>21</sup> while the CVLT was the most common validated task used to assess episodic verbal memory in previous MS studies<sup>6,8</sup>. The SRT-LTS (Long Term Storage) and the CVLT-immediate recall were considered as measures of learning performance, and DR-SRT (Delayed Free Recall) and DR-CVLT as measures of long term recall performance. Each subject also completed a standard questionnaire concerning depressive symptoms (Beck Depression Inventory, BDI).

Each PwCIS or PwMS was compared with the appropriate control group (n=54 and n=22 respectively), tightly matched for age, sex and educational level to calculate a z-score for each test:

$$z = (\text{patient's score} - \text{mean value of the matched control group}) / \text{standard deviation of the matched control group.}$$

Lower z-score indicates lower performance. A patient was considered impaired in a given cognitive domain if his/her z-score was < -1.5, according to agreed-upon threshold<sup>22</sup>.

### ***MRI acquisition***

All PwCIs, PwMS and a representative subset of 36 HC were scanned on a 3T Philips Achieva MRI system with an 8-channel SENSE head coil. The protocol included a 3D gradient-echo T1-weighted sequence (TR/TE/TI/flip angle=8.2ms/3.5ms/982ms/7°, resolution 1x1x1mm, 256mm FOV) and a 2D axial fluid attenuated inversion recovery (FLAIR) sequence (TR/TE/TI=11000ms/140ms/2800ms, resolution 1x1.1x3mm, 230mm FOV). A diffusion tensor echo-planar-imaging (EPI) pulse sequence was also acquired: TR/TE=11676ms/60ms, 1.6x1.6x1.6mm resolution, 230mm FOV, with b=1000s/mm<sup>2</sup> ( $\Delta=29.4\text{ms}$ ,  $\delta=12.9\text{ms}$ ) in 20 non-co-linear directions and 4 sets of b=0s/mm<sup>2</sup>.

### ***MRI analyses***

Lesion load was determined using co-registered T1 and FLAIR sequences and a semi-automated segmentation pipeline based on local thresholding<sup>23</sup> followed by manual correction by a blinded expert (V.P., a neurologist with 4 years of experience).

For volumetric analyses of brain structures, T1-weighted images were processed using the volBrain system (<http://volbrain.upv.es>). After denoising<sup>24</sup>, images were affine-registered<sup>25</sup> into the Montreal Neurological Institute (MNI) space and the total brain volume was

estimated. Hippocampus was automatically segmented with a patch-based multi-templates method described in details elsewhere<sup>26</sup> that uses expert manual segmentations in MNI space as priors. Anatomical boundaries of the hippocampus were defined according to the EADC-ADNI Harmonized Protocol<sup>27</sup>. Every mask was then blindly checked and manually corrected (V.P.) for inappropriate inclusion of para-hippocampal T1-hypointense lesions, choroidal plexus and/or CSF “pockets”. To control for variations in head size, total brain volumes and hippocampal volumes were scaled using the volumetric scaling factor determined through the affine registration to the MNI brain template.

An in-house pipeline (dtiBrain) was used to process diffusion weighted images (DWI). First, images were denoised<sup>28</sup> in order to improve signal-to-noise ratio. Then, head displacement and distortions induced by eddy currents were corrected by performing affine registration<sup>25</sup> of all DWI to the b0 images. The direction table was updated with the estimated motion matrices. To compensate for EPI distortion, a non-rigid registration of DWI to the subject’s T1-weighted images in MNI space was performed by using ANTs<sup>25</sup>. For that purpose, we found that registration of mean diffusivity map, derived from DWI, to CSF probability map, derived from T1, provided the most accurate strategy by visual inspection of the hippocampal areas. Then, a diffusion tensor model was fitted at each voxel using FSL 5.0 (<http://fsl.fmrib.ox.ac.uk/fsl>) to measure mean fractional anisotropy (FA) and mean diffusivity (MD) within the hippocampal masks previously generated from T1-weighted images (Fig. 1A, B and C).

### **Statistical Analyses**

Right and left hippocampal values were averaged. Statistical analyses were performed with Stata software 12 (StataCorp) and Prism software 6 (Graphpad). The distribution of all continuous data was tested with the Shapiro-Wilk test. We first compared clinical and imaging characteristics between the three groups (HC, CIS, MS) by using the Chi-squared test for categorical variables, and ANOVA or Kruskal-Wallis test (when assumptions of ANOVA were not met) for ordinal variables followed by appropriate *post-hoc* tests (Tukey-Kramer or Dunn test, respectively), and adjustment on age and gender. If only two groups had to be compared, Student’s t-test or Mann-Whitney test was used as appropriate. Cohen’s d was used to measure the effect size. Then, relationships between clinical scores and quantitative imaging variables were assessed using correlation coefficients (Pearson or Spearman according to

statistical distribution) for CIS and MS groups respectively. The associations were further tested in multivariate context to take into account adjustment on covariables fixed according to univariate results and clinical relevance: age, gender, depression and T2 lesion load. For that purpose, cognitive performances (dependent variables) were predicted with regression models. Linear regression model was used whenever possible while logistic regression was seen as the appropriate alternative for categorical outcome variables by dichotomizing the performances; a log transformation was applied when needed to achieve normality. Considering the issue of multiple comparisons, Sidak's correction was used to reduce the risk of type I error. Lastly, Receiver Operating Characteristic (ROC) analysis was performed to test the value of DTI to discriminate between memory-impaired PwCIS (z-score DR-SRT < -1.5) *versus* those with normal memory performance. All tests were two-tailed, with a type I error set at  $\alpha=0.05$ .

## Results

	Controls with MRI (n=36)	CIS (n=37)	MS (n=32)	p-value
<b>Clinical features</b>				
Mean age, years [range]	37.8 [21 – 60]	37.4 [19 – 59]	41.3 [28 – 50]	0.18
Sex ratio (F/M)	24/12	29/8	23/9	0.53
Mean disease duration, months [range]	-	<6	107[12 – 216]	<0.0001
Education level (High/Low <sup>s</sup> )	29/7	24/13	19/13	0.14
Median EDSS score [range]	-	1.0 [0 – 6]	3.0 [0 – 8]	<0.0001
Median depression (BDI) score [range]	3.5 [0 – 13]	9.0** [0 – 36]	14.0*** [0 – 26]	<0.0001
<b>Imaging features</b>				
Median T2 lesion volume,ml [range]	-	2.11 [0.18 – 60.28]	8.38 [1.25 – 65.69]	0.001
Median normalized brain volume, ml [range]	1564 [1475 – 1676]	1570 [1335 – 1657]	1485*** [1276 – 1667]	0.0002

Table 1: Clinical and general MRI features. BDI = Beck Depression Inventory; CIS = Clinically Isolated Syndrome; MS = Multiple Sclerosis; EDSS = Expanded Disability Status Scale. § Education level was considered as high or low according to French baccalaureate (equivalent to A-level). \*\*  $p < 0.01$  and \*\*\* $p < 0.001$ , patients vs controls.

### Clinical characteristics and general MRI features

A total of 37 PwCIS, 32 PwMS and 36 HC assessed with MRI were included (Table 1). Groups were comparable for age, sex ratio and educational level. PwCIS and PwMS showed significantly higher depression scores than controls but they were not significantly different from each other ( $p = ns$ ;  $d = 0.39$ ). As expected, EDSS and T2-lesion load were significantly lower in PwCIS than in PwMS. PwCIS presented no global brain atrophy compared to HC whereas PwMS did.

### Cognitive assessment

Median z-scores and percentages of impaired PwCIS and PwMS ( $z\text{-score} < -1.5$ ) are reported in table 2. Regarding mean or median z-scores, as expected, PwMS performed significantly worse than PwCIS for all the tests. Verbal episodic memory performance was the most frequently affected domain in PwCIS (27.0%) whereas slowing of IPS was the most frequently affected domain in PwMS (78.1%).

	CIS (n=37)		MS (n=32)	
	Impaired patients (%)	Median z-score [range]	Impaired patients (%)	Median z-score [range]
<b>Information processing speed</b>	13.9	-0.628 [-3.78 - +1.74]	78.1	-2.217 [-4.48 - +0.17]
<b>Attention/Working memory</b>	18.9	-0.525 [-1.50 - +1.43]	21.9	-1.324 [-2.45 - +2.06]
<b>Episodic verbal memory</b>				
- learning trials	27.0	-0.269 [-5.27 - +1.21]	65.6	-3.234 [-9.43 - +0.90]
- long term recall	27.0	+0.611 [-9.16 - +0.61]	62.5	-1.767 [-7.45 - +0.67]

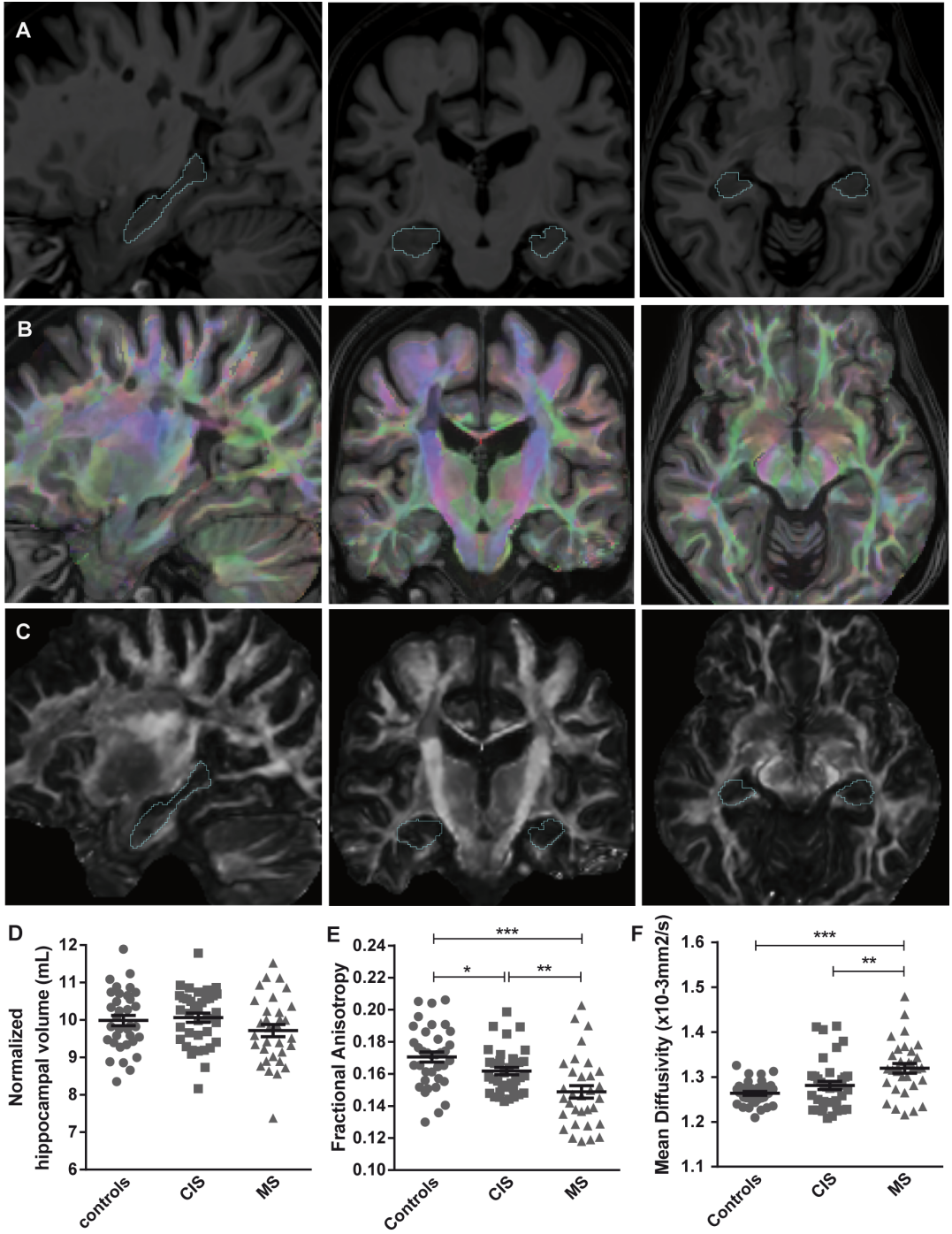
Table 2: Neuropsychological performances of persons with CIS and persons with MS. CIS = Clinically Isolated Syndrome; MS = Multiple Sclerosis. The threshold to dichotomize impaired/non impaired patients was set at  $z\text{-score} < -1.5$  ( $z\text{-scores}$  were computed relative to appropriate control groups for CIS and MS, see method).

### **Hippocampal volume and DTI measures**

Hippocampal volumes normalized for head size were not significantly different between groups ( $p=0.19$ ). PwMS showed slightly lower volumes compared to HC even though this difference didn't reach significance (mean volume 9.72 ml and 9.99 ml respectively,  $d=0.31$ , Fig.1D). Interestingly, PwCIS and HC were thoroughly similar for their hippocampal volumes (mean volume 10.06 ml and 9.99 ml respectively,  $d=0.09$ , Fig.1D).

Hippocampal FA and MD were significantly different between groups ( $p<0.0001$  for both measures, adjusted for age and gender: FA=0.171, 0.162 and 0.149; MD=1.269, 1.281 and  $1.319 \times 10^{-3} \text{ mm}^2/\text{s}$  for HC, CIS and MS groups respectively; Fig. 1E and F). *Post-hoc* analyses showed that FA was significantly decreased in PwCIS compared to HC ( $p=0.050$ , adjusted for age and gender;  $d=0.53$ ), as well as in PwMS compared to HC ( $p<0.0001$ ;  $d=1.05$ ) and compared to PwCIS ( $p=0.007$ ;  $d=0.70$ ). In PwMS, MD was significantly increased compared to HC ( $p<0.0001$ ;  $d=1.21$ ) and compared to PwCIS ( $p=0.004$ ;  $d=0.65$ ). The difference in MD between PwCIS and HC did not reach a statistically significant level ( $p=0.093$ ;  $d=0.41$ ), but the graphical distribution of hippocampal MD values in the CIS group showed a sub-group with distinctly higher MD values compared to HC.

*Figure 1: Hippocampal volumes and DTI measures in patients and controls. (A-C) Examples of MRI from a patient with MS. (A). T1-weighted images were used for hippocampi segmentation (cyan lines). (B). Color-coded FA maps superimposed to T1-weighted images. (C). FA maps registered in the MNI space with the same hippocampal masks. (D). Plots of the normalized hippocampal volumes of the three groups. (E). Plots of the fractional anisotropy values within the hippocampal masks of the three groups. (F). Plots of the mean diffusivity values within the hippocampal masks of the three groups. Each point is an individual measure and bars are mean and standard error of the mean. CIS = Clinically Isolated Syndrome; MS = Multiple Sclerosis. \* $p<0.05$ , \*\* $p<0.01$ , \*\*\* $p<0.001$  adjusted on age and gender.*



**Correlations between MRI measures and cognitive performance (table 3)**

In the CIS group, in univariate analyses, the hippocampal MD was the only metric strongly correlated with long-term recall ( $r=-0.57$ ,  $p=0.0002$ ); a correlation that remains significant even after correction for the 32 multiple comparisons run between MRI and clinical data ( $p=0.0050$ ). By contrast, hippocampal volume and T2-lesion load were not correlated with episodic memory. In multivariate analysis, after adjusting for age, gender, depression and T2-lesion load, the correlation between hippocampal MD and performances on long term recall remained significant with an odds ratio of 0.058 (95%CI=0.0057-0.59,  $p=0.016$ ).

CIS (n=37)	T2 Lesion load	Hippocampal Volume	Hippocampal FA	Hippocampal MD
Information processing speed	$r=-0.13$ , $p=0.45$	$r=0.04$ , $p=0.84$	$r=0.10$ , $p=0.54$	$r=-0.23$ , $p=0.18$
Attention/Working memory	$r=-0.16$ , $p=0.36$	$r=-0.11$ , $p=0.53$	$r=-0.17$ , $p=0.31$	$r=-0.01$ , $p=0.98$
Episodic verbal memory (learning trials)	$r=-0.24$ , $p=0.14$	$r=0.02$ , $p=0.93$	$r=-0.07$ , $p=0.67$	$r=-0.29$ , $p=0.08$
Episodic verbal memory (long term recall)	$r=-0.07$ , $p=0.68$	$r=0.02$ , $p=0.89$	$r=0.01$ , $p=0.96$	<b><math>r=-0.57</math>, <math>p=0.0002</math> (<math>p=0.016</math>)<sup>#</sup></b>
MS (n=32)	T2 Lesion load	Hippocampal Volume	Hippocampal FA	Hippocampal MD
Information processing speed	<b><math>r=-0.51</math>, <math>p=0.004</math> (<math>p=0.033</math>)<sup>†</sup></b>	$r=0.25$ , $p=0.18$	<b><math>r=0.36</math>, <math>p=0.04</math> (n.s.)<sup>#</sup></b>	<b><math>r=-0.52</math>, <math>p=0.002</math> (<math>p=0.012</math>)<sup>#</sup></b>
Attention/Working memory	$r=-0.16$ , $p=0.38$	$r=0.17$ , $p=0.35$	$r=0.16$ , $p=0.40$	$r=-0.05$ , $p=0.76$
Episodic verbal memory (learning trials)	$r=-0.15$ , $p=0.41$	<b><math>r=0.44</math>, <math>p=0.01</math> (<math>p=0.032</math>)<sup>#</sup></b>	$r=0.19$ , $p=0.31$	$r=-0.30$ , $p=0.09$
Episodic verbal memory (long term recall)	$r=-0.10$ , $p=0.60$	$r=0.29$ , $p=0.10$	$r=0.12$ , $p=0.52$	$r=-0.12$ , $p=0.52$

Table 3: Correlations between MRI measures and neuropsychological z-scores. CIS = Clinically Isolated Syndrome; FA = Fractional Anisotropy; MD= Mean Diffusivity; MS = Multiple Sclerosis. #, adjusted on age, gender, depression and T2-lesion load; †, adjusted on age, gender and depression. To explore multiple leads, p values were uncorrected for multiple comparisons in this table.

In the MS group, the performances on learning trials were correlated with hippocampal volumes ( $r=0.44$ ,  $p=0.01$  and  $\beta=1.23$ , 95%CI=0.12-2.34,  $p=0.032$  after adjustments). IPS measures were correlated with T2-lesion load ( $r=-0.51$ ,  $p=0.004$  and  $\beta=-3.5 \times 10^{-5}$ , 95%CI=  $6.8 \times 10^{-5}$ -- $3.12 \times 10^{-6}$ ,  $p=0.033$  after adjustments) but also with both hippocampal FA and MD

(respectively  $r=0.36$ ,  $p=0.04$ , non-significant after adjustments and  $r=-0.52$ ,  $p=0.002$ ;  $\beta=-8.95$ ,  $95\%CI=-15.77--2.13$ ,  $p=0.012$  after adjustments).

### **Hippocampal MD discriminates between memory-impaired and memory-preserved PwCIS**

Regarding the strong association between hippocampal MD and long-term recall memory performances, we tested whether this parameter could discriminate memory-impaired PwCIS from those with normal long-term recall. PwCIS were dichotomized in two subgroups according to their long-term memory performances (*i.e.* DR-SRT z-score  $<-1.5$ ). Using ROC analysis we showed that a threshold MD value ( $MD=1.278 \times 10^{-3} \text{mm}^2/\text{s}$ ) was discriminating these two subgroups with 90.0% sensitivity, 70.3% specificity, 52.9% positive predictive value (PPV) and 95.0% negative predictive value (NPV) (area under the curve = 0.77,  $95\%CI=0.62-0.92$ ,  $p=0.013$ , Fig. 2A). Hippocampal MD was the only demographical, clinical or radiological characteristic significantly different between memory-impaired and memory-preserved PwCIS ( $p=0.011$ , Fig. 2B and table 4).

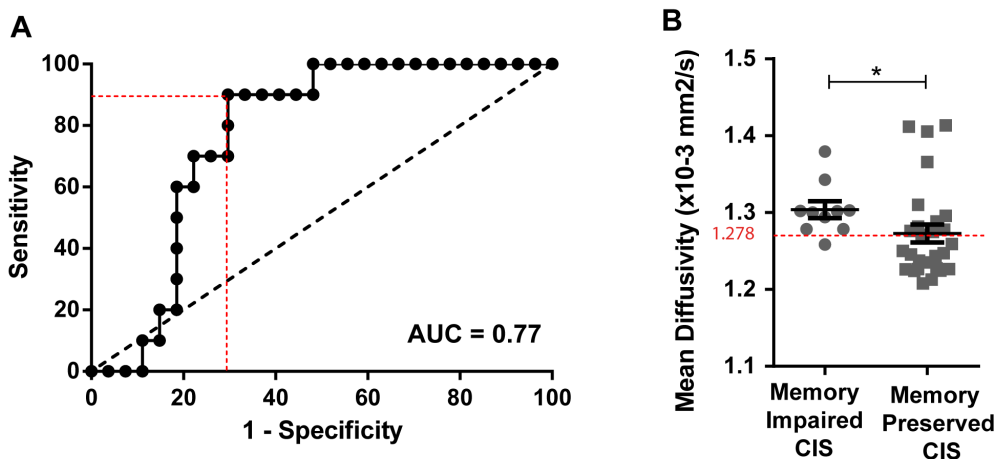


Figure 2: Hippocampal MD discriminates between memory-impaired and memory-preserved persons with CIS. (A). ROC curve defined a threshold MD value ( $1.278 \times 10^{-3} \text{mm}^2/\text{s}$ , red dashed line) that classified memory-impaired and memory-preserved patients (*i.e.* patients with DR-SRT z-score  $<-1.5$ ) with a sensitivity of 90.0% and a specificity of 70.3%. (B). Plots of mean diffusivity values in memory impaired and memory-preserved patients with CIS.  $*p=0.011$ . AUC = Area Under the Curve; CIS = Clinically Isolated Syndrome; DR-SRT = Delayed Recall-Selective Reminding Test.

CIS	Memory-impaired (n=10)	Memory-preserved (n=27)	p-value
<b>Median memory z-score</b> [range]	-2.44 [-9.16 – -1.83]	0.61 [-0.61 – 0.61]	<b>&lt;0.0001</b>
<b>Mean age</b> , years [range]	37.5 [19 – 59]	37.3 [23 – 58]	0.96
<b>Sex</b> (F/M)	6/4	23/4	0.17
<b>Educational level</b> (High/Low)	5/5	19/8	0.27
<b>Median T2 lesion volume</b> , ml [range]	2.05 [0.24 – 15.54]	1.80 [0.18 – 60.28]	0.89
<b>Median normalized brain volume</b> , ml [range]	1546 [1454 – 1647]	1587 [1335 – 1657]	0.33
<b>Median normalized hippocampal volume</b> , ml [range]	10.4 [8.16 – 10.86]	10.2 [8.73 – 11.79]	0.72
<b>Median hippocampal FA</b> [range]	0.1650 [0.1471 – 0.1695]	0.1577 [0.1429 – 0.1986]	0.69
<b>Median hippocampal MD</b> , x10 <sup>-3</sup> mm <sup>2</sup> /s [range]	1.301 [1.258 – 1.379]	1.250 [1.208 – 1.469]	<b>0.011</b>

Table 4: Clinical and MRI characteristics of memory-impaired vs memory-preserved patients with CIS. CIS = Clinically Isolated Syndrome; FA = Fractional Anisotropy; MD = Mean Diffusivity

## Discussion

In this study, hippocampal microstructural alterations measured by DTI appear to be already present in the early stages of MS (PwCIS), while no significant hippocampal or global brain atrophy compared to HC is evident. Furthermore, increased hippocampal MD was associated with early memory impairment in these PwCIS.

A quarter of our population of PwCIS showed episodic verbal memory impairment in learning and retrieval tasks which is consistent with previous studies using the same test<sup>9,10</sup>. Interestingly, memory impairment was more frequent than slowing of IPS in PwCIS. This observation suggests that a neurodegenerative process starts early within the hippocampus contributing to memory decline, even at a stage where IPS is relatively preserved because complete disconnection phenomena due to widespread demyelination are generally lower at the CIS stage than later on<sup>4</sup>. Furthermore, our PwCIS were not treated with disease modifying therapies, avoiding bias linked to heterogeneous therapeutic response.

Our data support the concept that early memory deficit in MS could be related to specific hippocampal vulnerability, independent of the extent of focal white matter lesions. Hippocampal FA was significantly decreased in the CIS group and even more in the MS group, in which a significant increase of hippocampal MD was also observed. In previous work assessing PwCIS, deep grey matter DTI changes were detected, while no hippocampal DTI

changes were apparent<sup>17</sup>. However, the sensitivity to DTI changes in the hippocampus might have been hampered by partial voluming effects due to a larger voxel size (3.33mm x 3.33mm x 3.00mm)<sup>17</sup>, compared with our 1.6mm<sup>3</sup> voxel size. We also believe that applying a denoising procedure further increased our sensitivity towards microstructural alterations detected by DTI, enabling our findings<sup>28</sup>.

In support of the clinical relevance of our finding of early hippocampal damage in PwCIS, we were able to show a strong and independent correlation of hippocampal MD with a hippocampus-dependent task (DR-SRT), but not with cognitive tasks that are not reliant on hippocampal function (*i.e.* IPS and attention/working memory, even though some authors argue for a continuum between working memory and long term memory encoding<sup>29</sup>). Hippocampal MD in PwCIS was correlated to hippocampal-dependent long-term recall in the absence of significant hippocampal volume loss, suggesting that hippocampal MD reflects an earlier pathophysiological process that likely precedes atrophy. Interestingly, and despite smaller differences between groups, the increase in MD appears to be more clinically relevant than the decrease in FA in the explored context. MD might be more stable and reproducible than FA in the hippocampus (*i.e.* smaller dispersion of the values, even in the control group), which can be reasonably expected in such a grey matter structure where diffusion tends to be more isotropic and therefore imperfectly represented by FA as a measure of fiber orientation. Therefore either FA and MD measure different underlying histological substrate or, more likely, FA is less reliable than MD in grey matter which is in line with previous results<sup>16,17</sup>. Higher MD might correspond to a mixture of hippocampal demyelination, neuronal or synaptic loss together with inflammatory cells as described in post-mortem studies of MS brains<sup>30</sup>.

We also showed that hippocampal MD discriminates memory-impaired from memory-preserved patients with a sensitivity of 90%, a specificity of 70.3% and a NPV of 95.0%. Among clinical and other MRI criteria, hippocampal MD was the only predictor of memory impairment in this group. Therefore, stabilization of low hippocampal MD might be an interesting candidate endpoint (surrogate marker with a very good NPV) in future proof-of-concept phase II clinical trials in CIS and early MS. Unambiguous monitoring of cognitive performances in the context of a neuroprotective agent in clinical trials is complicated by the length of the cognitive testing, the test/retest effect and confounding factors such as participation of the subject, fatigue or depression<sup>31</sup>. In this context, stabilization of low hippocampal MD might provide a complementary and unbiased endpoint. DTI of the hippocampus might also help to

improve patient selection by stratifying those with and without hippocampal damage, therefore powering future neuroprotective trials by including more homogeneous population in comparison groups.

In contrast, in PwMS, episodic memory correlated with hippocampal volume, but the correlation between hippocampal MD and memory scores was not significant. This finding suggests that at a more advanced stage, assessing the microstructure of the hippocampus with DTI might no longer be sensitive and relevant. Furthermore, T2-lesion load and hippocampal DTI metrics were correlated with IPS scores. These findings can suggest that hippocampus is involved in IPS but also that hippocampal DTI at the stage of clinically definite MS reflects more general brain damage and in turn correlate better with IPS that has been associated to global cerebral damage<sup>2</sup>. This is consistent with data in the literature showing that cognitive impairment is associated with several imaging metrics in more advanced MS<sup>32</sup> because cognitive impairment is probably the result of a complex interplay between several alterations at this stage<sup>33</sup>.

We acknowledge an important shortcoming of this meta-analysis of our data, namely that the cognitive testing was different for the CIS and MS groups, limiting our ability to directly compare PwCIS to PwMS. Nevertheless, a previous paper reported no difference in sensitivity between SRT and CVLT<sup>34</sup> and furthermore, we believe that the insights gained by separately comparing these groups of patients to matched HC explored with the same tests maintain full validity. We also acknowledge that the sample size of each group is relatively small and therefore these results can be viewed as preliminary and need confirmation in a larger cohort of PwCIS. Another limitation is that we didn't acquire 3D-double inversion recovery MRI, limiting our ability to detect focal hippocampal lesions<sup>35</sup>. Therefore, our DTI findings might reflect focal, as well as more diffuse alterations in the hippocampus. Because the PPV was only 52.9%, it will be of great interest for future studies to assess whether PwCIS with increased hippocampal MD but preserved memory functions display compensatory mechanisms measured by hippocampal activation and functional connectivity, as demonstrated in PwMS<sup>36</sup>. Similarly, longitudinal data should identify whether those patients are likely to show memory alterations in long-term follow-up. DTI could also be combined with susceptibility weighted imaging that could also reveal subtle alterations because it has been demonstrated that iron deposition is present within the hippocampus at the stage of CIS<sup>37</sup>.

In conclusion, episodic memory impairment was correlated with hippocampal DTI changes at the stage of CIS, in the absence of a significant effect of global lesion volume or atrophy on any of the cognitive measures. This argues for a clinically relevant neurodegenerative process occurring in the hippocampus in the early stages of MS, and suggests that DTI measurement in this structure might provide a sensitive indicator of early neurodegenerative changes.

### **Study funding**

This study was supported by the ARSEP Fondation, Bordeaux University Hospital and TEVA and Merck-Sereno laboratories. The work was further supported by public grants from the French Agence Nationale de la Recherche within the context of the Investments for the Future program referenced ANR-10-LABX-57 named TRAIL (project IBIO-NI and HR-DTI) and ANR-10-LABX-43 named BRAIN (Project MEMO-MS). This study has also been carried out with financial support from the "Investments for the future" Programme IdEx Bordeaux - CPU (ANR-10-IDEX-03-02) and the CNRS multidisciplinary project "Défi ImagIn" HL-MRI. The sponsors did not participate in any aspect of the design or performance of the study, including data collection, management, analysis, and interpretation or the preparation of the manuscript.

### **Disclosures**

VP received travel expenses from ARSEP Fondation, Biogen, Teva-Lundbeck and Merck-Serono. AR received research grants and/or consulting fees from Novartis, Biogen, Merck-Serono, Bayer Healthcare, Roche, Teva, and Genzyme unrelated to the submitted work. BB serves on scientific advisory boards for and has received honoraria or research support for its institution from Biogen-idec, Merck-Serono, Novartis, Genzyme, Teva, Roche, Medday and Bayer outside the submitted work. CRGG is the recipient of a grant from Sanofi, and holds shares in Roche, Novartis, GSK, Alnylam, Protalix, Agenus, Arrowhead, and Cocrystal.

### **Acknowledgments**

The authors thank Julie Charré-Morin and Aurore Saubusse (Bordeaux University Hospital) for neuropsychological testing.

## References

1. Chiaravalloti ND, DeLuca J. Cognitive impairment in multiple sclerosis. *Lancet Neurol.* 2008; 7(12):1139–1151.
2. Rocca MA, Amato MP, De Stefano N, et al. Clinical and imaging assessment of cognitive dysfunction in multiple sclerosis. *Lancet Neurol.* 2015; 14(3):302–317.
3. Ruet A, Deloire M, Hamel D, et al. Cognitive impairment, health-related quality of life and vocational status at early stages of multiple sclerosis: a 7-year longitudinal study. *J. Neurol.* 2013; 260(3):776–784.
4. Dineen RA, Vilisaar J, Hlinka J, et al. Disconnection as a mechanism for cognitive dysfunction in multiple sclerosis. *Brain.* 2009; 132(Pt 1):239–249.
5. Sicotte NL, Kern KC, Giesser BS, et al. Regional hippocampal atrophy in multiple sclerosis. *Brain.* 2008; 131(Pt 4):1134–1141.
6. Benedict RHB, Ramasamy D, Munschauer F, Weinstock-Guttman B, Zivadinov R. Memory impairment in multiple sclerosis: correlation with deep grey matter and mesial temporal atrophy. *J. Neurol. Neurosurg. Psychiatry.* 2009; 80(2):201–206.
7. Longoni G, Rocca MA, Pagani E, et al. Deficits in memory and visuospatial learning correlate with regional hippocampal atrophy in MS. *Brain Struct. Funct.* 2015; 220(1):435–444.
8. Koenig KA, Sakaie KE, Lowe MJ, et al. Hippocampal volume is related to cognitive decline and fornical diffusion measures in multiple sclerosis. *Magn. Reson. Imaging.* 2014; 32(4):354–358.
9. Achiron A, Barak Y. Cognitive impairment in probable multiple sclerosis. *J. Neurol. Neurosurg. Psychiatry.* 2003; 74(4):443–446.
10. Feuillet L, Reuter F, Audoin B, et al. Early cognitive impairment in patients with clinically isolated syndrome suggestive of multiple sclerosis. *Mult. Scler.* 2007; 13(1):124–127.
11. Henry RG, Shieh M, Okuda DT, et al. Regional grey matter atrophy in clinically isolated syndromes at presentation. *J. Neurol. Neurosurg. Psychiatry.* 2008; 79(11):1236–1244.
12. Rocca MA, Preziosa P, Mesaros S, et al. Clinically Isolated Syndrome Suggestive of Multiple Sclerosis: Dynamic Patterns of Gray and White Matter Changes-A 2-year MR Imaging Study. *Radiology.* 2016; 278(3):841–853.
13. Calabrese M, Rinaldi F, Mattisi I, et al. The predictive value of gray matter atrophy in clinically isolated syndromes. *Neurology.* 2011; 77(3):257–263.
14. Audoin B, Zaaraoui W, Reuter F, et al. Atrophy mainly affects the limbic system and the deep grey matter at the first stage of multiple sclerosis. *J. Neurol. Neurosurg. Psychiatry.* 2010; 81(6):690–695.
15. Bergsland N, Horakova D, Dwyer MG, et al. Subcortical and cortical gray matter atrophy in a large sample of patients with clinically isolated syndrome and early

- relapsing-remitting multiple sclerosis. *AJNR Am. J. Neuroradiol.* 2012; 33(8):1573–1578.
16. Preziosa P, Rocca MA, Mesaros S, et al. Intrinsic damage to the major white matter tracts in patients with different clinical phenotypes of multiple sclerosis: a voxelwise diffusion-tensor MR study. *Radiology.* 2011; 260(2):541–550.
17. Cappellani R, Bergsland N, Weinstock-Guttman B, et al. Diffusion tensor MRI alterations of subcortical deep gray matter in clinically isolated syndrome. *J. Neurol. Sci.* 2014; 338(1–2):128–134.
18. Deppe M, Krämer J, Tenberge J-G, et al. Early silent microstructural degeneration and atrophy of the thalamocortical network in multiple sclerosis. *Hum. Brain Mapp.* 2016.
19. Douaud G, Menke RAL, Gass A, et al. Brain microstructure reveals early abnormalities more than two years prior to clinical progression from mild cognitive impairment to Alzheimer’s disease. *J. Neurosci.* 2013; 33(5):2147–2155.
20. Polman CH, Reingold SC, Edan G, et al. Diagnostic criteria for multiple sclerosis: 2005 revisions to the ‘McDonald Criteria’. *Ann. Neurol.* 2005; 58(6):840–846.
21. Boringa JB, Lazeron RH, Reuling IE, et al. The brief repeatable battery of neuropsychological tests: normative values allow application in multiple sclerosis clinical practice. *Mult. Scler.* 2001; 7(4):263–267.
22. Benedict RHB, Zivadinov R. Reliability and validity of neuropsychological screening and assessment strategies in MS. *J. Neurol.* 2007; 254 Suppl 2:II22-II25.
23. Van Leemput K, Maes F, Vandermeulen D, Colchester A, Suetens P. Automated segmentation of multiple sclerosis lesions by model outlier detection. *IEEE Trans. Med. Imaging.* 2001; 20(8):677–688.
24. Manjón JV, Coupé P, Martí-Bonmatí L, Collins DL, Robles M. Adaptive non-local means denoising of MR images with spatially varying noise levels. *J. Magn. Reson. Imaging.* 2010; 31(1):192–203.
25. Avants BB, Tustison NJ, Song G, et al. A reproducible evaluation of ANTs similarity metric performance in brain image registration. *NeuroImage.* 2011; 54(3):2033–2044.
26. Coupé P, Manjón JV, Fonov V, et al. Patch-based segmentation using expert priors: application to hippocampus and ventricle segmentation. *NeuroImage.* 2011; 54(2):940–954.
27. Frisoni GB, Jack CR, Bocchetta M, et al. The EADC-ADNI Harmonized Protocol for manual hippocampal segmentation on magnetic resonance: Evidence of validity. *Alzheimers Dement.* 2015; 11(2):111–125.
28. Manjón JV, Coupé P, Concha L, et al. Diffusion weighted image denoising using overcomplete local PCA. *PLoS One.* 2013; 8(9):e73021.
29. Leszczynski M. How does hippocampus contribute to working memory processing? *Front. Hum. Neurosci.* 2011; 5:168.
30. Dutta R, Chang A, Doud MK, et al. Demyelination causes synaptic alterations in hippocampi from multiple sclerosis patients. *Ann. Neurol.* 2011; 69(3):445–454.

31. Benedict RHB, Zivadinov R. Risk factors for and management of cognitive dysfunction in multiple sclerosis. *Nat. Rev. Neurol.* 2011; 7(6):332–342.
32. Daams M, Steenwijk MD, Schoonheim MM, et al. Multi-parametric structural magnetic resonance imaging in relation to cognitive dysfunction in long-standing multiple sclerosis. *Mult. Scler.* 2016; 22(5):608–619.
33. Preziosa P, Rocca MA, Pagani E, et al. Structural MRI correlates of cognitive impairment in patients with multiple sclerosis: A Multicenter Study. *Hum. Brain Mapp.* 2016; 37(4):1627–1644.
34. Strober L, Englert J, Munschauer F, et al. Sensitivity of conventional memory tests in multiple sclerosis: comparing the Rao Brief Repeatable Neuropsychological Battery and the Minimal Assessment of Cognitive Function in MS. *Mult. Scler.* 2009; 15(9):1077–1084.
35. Calabrese M, Battaglini M, Giorgio A, et al. Imaging distribution and frequency of cortical lesions in patients with multiple sclerosis. *Neurology.* 2010; 75(14):1234–1240.
36. Hulst HE, Schoonheim MM, Van Geest Q, et al. Memory impairment in multiple sclerosis: Relevance of hippocampal activation and hippocampal connectivity. *Mult. Scler.* 2015.
37. Hagemeyer J, Weinstock-Guttman B, Bergsland N, et al. Iron deposition on SWI-filtered phase in the subcortical deep gray matter of patients with clinically isolated syndrome may precede structure-specific atrophy. *AJNR Am. J. Neuroradiol.* 2012; 33(8):1596–160.



**Early dentate gyrus disruption  
in experimental multiple sclerosis**



## Chapter 3: Early dentate gyrus disruption in experimental multiple sclerosis

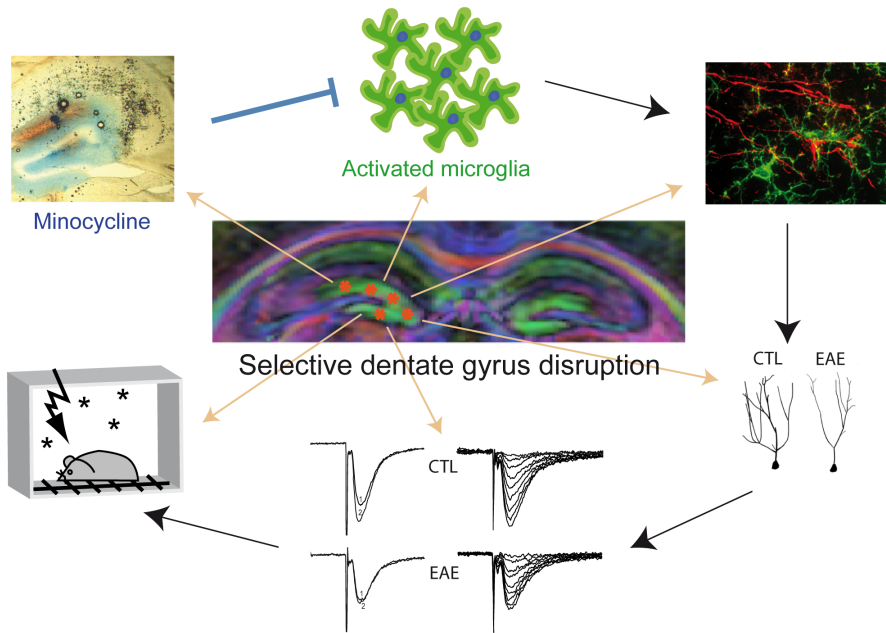
### 1. Summary page

**Rationale:** We have demonstrated that hippocampal microstructural damage was already present early during the course of multiple sclerosis (MS) and associated with memory performances (chapter 2). However, the underlying neuropathological process needs to be characterized. Furthermore, because measurements were done in the whole hippocampus of patients, it remains unknown whether some hippocampal regions could be more vulnerable than others.

**Summary of the methods:** We explored experimental autoimmune encephalomyelitis (EAE) mice (a mouse model of multiple sclerosis) and their controls at the acute stage (20 days post immunization) with a combination of behavioral, *in vivo* MRI, histological, electrophysiological and pharmacological approaches.

**Main results:** By using a particular contextual fear conditioning paradigm, we first demonstrated that hippocampal-dependent memory was impaired at the early stage of EAE (similarly to what was observed in patients with MS) while controlling confounding factors such as motor/sensory deficits or slowing of information processing speed. Then, using *in vivo* diffusion-tensor imaging (DTI) at ultra-high resolution to screen for regional vulnerability within the hippocampus, we found decreased fractional anisotropy selectively in the molecular layer of the dentate gyrus of EAE-mice compared to controls while the other hippocampal subfields did not show any modification. Histological and morphometric analyses of dendritic length and complexity confirmed the occurrence of a selective neurodegenerative process in the dentate gyrus, correlated to the *in vivo* reduced fractional anisotropy. Glutamatergic synaptic transmission and long-term synaptic potentiation were also impaired in the dentate gyrus but not in CA1. To understand what could drive such structural and functional alterations, we investigated glial cells and found a more severe pattern of microglial activation in this subfield. Systemic injections of the microglial inhibitor minocycline by daily intra-peritoneal injections prevented DTI, morphological, electrophysiological and behavioral impairments in EAE-mice. Furthermore, the selective inhibition of microglial activation by daily

intra-dentate gyrus infusions of minocycline through implanted cannulae was sufficient to prevent memory impairment in EAE-mice while infusion of minocycline within CA1 was inefficient.



*Summary Figure: Microglial activation causes selective dentate gyrus disruption and memory impairment in experimental MS. Some of these features can be identified with in vivo diffusion MRI.*

**Comments:** These results are the first to link early memory impairment in multiple sclerosis to a selective disruption of the dentate gyrus by demonstrating that dentate gyrus structure and function are more vulnerable than other hippocampal regions, which might be due to the neurotoxic effect of microglial activation. These results open new pathophysiological, imaging, and therapeutic perspectives for memory impairment in multiple sclerosis.

The results suggest that the alterations of DTI measured within the whole hippocampus in patients with CIS (chapter 2) are mainly driven by alterations specifically located with the dentate gyrus. Nevertheless, the demonstration of such selective dentate gyrus vulnerability in EAE-mice needs to be confirmed in humans.

## 2. Article

### **Selective dentate gyrus disruption causes memory impairment at the early stage of experimental multiple sclerosis**

Vincent Planche<sup>1,2,3</sup>, Aude Panatier<sup>1,2</sup>, Bassem Hiba<sup>2,4</sup>, Eva-Gunnel Ducourneau<sup>1,2</sup>, Gerard Raffard<sup>2,5</sup>, Nadège Dubourdiou<sup>1,2</sup>, Marlène Maitre<sup>1,2</sup>, Thierry Lesté-Lasserre<sup>1,2</sup>, Bruno Brochet<sup>1,2,6</sup>, Vincent Dousset<sup>1,2,6</sup>, Aline Desmedt<sup>1,2</sup>, Stéphane H. Oliet<sup>1,2</sup> and Thomas Tourdias<sup>1,2,6</sup>.

<sup>1</sup>INSERM, U1215, Neurocentre Magendie, F-33000 Bordeaux, France

<sup>2</sup>Univ. Bordeaux, F-33000 Bordeaux, France

<sup>3</sup>CHU de Clermont-Ferrand, F-63000 Clermont-Ferrand, France

<sup>4</sup>CNRS UMR 5287, Institut de Neurosciences Cognitives et Intégratives d'Aquitaine, F-33000, Bordeaux, France

<sup>5</sup>CNRS UMR 5536, Centre de Résonance Magnétique des Systèmes Biologiques, F-33000, Bordeaux, France

<sup>6</sup>CHU de Bordeaux, F-33000 Bordeaux, France

***Brain Behav Immun. (2016) doi:10.1016/j.bbi.2016.11.010***

## Abstract

Memory impairment is an early and disabling manifestation of multiple sclerosis whose anatomical and biological substrates are still poorly understood. We thus investigated whether memory impairment encountered at the early stage of the disease could be explained by a differential vulnerability of particular hippocampal subfields. By using experimental autoimmune encephalomyelitis (EAE), a mouse model of multiple sclerosis, we identified that early memory impairment was associated with selective alteration of the dentate gyrus as pinpointed *in vivo* with diffusion-tensor-imaging (DTI). Neuromorphometric analyses and electrophysiological recordings confirmed dendritic degeneration, alteration in glutamatergic synaptic transmission and impaired long-term synaptic potentiation selectively in the dentate gyrus, but not in CA1, together with a more severe pattern of microglial activation in this subfield. Systemic injections of the microglial inhibitor minocycline prevented DTI, morphological, electrophysiological and behavioral impairments in EAE-mice. Furthermore, daily infusions of minocycline specifically within the dentate gyrus were sufficient to prevent memory impairment in EAE-mice while infusions of minocycline within CA1 were inefficient. We conclude that early memory impairment in EAE is due to a selective disruption of the dentate gyrus associated with microglia activation. These results open new pathophysiological, imaging, and therapeutic perspectives for memory impairment in multiple sclerosis.

## Introduction

Multiple sclerosis is the most frequent inflammatory disorder of the central nervous system<sup>1</sup>. Among symptoms, episodic memory impairment is frequent<sup>2</sup>, greatly impacts quality of life<sup>3</sup> and occurs early during the course of the disease<sup>4</sup>. Evidence from clinical studies links episodic memory impairment with hippocampal alteration. Nevertheless, these human data are either post-mortem histological studies inherently biased toward the chronic stage of the disease<sup>5,6</sup>, or *in vivo* studies based on measurement of hippocampal atrophy on magnetic resonance imaging (MRI), which reflects again a late process and don't inform on the underlying cellular modifications<sup>7,8</sup>. Therefore, there is a need for a better understanding of the substrate of early memory deficit associated with multiple sclerosis.

The cellular mechanisms that could be potentially disrupted in the hippocampus during the early stage of multiple sclerosis are mainly those involved in long-term synaptic plasticity within the trisynaptic loop, which is one of the major substrates for learning and memory<sup>9</sup>. These mechanisms can only be explored by using experimental autoimmune encephalomyelitis (EAE), the most widely accepted animal model of multiple sclerosis<sup>10</sup>. Early synaptic dysfunctions have been reported in EAE and associated with pro-inflammatory cytokines released by macrophages, microglia or astrocytes<sup>11,12,13,14</sup>, leading to the concept of "inflammatory synapthopathy"<sup>15</sup>. However, it is currently unknown whether some particular synaptic pathways could be differentially targeted by activated glial cells during the course of multiple sclerosis or EAE.

Indeed, the hippocampus is composed of different interconnected regions and layers (the Cornu Ammonis subfields, the dentate gyrus and the subiculum) which are very different in their morphological, molecular, electrophysiological and functional profiles. This implies that it is not enough to consider the hippocampus as a unitary and homogeneous entity. By analogy with other diseases such as Alzheimer or post-traumatic stress disorder that differentially target distinct subregions of the hippocampus circuit, we can envision that groups of hippocampal neurons are afflicted at the early stage of multiple sclerosis while neighboring ones are not<sup>16,17</sup>. Human MRI data also suggest that some hippocampal regions could be more affected than others in multiple sclerosis because some authors have reported hippocampal volume loss localized to specific subfields<sup>7,18,19,20</sup>. However, these studies provide controversial

results which may come from measure of atrophy performed at different stages and with different methodology. Whether hippocampal regions/subfields could be differentially vulnerable to early pathophysiological mechanisms in multiple sclerosis (prior to atrophy) is therefore currently unclear and can only be addressed with the EAE model.

Consequently, in this study, we looked for the substrate of early memory impairment in multiple sclerosis by combining multi scale complementary approaches in the different hippocampal subfields of EAE-mice. Similarly to the human disease, we demonstrated that EAE-mice showed hippocampal-dependent memory impairment prior to hippocampal atrophy. Then, we used diffusion tensor imaging (DTI) as an *in vivo* “screening procedure” to pinpoint potential regional vulnerability and focus the other experiments. We identified the locus of early hippocampal disruption in the dentate gyrus with concordant DTI, morphological and electrophysiological experiments. This selective vulnerability was associated with early microglial activation and was prevented with systemic injections or local intra-dentate gyrus infusions of the microglial inhibitor minocycline. Hence, we identified the anatomical source of memory impairment in early multiple sclerosis which could be exploited to clarify pathogenesis and which could be translated to patients as it can be captured with *in vivo* imaging.

## **Materials and methods**

### ***Animals and Experimental Autoimmune Encephalomyelitis (EAE)***

Experiments were performed on 7 to 9-week-old females C57BL6/J (Janvier Labs). EAE was induced with a subcutaneous injection of 150µg of Myelin Oligodendrocyte Glycoprotein peptide 35-55 (MOG35-55, Anaspec) emulsified in 150µL of Complete Freund’s Adjuvant (CFA, Difco) containing 6mg/mL of desiccated *Mycobacterium Tuberculosis* (H37Ra, Difco). Animals received intraperitoneal (IP) injections of Pertussis Toxin (Sigma) on the day of immunization and 2 days later (250ng/injection). Control mice were injected with 150µL of CFA emulsified in phosphate-buffered saline (PBS). All animals were weighted daily and scored for clinical symptoms using the standard grading scale: 0, unaffected; 1: flaccid tail; 2: hind limb weakness and/or ataxia; 3: hind limb paralysis; 4: paralysis of all four limbs and 5: moribund.

All experiments reported in this article were performed early in the course of the disease at 20 days post-injection (d.p.i), except electrophysiological experiments which were performed between 18 and 22 d.p.i. All animal care and experiments were conducted in accordance with the European directive (2010/63/EU) and after approval of the local ethical committee (approval number 02046.01).

### ***Contextual fear conditioning***

Memory functions were assessed with a particular contextual fear conditioning procedure (Fig. 1B) that does not require important motor skills unlike other tests, such as the Morris water maze. Acquisition of fear conditioning took place in a Plexiglas box (30x24x22 cm, Imetronic) in a brightness of 60 lux, given access to different visual-spatial cues in the experimental room. The floor of the chamber consisted of stainless-steel rods connected to a shock generator. The box was cleaned with 70% ethanol. The training procedure consisted on a pseudo-random distribution of tones and shocks as followed (tone-shock unpairing procedure): 100s after being placed into the chamber, animals received a footshock (0.4mA squared signal, 1s), then, after 20s, a tone (65dB, 1kHz, 15s) was presented twice (30s delay); finally, after 30s, mice received a second shock and returned to the home cage 20s after. One day after the acquisition, mice were re-exposed to the tone alone during 2 minutes in a safe and familiar chamber where they had been pre-exposed the day before conditioning (opaque PVC chamber with opaque floor, brightness of 15 lux, cleaned with 4% acetic acid). One hour later, animals were re-exposed to the conditioning context alone, without the tone. Animals were recorded on videotape for off-line manual scoring of freezing behavior. We previously repeatedly showed that such conditioning procedure normally leads to the identification of the conditioning context as the correct predictor of the threat (i.e. footshock) as animals display conditioned fear when re-exposed to the context but not to the discrete tone<sup>21,22,23</sup>.

Conditioned fear to the context was assessed by measuring the percentage of total time spent freezing during the first 2 minutes period of context re-exposure. In order to assess conditioned fear to the tone, a freezing ratio was calculated as follow: [% freezing during the tone presentation – (% pre-tone period freezing + % post-tone period freezing)/2] / [% freezing during the tone presentation + (% pre-tone period freezing + % post-tone period

freezing)/2]. Two different observers performed the measurements independently and blinded of experimental groups (EAE, n=12 and CFA, n=12).

Slowing of information processing speed is frequent in multiple sclerosis<sup>24</sup> and can confound memory tests. Thus, we reasoned that EAE-mice could need more time than CFA-mice to process and memorize a new context independently of hippocampal dysfunction. To disentangle these phenomena, we designed a new experimental procedure where the conditioning period was longer: 130s into the chamber, first shock, 40s delay, first tone, 50s delay; second tone, 50s delay, second shock, 20s and back to the home cage. Tone, shock, context parameters and testing conditions were the same as described above (EAE, n=12 and CFA, n=12).

### ***Magnetic Resonance Imaging: acquisition and analyses***

The afternoon following contextual fear conditioning, the same animals underwent MRI exploration. Imaging was performed on a 4.7T scanner (Biospec 47/20, Bruker) equipped with a high-performance gradient system (capable of 660 mT/m maximum strength and 110 $\mu$ s rise time). A 86mm-diameter volume coil was used for radio frequency pulse transmission and a four-elements phased array surface coil for signal detection. Mice anesthetized with isoflurane in air (1-2% concentration to obtain a respiratory rate between 25/s and 35/s) were immobilized in a head holder with ear bars and their body temperature was kept at 37°C.

We first collected standard T2-weighted images to assess hippocampal volumetry. This was acquired using a fat-suppressed turbo spin echo axial sequence (Turbo-RARE, TR=4843ms, effective TE=66ms, matrix=196x196 pixels, FOV=20x16mm<sup>2</sup>, spatial resolution=102x82x300 $\mu$ m, 15 averages, 25 axial slices, scan time=14 minutes 32s).

To analyze microstructural changes in the three main hippocampal layers (i.e. the stratum radiatum, the stratum lacunosum-moleculare and the molecular layer of the dentate gyrus), we designed and optimized a new DTI pulse sequence based on a 3D-sampling of Fourier-space. Each of these hippocampal layers is about 200 $\mu$ m thick in the coronal plane, oriented perpendicular to the longitudinal axis of the dorsal hippocampus. We postulated that the in-plane resolution of the obtained diffusion-weighted images should be less than 100 $\mu$ m, to get at least 2 voxels per layer in the dorso-ventral axis. Because of little through-plane anatomical variation of the hippocampus in its dorsal part, we favored in-plane resolution with thicker

slices to recover enough signal (anisotropic voxel). Furthermore, we favored a high b-value in a high number of directions, to be more sensitive to restricted diffusion in a complex and heterogeneous structure such as the hippocampus<sup>25</sup>. We obtained the best tradeoff between signal-to-noise ratio, scan time, spatial resolution and b-value with a multi-shot echo-planar-imaging (EPI) pulse sequence as follow: TR=2000ms, TE=38ms, matrix=196x148, FOV=16x12mm<sup>2</sup>, 2 segments, spatial resolution=82x81x203μm, 32 coronal slices including the whole hippocampus in the rostro-caudal axis. Two images without diffusion weighting were acquired and 30 images with diffusion weighting ( $\Delta=10\text{ms}$ ,  $\delta=3\text{ms}$ , b-value 2000s/mm<sup>2</sup>) were collected in 30 different diffusion directions. All exams began with a higher order shim procedure to optimize first and second order shims based on a 3D field map acquired over the whole brain. The total acquisition time for in vivo DTI was 51 minutes 12s.

Images were post-processed off-line for volumetric analyses and extraction of diffusion metrics within each hippocampal layer. T2-weighted images were analyzed using the 3D-Slicer software (slicer.org). Hippocampal boundaries were manually traced on contiguous axial slices by an investigator blinded of the experimental conditions. Diffusion-weighted data were processed and analyzed using FMRIB Software Library (FSL, fmrib.ox.ac.uk). Eddy current distortions were firstly corrected and then, the diffusion tensor was calculated using mono-exponential diffusion tensor model. Color-coded fractional anisotropy (FA) maps were used to manually outline regions of interest (ROIs) in the stratum radiatum of CA1, stratum lacunosum-moleculare and molecular layer of the dentate gyrus, on 3 consecutive slices, within the dorsal part of the hippocampus (known to be the part of the hippocampus linked to memory processes<sup>26</sup>) (Fig. 2A and B). CA3 hippocampal subfield was not properly analyzed because of its rotation in the coronal plane that does not allow its clear individualization in color-coded FA maps. Right and left hippocampi were averaged because no difference was observed between the two sides. The mean FA, the mean eigenvalues ( $\lambda_1$ ,  $\lambda_2$ ,  $\lambda_3$ ) and the mean diffusivity within the ROIs were obtained using FSL and then, axial ( $\lambda_1$ ) and radial diffusivity ( $(\lambda_2 + \lambda_3)/2$ ) were calculated. The analysis was performed blinded of the animal groups (EAE, CFA, treatment) and all the measures were repeated twice, one month apart, with very good reproducibility (intra-class correlation coefficient was 0.80 for FA and 0.97 for axial diffusivity (AD)). The two measured values were averaged to perform further statistical analyses.

### ***Immunohistochemistry***

To allow MRI-histological correlations, animals were sacrificed immediately following MRI. Mice were deeply anesthetized with pentobarbital and perfused transcardially with a phosphate-buffered solution containing 2% paraformaldehyde and 0.2% picric acid, for 20 minutes. The brain and the spinal cord were then removed and transferred into a Tris-buffered saline (TBS) containing 30% sucrose and 0.05% sodium azide and left at 4°C until use. A 0.8mm block containing the dorsal hippocampus (*i.e.*; from approximately bregma -1.34 to bregma -2.14 in the Paxino's atlas) was cut using 30µm thick coronal sections on a freezing microtome. For direct comparison, both MRI and histological sections were perpendicular to the flat skull position.

For immunofluorescence, free-floating sections were rinsed in TBS and then incubated in a solution of 0.25% Triton X-100 and 1% normal donkey serum with the primary antiserum overnight. After incubation, tissue sections were washed in TBS and incubated with the appropriate secondary antibody solution (0.25% Triton X100) for 2 h. The following primary antibodies were used: rabbit anti-MBP for myelin (Myelin Basic Protein, ab 40390, Abcam, 1:1000), mouse anti-SMI-32 for dendrites (Neurofilament H non-phosphorylated, SMI-32R, Sternberger, Covance, 1:1500), rabbit anti-GFAP for astrocytes (Glial Fibrillary Acid Protein, Z0334, Dako, 1:1000), rabbit anti-Iba1 for microglia (Ionized calcium-binding Adaptor molecule 1, 019-19741, Wako, 1:2000), rabbit anti-CD3 for T lymphocytes (ab 5690, Abcam, 1:200), rat anti-ED1 for macrophages (anti-CD-68, MCA 1957, AbD Serotec, 1:200), goat anti-DCX for immature neurons (Doublecortin, sc-8066, Santa Cruz, 1:1000) and rabbit anti-active Caspase 3 for apoptosis (ab 13847, Abcam, 1:1000). The following secondary antibodies were used (donkey IgGs): anti-mouse Alexa Fluor-568 (ab 175472, Abcam, 1:1000), anti-rabbit Alexa Fluor 488 (711-545-152, Jackson Laboratories, 1:1000), anti-goat Cyanine 3 (705-165-003, Jackson Laboratories, 1:1000), anti-rat DyLight 488 (712-485-150, Jackson Laboratories, 1:500) and anti-rat Rhodamine Red-X (712-295-150, Jackson Laboratories, 1:500).

### ***Histological processing and NeuroLucida reconstruction***

Shortly after being processed, sections were imaged for quantitative analyses with a video-spinning-disk laser confocal microscope (Leica DMI 6000) equipped with a 20x objective and

with a camera Coolsnap HQ2 (Photometrics). These systems were driven by Metamorph software (Molecular Devices) and the “scan slide” technique was used in order to visualize and reconstruct the whole hippocampus (mosaic images) for layer analyses. Individual optical sections of 1 $\mu$ m were acquired and analyzed. Identical laser intensity and exposure settings were applied to all images taken for each experimental set. For all immunostaining experiments, at least 2 slices containing the dorsal hippocampus were randomly selected and quantitative results were averaged. Images were analyzed using ImageJ software (imagej.nih.gov). Similar ROIs as the ones used in MRI studies were manually drawn on the mosaic. Within the ROIs, the number of microglial cells (Iba1+/DAPI+), astrocytes (GFAP+/DAPI+) were counted manually and normalized by the size of the ROI. GFAP, Iba1, MBP and SMI-32 staining area were quantified automatically as percent area of immunoreactivity (after subtracting background and thresholding identically all the images for conversion to binary masks). The dendritic marker SMI-32 (non-phosphorylated neurofilament H) is widely used in multiple sclerosis and EAE pathological studies, including hippocampal exploration<sup>6</sup> and provides a sparse labeling of mature dendrites and perikarya in both pyramidal and granular neurons<sup>27</sup>, facilitating the analysis. Newborn neurons (DCX+/DAPI+) were counted manually within the subgranular and granular layer of the dentate gyrus (DCX+ perikarya with short processes parallel to the longest axis of the granular cell layer) and normalized by the size of the granular layer.

To provide further quantification of the dendritic arbor, the morphometric analyses of SMI-32+ neurons were performed with a 40x objective using a manual neuron tracing system (NeuroLucida, MBF Bioscience). Two neurons per animal (n=24 per condition) were analyzed within the molecular layer of the dentate gyrus and the stratum radiatum. Neurons were selected based on the standard following criteria: (i) the cell body should be contained in the slice, (ii) the dendrites should be vertically oriented within the molecular layer or the stratum radiatum, (iii) the overlap with the dendrites of the adjacent cells should be minimal, to avoid ambiguous tracing of the dendritic tree. The complexity of the dendritic trees was analyzed using the concentric analysis of Sholl (Neuroexplorer). For each neuron, the total dendritic length and the total number of intersections between dendrites and the surface of concentric spheres with a radius increment of 10 $\mu$ m were analyzed.

To detect apoptotic neurons, observation and quantification of Caspase-3+/SMI-32+ cell bodies were performed on epifluorescence microscope (Zeiss Axiophot 1) with a 40x objective. Because the occurrence of Caspase-3 expression was low, two to four hippocampal sections per animal were screened (n=36 per condition), in different focal planes, in the granular layer of the dentate gyrus and in the pyramidal layer of CA1. Only the occurrence of typical staining (with nuclear and cytoplasmic condensations) was taken into account for quantitative analyses.

To obtain illustrative images (SMI-32/Iba-1 and Caspase-3/SMI-32 co-stainings), a 63x-oil objective was used and z-stack acquisitions were performed on the station previously described.

### ***Laser capture microdissection (LCM) and quantitative real-time PCR (qPCR) analyses***

For RNA analyses other EAE and CFA mice were followed and their brains were quickly extracted, flash-frozen in a vial of isopentane that was immersed in dry ice and subsequently stored at  $-80^{\circ}\text{C}$  until sectioning. Brains were cut using  $50\mu\text{m}$  thick coronal sections on a freezing microtome (CM3050 S Leica) at  $-22^{\circ}\text{C}$  to prevent RNA degradation. Tissue sections were mounted on PEN-membrane 1 mm glass slides (P.A.L.M. Microlaser Technologies AG, Bernried, Germany) that had been pretreated to inactivate RNase. Frozen sections were fixed in a series of precooled ethanol baths (40s in 95%, 75% and 30s in 50%) and stained with cresyl violet 1% for 20s. Subsequently, sections were dehydrated in a series of precooled ethanol baths (30s in 50%, 75% and 40s in 95% and in anhydrous 100% twice). Immediately after dehydration LCM was performed with a P.A.L.M MicroBeam microdissection system version 4.0-1206 equipped with a P.A.L.M. RoboSoftware (P.A.L.M. Microlaser Technologies AG, Bernried, Germany). Laser power and duration were adjusted to optimize capture efficiency. Microdissection was performed at 5 $\times$  magnification. The molecular layer of the dentate gyrus and the stratum radiatum of the CA1 were selectively captured (see supplementary method A.1 for example) in adhesive caps (P.A.L.M Microlaser Technologies AG, Bernried, Germany). Following LCM,  $150\mu\text{l}$  of extraction buffer provided in a ReliaPrep™ RNA Cell Miniprep System (Promega) were added to the caps and stored at  $-80^{\circ}\text{C}$  until RNA isolation. Total RNA was extracted from microdissected tissues by using the ReliaPrep™ RNA Cell Miniprep System (Promega, Madison, USA) according to the manufacturer's protocol and eluted with  $14\mu\text{l}$  of

RNAse-free water. The concentration of RNA was determined with Nanodrop 1000. RNA qualities were performed using Agilent RNA 6000 Pico Kit on 2100 Bioanalyzer (Agilent Technologies, Santa Clara, CA).

RNA was processed and analyzed according to an adaptation of published methods<sup>28</sup>. Briefly, cDNA was synthesized from 75ng of total RNA for each structure by using qSript<sup>TM</sup> cDNA SuperMix (Quanta Biosciences). qPCR was performed with a LightCycler<sup>®</sup> 480 Real-Time PCR System (Roche, Meylan, France). qPCR reactions were done in duplicate for each sample by using LightCycler 480 SYBR Green I Master (Roche) in a final volume of 10 $\mu$ l. The qPCR data were exported and analyzed in an informatics tool (Gene Expression Analysis Software Environment) developed at our institute. The Genorm method was used to determine the reference gene<sup>28</sup>. Relative expression analysis was normalized against two reference genes. In particular, succinate dehydrogenase complex subunit (Sdha) and non-POU-domain-containing, octamer binding protein (Nono) were used as reference genes. To estimate the PCR amplification efficiency, standard curves were determined, and all the primers chosen were 100% efficient. The relative level of expression was calculated with the comparative ( $2^{-\Delta\Delta CT}$ ) method (n=4 to 10 animals per analyses). Primer sequences are reported in supplementary method A.2.

### ***Electrophysiology: slice preparation and extracellular recordings***

Sagittal hippocampal slices (350  $\mu$ m) were carried out from additional EAE and CFA-mice at 18 to 22 d.p.i. Mice were deeply anesthetized with isoflurane and then decapitated. Brains were rapidly removed and chilled in an ice-cold carbogenated (*i.e.* bubbled with 95% O<sub>2</sub> and 5% CO<sub>2</sub>) cutting solution containing (in mM): 120 Choline-Cl, 1.25 NaH<sub>2</sub>PO<sub>4</sub>, 17 glucose, 3 KCl, 1.3 MgCl<sub>2</sub> and 26 NaHCO<sub>3</sub>. Sagittal slices were cut from a block of tissue using a vibratome (Microm HM650V) and then incubated in artificial cerebrospinal fluid (aCSF) 20 minutes at 32°C and then 1h at room temperature. Artificial CSF was saturated with 95% O<sub>2</sub> and 5% CO<sub>2</sub> and contained (in mM): 125 NaCl, 1.25 NaH<sub>2</sub>PO<sub>4</sub>, 5 glucose, 2.5 KCl, 2 CaCl<sub>2</sub>, 1.3 MgCl<sub>2</sub>, and 26 NaHCO<sub>3</sub>.

Slices were individually transferred to a submerged recording chamber and continuously perfused (2.5–3.5 mL/min) with carbogenated and warm (30–32°C) aCSF containing 100  $\mu$ M picrotoxin (Tocris). Field excitatory post-synaptic potentials (fEPSPs) were recorded using a

glass pipette (2.5–4.9 M $\Omega$ ) filled with aCSF and placed in the molecular layer of the dentate gyrus or in the stratum radiatum of the CA1 region. The medial perforant pathway (MPP) in the dentate gyrus or the Schaffer collaterals in the CA1 region were stimulated using a glass electrode placed at 200 $\mu$ m away from the recording pipette (Fig. 4 A and D). MPP stimulation was corroborated by observing paired-pulse depression at 50 ms interpulse intervals. Basal glutamatergic synaptic transmission, evoked at 0.033Hz, was examined by generating input/output relationships. For long-term potentiation (LTP) experiments, the stimulation intensity was set to the one producing 35-40% of maximum fEPSP slopes. Then, LTP was induced by applying a high frequency stimulation (HFS) protocol consisting of: 100Hz trains of stimuli for 1s repeated at 20s interval 2 times at CA3-CA1 synapses and 4 times at MPP-DG synapses. After HFS, fEPSPs were recorded during additional 60 minutes. fEPSP slopes were measured and normalized to the mean of the last 10 minutes of the baseline. Recordings were obtained using an Axon Multiclamp 700B amplifier (Molecular Devices). Signals were filtered at 2 kHz, digitized at 20 kHz, and analyzed using Axon Clampfit software (Molecular Devices).

### ***Systemic injection of minocycline***

Minocycline hydrochloride (Sigma) was used as a potent microglial inhibitor<sup>29</sup>. Minocycline was dissolved few minutes before injections in sterile isotonic PBS and administrated every 24h by intra-peritoneal (IP) injections at a dosage of 50mg/kg. EAE mice (EAE-MINO, n=15) were treated from 7 d.p.i (the beginning of the motor symptoms) to 20 d.p.i. A placebo group (EAE-PBS, n=15) received daily IP injections of PBS. The EAE score was evaluated daily by investigators blinded of the experimental conditions.

### ***Surgical procedures and intra-hippocampal infusions of minocycline***

To determine if the selective inhibition of microglial activation in the dentate gyrus was sufficient to prevent memory impairment in EAE-mice, we performed chronic local infusions of minocycline in different hippocampal subfields. Surgery and intra-hippocampal infusions were performed as described previously<sup>23</sup>. Briefly, mice were anesthetized with isoflurane (2%) and secured in a Kopf stereotactic apparatus. For every mouse, stainless-steel guide cannulae (26 gauge, 8mm length) were implanted bilaterally above the dorsal hippocampus (anteroposterior: -2mm, mediolateral: +1.3mm, dorsoventral: 0.8mm; relative to dura and bregma) and then fixed to the skull with dental cement. Mice were then allowed to recover 2

to 3 days in their home cage before EAE induction (*i.e.* 3 weeks before behavioural experiments).

EAE-mice received every day intra-dentate gyrus or intra-CA1 bilateral infusions of minocycline (500µg/mL, diluted in sterile PBS) or PBS alone from 7 d.p.i to 20 d.p.i. (EAE-MINO-DG, n=17; EAE-MINO-CA1, n=15 and EAE-MINO-PBS, n=14; Fig. 7A and B). For infusions, the stylets normally protruding the guide cannulae were removed. Stainless-steel cannulae (32 gauge) attached to 1µL Hamilton syringes with catheter tubing were inserted through the guide cannulae. Cannulae had different lengths regarding the targeted subfield and infusions were performed 1.8mm under the dura for CA1 and 2.6mm for dentate gyrus. The syringes were fixed in a constant rate infusion pump. After preliminary experiments using Pontamine blue dye (Fig. 7A and B), we determined that a volume of 0.2 µL (per side) injected at 0.1 µL/min was optimum to allow a specific and local diffusion of drug within dorsal CA1 or dentate gyrus (Fig. 7A and B). The cannulae were left in place for an additional 90 seconds before removal to allow diffusion of the drug away from the tips.

### **Statistical analyses**

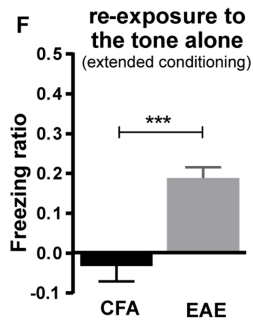
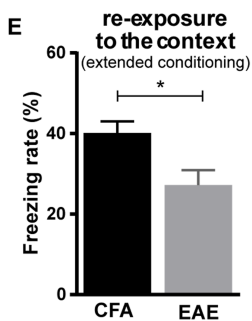
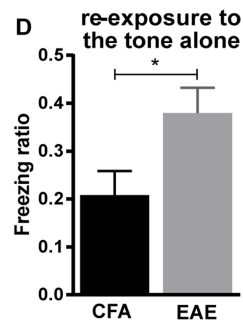
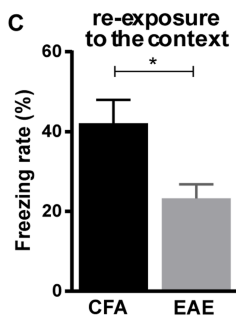
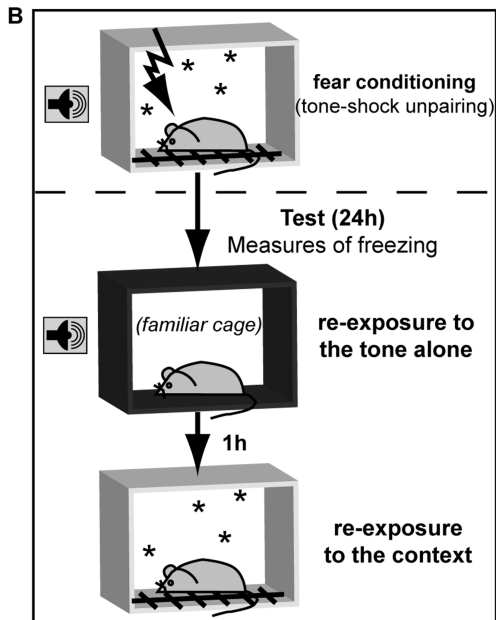
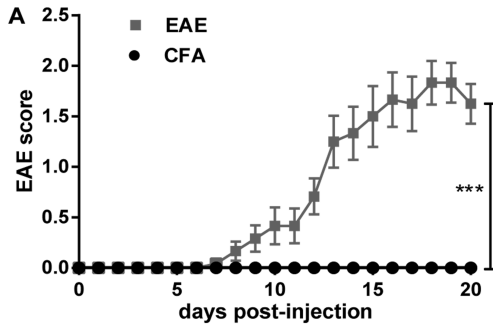
Data are presented as the mean ±SEM. The Gaussian distribution was tested with Shapiro-Wilk normality test. Clinical scores and input/output curves were analyzed with two-way ANOVA. Behavioral, MRI, histological and electrophysiological quantitative data were compared between groups using ANOVA when more than two groups were compared (and Tukey's multiple comparisons test for *post hoc* multiple comparisons) or unpaired t-tests (or Mann-Whitney tests) when two groups were compared (except for quantification of Caspase-3 staining where a Fisher's exact test was used). In order to perform MRI-histological correlation, we used Pearson's correlations for univariate analyses and then multiple linear regressions to model the relationship between MRI data (dependent variables) and histological data (independent variables). Statistical analyses were performed with Prism 6.0 (GraphPad). A p-value<0.05 was deemed significant.

## Results

### ***EAE-mice presented an early hippocampal-dependent memory deficit***

Twenty days post-immunisation (d.p.i), EAE-mice were experiencing first clinical expression of motor symptoms but were all still ambulatory with a mean clinical score of  $1.6 \pm 0.20$  (Fig. 1A). To assess hippocampal long-term memory we used a dedicated contextual fear conditioning procedure (Fig. 1B). EAE-mice displayed significantly less conditioned freezing than control CFA-mice, when they were re-exposed to the predictive context (freezing rate: 23.3% vs 42.1%,  $p=0.011$ , Fig. 1C and Fig. A.1A). This suggests that the functional integrity of the hippocampus was impaired because mice showed a deficit in the identification of the environment in which they previously received footshocks as predictor of the threat. Moreover, the same EAE-mice displayed significantly more freezing than CFA-mice when they were re-exposed to the tone alone (which was not the relevant predictor of the threat), in a safe and familiar environment (freezing ratio: 0.380 vs 0.208,  $p=0.028$ , Fig. 1D and Fig. A.1B).

*Figure 1: Clinical and memory-related behavioral data of mice with experimental autoimmune encephalomyelitis (EAE) and control mice (CFA). (A) Motor signs began 7 days post-injection (d.p.i) and were moderately severe at 20 d.p.i. when mice were tested for memory performances (\*\* $p<0.001$ ,  $F=41.61$ , two-way ANOVA,  $n=12$  per group). (B) Schematic representation of the contextual fear conditioning paradigm: because the discrete tone and the footshock are pseudo-randomly distributed (tone-footshock unpairing), the background context is the only predictive factor of the footshock occurrence. Acquisition of an adaptive conditioned fear to the context is attested 24h later when mice are re-exposed to the discrete tone alone in a familiar context, then to the conditioning context alone. (C) EAE-mice displayed less conditioned freezing to the predictive conditioning context than CFA-mice. (D) However, EAE-mice exhibited a paradoxical and maladaptive freezing behavior to the tone when re-exposed to it in a familiar and safe box. (E and F) The same differences between groups were observed even if time exposure to the context was extended by 40%. (\* $p<0.05$  and \*\*\* $p<0.001$ , t-test,  $n=12$  per group).*



This paradoxical fear response to the tone first demonstrates that EAE-mice can freeze and even display higher conditioned fear than CFA-mice to some irrelevant cues, excluding potential bias linked to sensory or motor symptoms that would have hindered EAE-mice to feel shock or to display freezing. Second, this maladaptive fear response to the tone attests of an altered hippocampal-amygdala interaction to the detriment of the hippocampal function in EAE-mice. Indeed, such amygdala-dependent elemental conditioning to the most salient and simple cue (the tone) has been previously repeatedly shown when the hippocampal-dependent processing of more complex contextual information was impaired<sup>21,22,23</sup>.

To definitely validate that the inability of EAE-mice to identify the complex predicting context was due to a proper hippocampal-dependent memory deficit and not to slowing of information processing speed, two other groups of EAE and CFA-mice were tested after an extended (+40%) conditioning period. As in the first experiment, EAE-mice displayed less conditioned freezing to the predictive conditioning context than CFA-mice (freezing rate: 27.2% vs 40.1%,  $p=0.012$ , Fig. 1E). EAE-mice also showed the same paradoxical fear response to the tone, even though the freezing ratio was less pronounced than with the shorter time exposure to the conditioning context (freezing ratio: 0.189 vs -0.033,  $p<0.001$ , Fig. 1F). This lower freezing ratio in both groups can be explained by the higher temporal distance between the tone and the shock in the extended fear conditioning paradigm, which might facilitate the processing of the tone as a non-predictive cue.

Taken together, these behavioral data indicate that a hippocampal-dependent memory deficit occurs early in the course of EAE.

### ***Hippocampal structural changes in EAE-mice***

Because we wanted to assess early cellular alteration occurring prior to irreversible atrophy, we first confirmed using *in vivo* MRI that the hippocampal volumes were not changed at this early time point. From T2-weighted images (Fig. A.2A), hippocampal volumetry (Fig. A.2B) showed no difference between EAE and CFA-mice at 20 d.p.i. ( $20.58\text{mm}^3$  vs  $20.67\text{mm}^3$ ,  $p=0.90$ , Fig. A.2C).

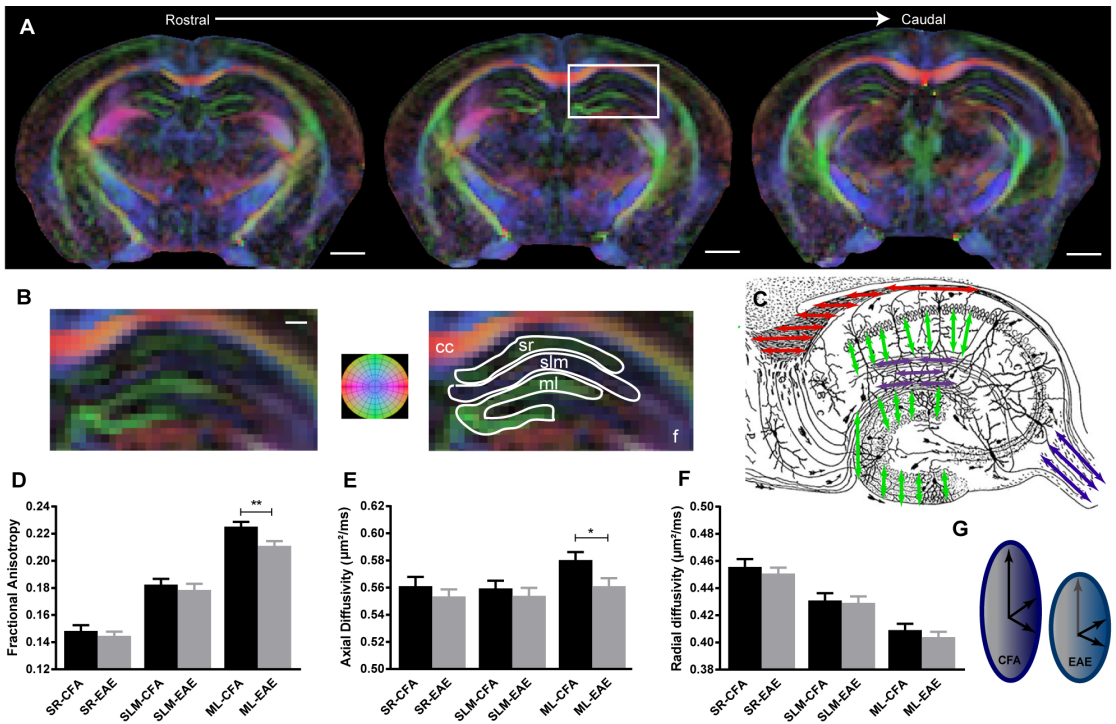


**Fig. 2: Diffusion-tensor imaging (DTI) of hippocampal layers revealed microstructural damages specific to the molecular layer of the dentate gyrus.** (A) Color-coded fractional anisotropy (FA) maps were used to draw 3 regions of interest (ROIs) within the hippocampus. The dorsal part of the right and left hippocampi were analyzed in three adjacent slices for each animal, along the rostral-caudal axis. (B) Magnification of the white box in (A) with the 3 ROIs overlaid in white. Directions for color-coding: blue, rostral-caudal; red, left-right; and green, dorsal-ventral. (C) Drawing adapted from Ramon y Cajal (1911) representing the orientation of the fibers within the different layers of the hippocampus and corroborating the color-coded FA map. (D-F) Quantification of FA, axial diffusivity (AD) and radial diffusivity in the three different ROIs for both EAE and CFA-mice. (G) Schematic representation of the tensor in the molecular layer of CFA and EAE-mice: diffusion directionality is decreased in EAE (lower FA) because of a loss of directivity in the main axis (lower AD). SR: stratum radiatum of CA1, SLM: stratum lacunosum-moleculare, ML: molecular layer of the dentate gyrus, cc: corpus callosum and f: fimbria. (\* $p < 0.05$ , \*\* $p < 0.01$ , t-test,  $n = 12$  animals per group). Scale bar: 1mm (A) and 200 $\mu\text{m}$  (B).

To screen for early regional vulnerability in the hippocampus of EAE-mice, we then used a cutting-edge high-resolution *in vivo* DTI sequence that we have optimized to allow quantifying the microscopic displacement of water within the three main hippocampal layers (Fig. 2A). Because water diffuses preferentially along the long axis of the fibers, the CA1 stratum-radiatum, the stratum-lacunosum moleculare and the molecular layer of the dentate gyrus whose fibers are perpendicularly oriented were well identified on the color-coded orientation map of the tensor (Fig. 2B, C). Quantitative measurement showed that fractional anisotropy (FA), was specifically decreased in the molecular layer of the dentate gyrus in EAE compared to CFA-mice (0.211 vs 0.225,  $p=0.0093$ , Fig. 2D) while FA was not significantly modified in the other layers (Fig. 2D). Such decrease of FA in the molecular layer of EAE mice was driven by a decrease of axial diffusivity (AD) ( $0.561$  vs  $0.580\mu\text{m}^2/\text{ms}$ ,  $p=0.030$ , Fig. 2E), while radial diffusivity (Fig. 2F) and mean diffusivity were not significantly changed (respectively  $0.404$  vs  $0.407\mu\text{m}^2/\text{ms}$ ,  $p=0.51$  and  $0.456$  vs  $0.465\mu\text{m}^2/\text{ms}$ ,  $p=0.18$ ). Finally, diffusivity parameters were not modified within the fimbria, which is the main myelinated output of the hippocampus. Taken together, these MRI experiments showed that prior to hippocampal atrophy, there was a selective decrease of the FA and AD in the molecular layer of the dentate gyrus.

#### ***Selective neurodegenerative process in the dentate gyrus of EAE-mice***

Because a significant decrease of axial diffusivity is usually associated with neuritic damage<sup>30</sup>, we first looked for potential early neuronal loss in the dentate gyrus of EAE-mice. Analysis of the dendritic marker SMI-32 revealed a dramatic decrease of the staining in the molecular layer of the dentate gyrus in EAE compared to CFA-mice (42% decrease in immunostained surface area,  $p=0.0076$ , Fig. 3A and B). Interestingly the dendrites of the pyramidal neurons in the stratum radiatum were relatively preserved (the stratum-lacunosum moleculare contains thin axons from the perforant path and was not stained by SMI-32). In the molecular layer of the dentate gyrus, SMI-32 staining was correlated with both fractional anisotropy ( $r=0.56$ ,  $p=0.0051$ , Fig. 3C) and axial diffusivity ( $r=0.47$ ,  $p=0.024$ ).

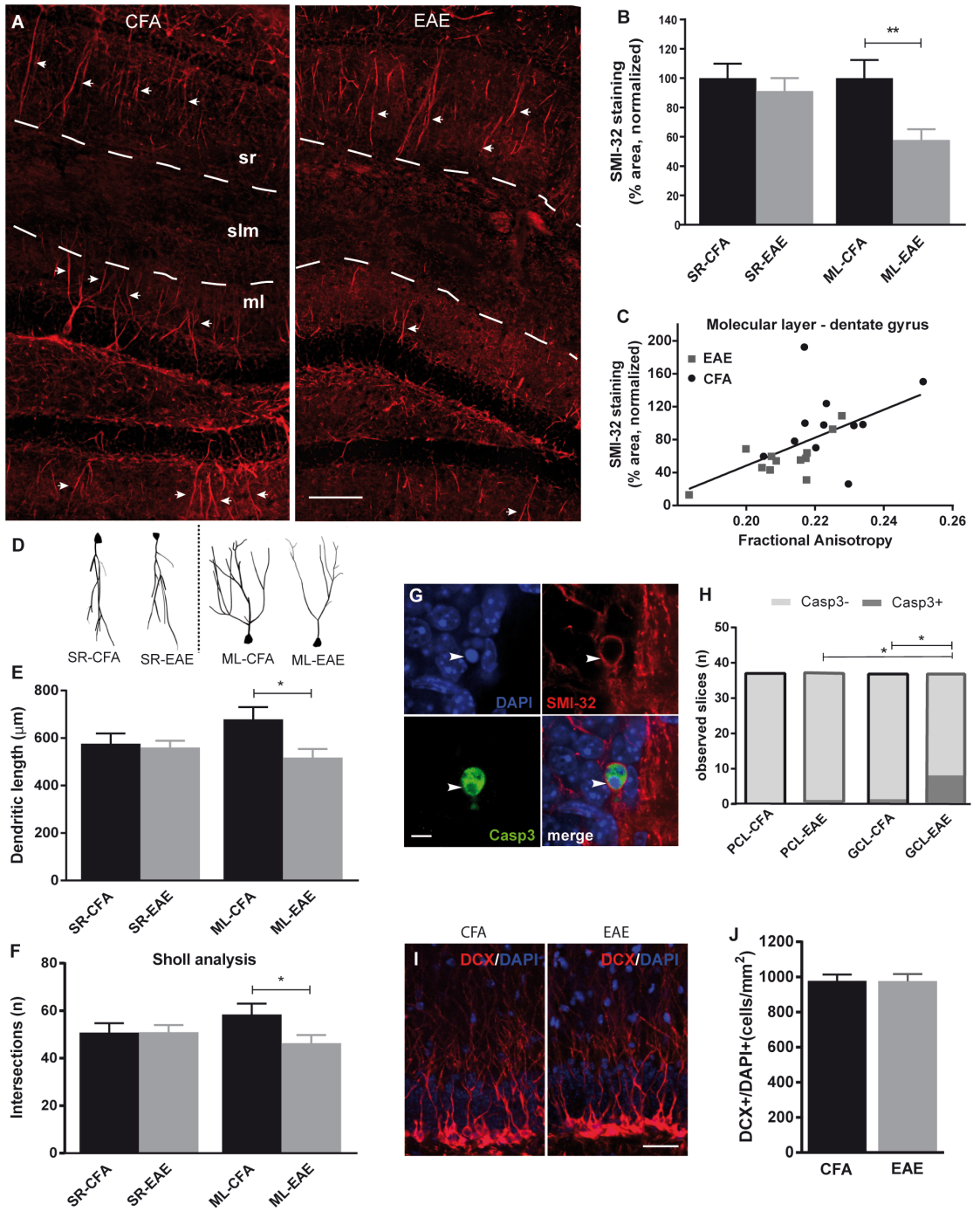


*Fig. 3: Selective dendritic loss and neuronal death in the dentate gyrus of EAE-mice. (A) Immunofluorescence staining for the dendritic marker SMI-32; white arrowheads show dendrites in the different layers. (B) Quantification of SMI-32 staining area in the stratum radiatum (SR) and the molecular layer (ML) in EAE and CFA-mice (\*\* $p < 0.01$ , t-test,  $n = 12$  per group). The stratum lacunosum-moleculare (SLM) contains thin axons of the perforant path, which are not stained by SMI-32. (C) Correlation between SMI-32 staining and fractional anisotropy in the molecular layer of the dentate gyrus ( $r = 0.56$ ,  $p = 0.0051$ , Pearson). (D-F) Neurolucida neuron tracing analyses with (E) quantification of the total dendritic length per neuron and (F) the number of intersections between dendrites and the surface of spheres with a radius increment of  $10\mu\text{m}$  ( $*p < 0.05$ , t-test,  $n = 24$  neurons per condition, from 12 animals) (see also Fig. A.3). Representative tracing of apical dendrites are shown in (D): dendrites from pyramidal cells of the pyramidal layer of CA1 and dendrites from the granular cells of the dentate gyrus. (G) Illustration of an apoptotic neuron in the granular layer of the dentate gyrus with nuclear (DAPI) and cytoplasmic (SMI-32) condensations (arrowheads), together with an intense activated-caspase 3 staining. (H) Contingency of Caspase 3+ neurons in the granular cell layer (GCL) of the dentate gyrus and the pyramidal cell layer (PCL) of CA1 was reported to the number of observed slices ( $*p < 0.05$ , Fischer's exact test,  $n = 36$  per condition). (I) Immunofluorescence staining for doublecortin (DCX), a marker of immature neurons. (J) DCX/DAPI cell counting did not show any difference between EAE and CFA-mice ( $n = 12$  per group).*

To better characterize this first evidence of selective vulnerability of the dentate gyrus, we performed neuromorphometric analyses of the granular neurons of the dentate gyrus, whose dendrites project in the molecular layer, and of CA1 pyramidal neurons, whose dendrites project in the stratum radiatum. Under our sampling conditions, there was no significant morphological difference between EAE and CFA-mice regarding the dendrites of CA1 pyramidal neurons in the stratum radiatum (Fig. 3D, E, F and Fig. A.3. A, B). However, the total dendritic length and the complexity of the dendritic arbor were decreased in the granular neurons of EAE-mice compared to CFA-animals (respectively  $517\mu\text{m}$  vs  $679\mu\text{m}$ ,  $p = 0.014$  and  $46.4$  vs  $58.5$  intersections,  $p = 0.039$ , Fig. 3D, E, F and Fig. A.3. C, D). These data demonstrate a selective neuritic degeneration in the molecular layer of the dentate gyrus. Thus, we decided to look at neuronal apoptosis in the granular cell layer of the dentate gyrus and the pyramidal cell layer of CA1 using activated Caspase-3 staining (Fig. 3G). The occurrence of Caspase-3 positive neurons in the dentate gyrus was significantly higher in slices obtained from EAE-mice compared to CFA-animals (8 neurons of 36 slices vs 1 neuron of 36 slices,  $p = 0.028$ , Fig. 3H). Such increase in Caspase-3 positive neurons in the dentate gyrus was not observed in the pyramidal cell layer of EAE-mice. These results further strengthen the hypothesis of a selective

neurodegenerative process that takes place at an early stage of the disease in the dentate gyrus and that is characterized by both dendritic loss and neuronal death (even though an alternative explanation could be an impaired phagocytosis of apoptotic cells rather than a decreased survival<sup>31</sup>).

Because one specific property of the dentate gyrus is its ability to produce newborn neurons throughout adulthood, we also analyzed doublecortin (DCX) immature neurons (less than 4 weeks old neuroblasts) in the sub-granular zone of EAE and CFA-mice (Fig. 3I). There was no significant difference between the two groups after DCX/DAPI cells counting (Fig. 3J) as previously reported at this early time point<sup>32</sup> even though these data do not preclude more subtle abnormalities in radial-glia cells for example.

Taken together, histological analyses are thus in agreement with our DTI results, thereby confirming the selective vulnerability of the dentate gyrus at this early stage of EAE.

#### ***Impaired excitatory synaptic transmission in the dentate gyrus of EAE-mice.***

To investigate functional consequences of this neurodegenerative process specifically in the dentate gyrus at this early stage of EAE, we analyzed excitatory glutamatergic synaptic transmission at two different synapses in acute hippocampal slice preparations. We first investigated excitatory synaptic transmission at synapses formed by the medial perforant path (MPP, axons coming from the entorhinal cortex) and the dendrites of dentate granule cells in the molecular layer of the dentate gyrus (Fig. 4A). To this end, fEPSPs were evoked at different stimulation intensities to assess the input/output (I/O) relationship at these synapses. Interestingly, fEPSPs slope were significantly lower in EAE-mice in comparison to CFA-mice ( $F=17.18$ ,  $p=0.0006$ , Fig. 4B). We then investigated the I/O relationship at CA3-CA1 excitatory synapses and no impairment was detected in EAE mice (Fig. 4D and E).

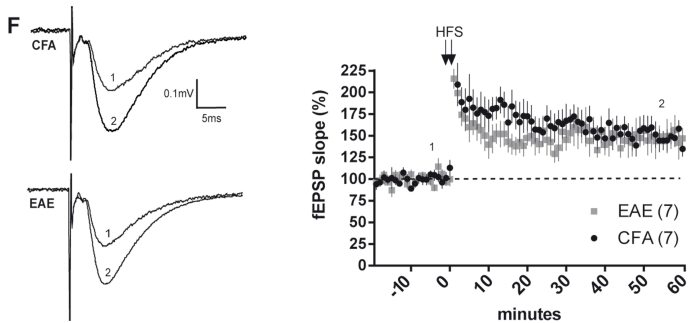
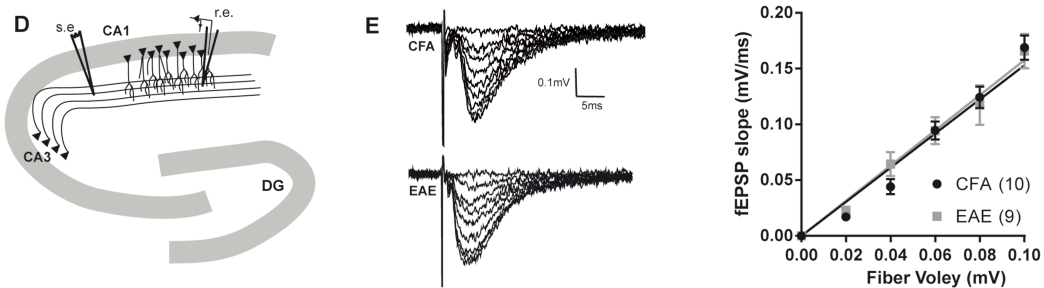
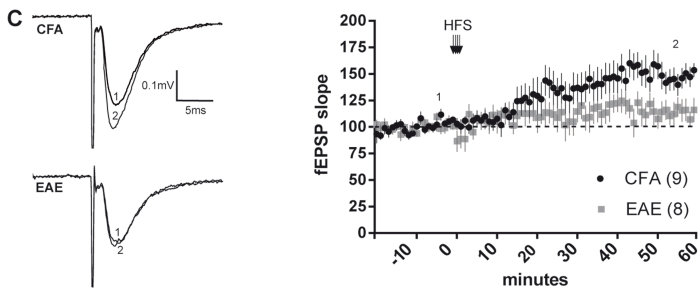
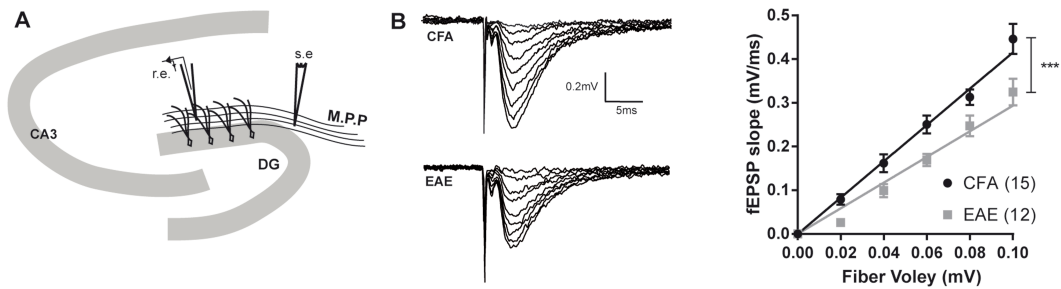


*Fig. 4: Excitatory synaptic transmission and long term potentiation are decreased in the dentate gyrus but not in the CA1 area. (A and D) Schematic representation of hippocampal circuits and position of the recording and stimulating electrodes (respectively r.e. and s.e.) at the medial perforant pathway (MPP) – dentate gyrus (DG) synapses (A) and the CA3-CA1 synapses (D). (B and E) (Left) Representative traces illustrating field excitatory post-synaptic potentials (fEPSPs) obtained in response to increasing stimulus intensity at the MPP-DG synapses (B) and at the CA3-CA1 synapses (E) and (Right) input/output relationship for EAE and CFA-mice at the MPP-DG synapses (EAE, n=15 and CFA, n=12 slices, \*\*\*p<0.001, two-way ANOVA, (B)) and at the CA3-CA1 synapses (EAE, n=10 and CFA, n=9, (E)). (C and F) (Left) Representative traces before and after LTP induction at the MPP-DG synapses (C) and at the CA3-CA1 synapses (F) (1: last 10 minutes of the baseline and 2: 60 minutes after HFS), (Middle) summary plot of the average time course of fEPSP slope (% of baseline) in response to HFS and (Right) histogram summarizing LTP amplitude at 60 minutes after HFS compared to the last 10 minutes of the baseline in EAE and CFA-mice at the MPP-DG synapses (EAE, n=9 and CFA, n=8 slices, \*\*p<0.01, Mann-Whitney test, (C)) and at the CA3-CA1 synapses (EAE, n=7 and CFA, n=7, (F)).*

These results confirm the selective vulnerability of the dentate gyrus to early pathophysiological processes in EAE. Indeed, the decreased basal synaptic excitatory transmission recorded at the MPP-DG synapses probably results from synaptic loss that is likely to be associated with the dendritic loss observed with DTI and histological methods.

***Decreased synaptic plasticity in the dentate gyrus of EAE-mice.***

We then tested whether LTP of hippocampal excitatory synaptic transmission, a process known as the cellular substrate of episodic memory<sup>33</sup>, was affected in EAE-mice and whether it could be synapse specific. LTP was elicited with a high-frequency stimulation (HFS) protocol of the MPP or the Schaffer collateral pathway and recorded in the molecular layer of the dentate gyrus or in CA1 stratum radiatum respectively. Importantly, there was a strong decrease in the level of LTP at the MPP-DG synapses in EAE compared to CFA-mice (110.2% vs 143.5%, p=0.001, Fig. 4C) whereas LTP was not impaired at the CA3-CA1 synapses (146.8% in EAE-mice vs 145.5% in CFA-mice, p=0.87, Fig. 4F). These results indicate that in the dentate gyrus of EAE-mice, on top of synaptic loss, the remaining synapses exhibit impaired plasticity properties.

### ***Differential microglial activation in the dentate gyrus of EAE-mice***

Because EAE potentially impacts all glial cells during the course of the disease and because all glial cell dysfunctions potentially impact neuronal function and survival<sup>34</sup>, we investigated possible myelin, astrocytic and microglial alterations in the hippocampus of EAE-mice. Myelin staining with MBP did not show any demyelinating area in the hippocampus, even after quantitative analysis (Fig. A.4A and C). There was also neither obvious difference in astrocyte morphology after the analysis of GFAP staining area nor increase of astrocyte number after GFAP/DAPI cell counting (Fig. A.4B and D) in none of the hippocampal layers. ED1(CD68) and CD3 staining revealed the absence of macrophages and T lymphocytes infiltration in the hippocampus of EAE-mice whereas these markers were detected in typical demyelinating lesions in the spinal cord (Fig. A.5), as classically reported at this stage of the disease<sup>10</sup>.

Microglial cells exhibited morphological changes including larger cell bodies, thicker processes (Fig. 5A) and higher percentage of staining area after quantitative analyses in both the stratum radiatum (respectively 7.24% for EAE-mice vs 3.95% for CFA-mice,  $p=0.011$ ) and in the molecular layer of the dentate gyrus (7.25% vs 3.57%,  $p=0.007$ ). We also found microglial proliferation in EAE-mice (50-70% increase after Iba-1/DAPI cell counting) in both the stratum radiatum (150.4 vs 101.6 cells/mm<sup>2</sup>,  $p=0.0004$ ) and the molecular layer of the dentate gyrus (165.3 vs 96.6 cells/mm<sup>2</sup>,  $p<0.0001$ ) (Fig. 5B). As morphological analyses show diffuse microglial proliferation in the whole hippocampus (although slightly higher in the dentate gyrus), we decided to look at mRNA expression profile in hippocampal sub-regions. Interestingly, mRNA expression level of microglial markers such as Iba-1 and ED1(CD68) was significantly increased in the molecular layer of the dentate gyrus of EAE-mice (1.64 in ML-EAE vs 1.00 in ML-CFA for Iba1,  $p=0.013$  and 1.55 in ML-EAE vs 1.01 in ML-CFA for ED1(CD68),  $p=0.012$ , Fig. 5C and E) but not significantly in CA1. Furthermore, mRNA overexpression of CD11b was higher in the molecular layer of the dentate gyrus than in the stratum radiatum of CA1 (1.94 in ML-EAE vs 1.02 in ML-CFA  $p=0.0030$  and 1.56 in SR-EAE vs 1.02 in SR-CFA,  $p=0.038$ , Fig. 5D).

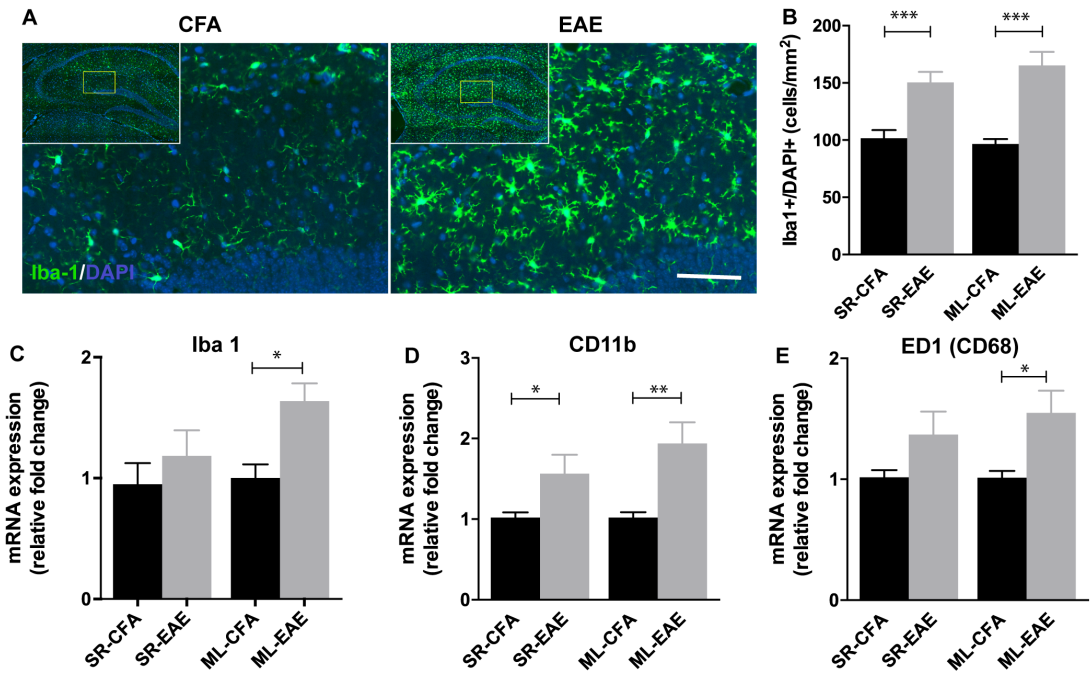


Fig. 5: Excitatory synaptic transmission and long term potentiation are decreased in the dentate gyrus but not in the CA1 area. (A and D) Schematic representation of hippocampal circuits and position of the recording and stimulating electrodes (respectively r.e. and s.e.) at the medial perforant pathway (MPP) – dentate gyrus (DG) synapses (A) and the CA3-CA1 synapses (D). (B and E) (Left) Representative traces illustrating field excitatory post-synaptic potentials (fEPSPs) obtained in response to increasing stimulus intensity at the MPP-DG synapses (B) and at the CA3-CA1 synapses (E) and (Right) input/output relationship for EAE and CFA-mice at the MPP-DG synapses (EAE,  $n=15$  and CFA,  $n=12$  slices,  $***p<0.001$ , two-way ANOVA, (B)) and at the CA3-CA1 synapses (EAE,  $n=10$  and CFA,  $n=9$ , (E)). (C and F) (Left) Representative traces before and after LTP induction at the MPP-DG synapses (C) and at the CA3-CA1 synapses (F) (1: last 10 minutes of the baseline and 2: 60 minutes after HFS), (Middle) summary plot of the average time course of fEPSP slope (% of baseline) in response to HFS and (Right) histogram summarizing LTP amplitude at 60 minutes after HFS compared to the last 10 minutes of the baseline in EAE and CFA-mice at the MPP-DG synapses (EAE,  $n=9$  and CFA,  $n=8$  slices,  $**p<0.01$ , Mann-Whitney test, (C)) and at the CA3-CA1 synapses (EAE,  $n=7$  and CFA,  $n=7$ , (F)).

To test whether such microglial activation is one of the biological substrates of DTI abnormalities observed in the hippocampus of EAE-mice (Fig. 2), we further looked for MRI-histological correlations. None of these glial alterations were sufficient by themselves to contribute independently to the signal measured *in vivo* with DTI. After a backward stepwise selection of all the histological metrics, the final model of MR-to-histology correlation amounted to a univariate relationship between FA/AD and dendritic loss ( $r^2 = 0.32$ ,  $p=0.0051$  and  $r^2 = 0.22$ ,  $p=0.024$  respectively, table A.1).

### ***Systemic inhibition of microglial activation prevented anatomical, electrophysiological and behavioral abnormalities***

The transcriptional profile of microglial markers in the molecular layer of the dentate gyrus, together with the selective neurodegeneration observed in this hippocampal subfield suggest a link between this 2 processes. Furthermore, the co-staining of Iba-1 and SMI-32 in the molecular layer of the dentate gyrus of EAE-mice revealed that microglia extended processes around dendrites and that microglial cell bodies were appended on swelling neurites, suggesting that these cells could induce the neurodegeneration described above (Fig. 6A). To test this hypothesis, we used minocycline, a well-known inhibitor of microglial activation<sup>35</sup>. Two groups of EAE-mice were treated daily with minocycline (EAE-MINO, 50mg/kg) or saline injection (EAE-PBS) after the onset of the motor symptoms (7 d.p.i).

Minocycline treatment significantly reduced motor symptoms in EAE-mice with an early stabilization of the neurological deficit ( $F=5.27$ ,  $p=0.029$ , Fig. 6B), as previously described<sup>36</sup>. As expected, on histological analyses, microglial proliferation was partially suppressed in EAE-MINO compared to EAE-PBS mice (147.8 vs 179.7 cells/mm<sup>2</sup>,  $p=0.019$ , Fig. 6C and Fig. A.6A and B). As a consequence, neurofilament staining was preserved in the molecular layer of EAE-MINO mice compared to EAE-PBS (35% increase,  $p=0.017$ , Fig. 6D and Fig. A.6C and D). Neuron tracing analyses (Fig A.6E and F) confirmed that dendritic length was higher in EAE-MINO mice than in EAE-PBS mice (784.8 $\mu$ m vs 616.5 $\mu$ m,  $p=0.0009$ , Fig. 6E) and that dendritic arbor complexity was also higher in EAE-MINO mice (68.8 vs 54.4 intersections,  $p=0.0022$ , Fig. 6F).

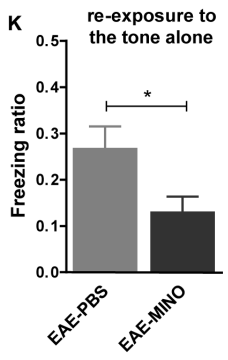
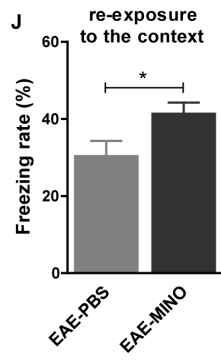
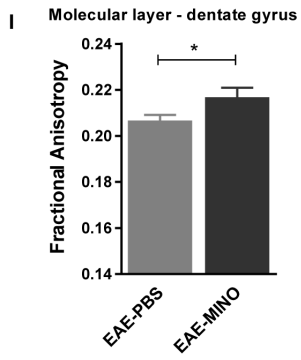
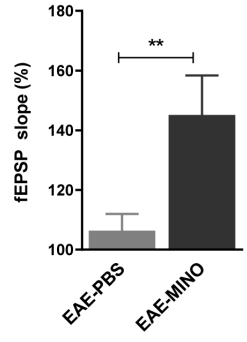
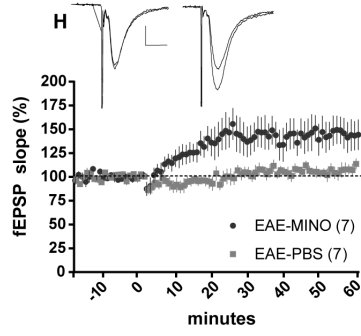
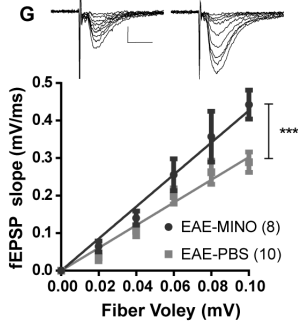
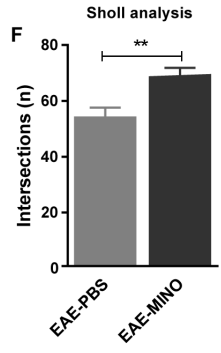
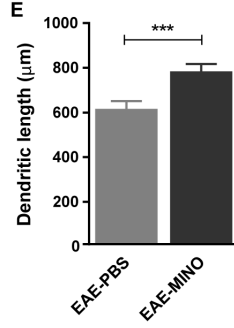
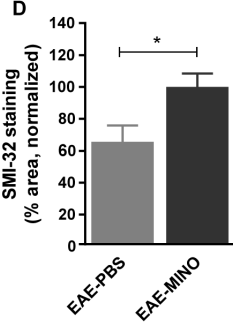
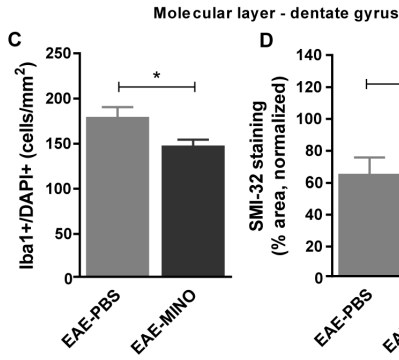
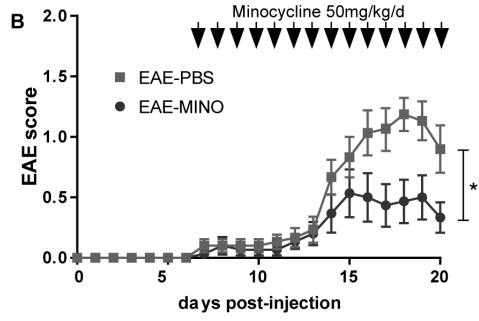
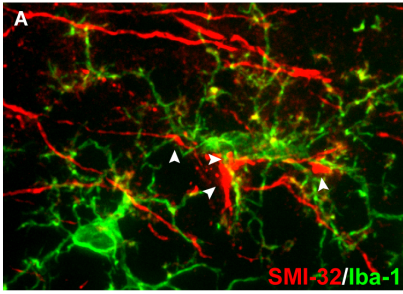


*Fig. 6: The inhibition of microglial activation with minocycline treatment prevented dentate gyrus neurodegeneration, DTI changes and memory impairment in EAE-mice. (A) Z-stack projection of confocal images from the molecular layer of an EAE-PBS mouse showing activated microglial cells (Iba1, large cell body and thick arms) in contact with swelling and degenerative dendrites (SMI-32, arrowheads). (B) EAE-mice received daily injections of minocycline (50mg/kg, n=15) or placebo (PBS, n=15) from 7 d.p.i. to sacrifice (vertical arrows). Treatment with minocycline decreased the clinical severity of EAE regarding the motor EAE-score (\* $p < 0.05$ , two-way ANOVA). (C-D) Histological analyses showed that there were less microglial cells but more dendrites in the molecular layer of minocycline-treated EAE-mice (EAE-MINO) compared to placebo-treated animals (EAE-PBS) (n=15 per group, \* $p < 0.05$ , t-test). (E-F) NeuroLucida neuron tracing analyses confirmed that the dendritic arbor of EAE-MINO mice were preserved compared to EAE-PBS mice (n=30 neurons per condition, from 15 animals, \* $p < 0.01$ , \*\*\* $p < 0.001$ , t-test). (G) (Upper) Representative traces illustrating field excitatory post-synaptic potentials (fEPSPs) obtained in response to increasing stimulus intensity at the MPP-DG synapses and (Lower) input/output relationship for EAE-MINO and EAE-PBS (n=8 and n=10 slices respectively, \*\*\* $p < 0.001$ , two-way ANOVA). (H) (Left) Representative traces before and after LTP induction at the MPP-DG synapses and summary plot of the average time course of fEPSP slope (% of baseline) in response to HFS in EAE-MINO and EAE-PBS mice and (Right) histogram summarizing LTP amplitude at 60 minutes after HFS compared to the last 10 minutes of the baseline and showing that LTP was preserved in EAE-MINO compared to EAE-PBS mice at the MPP-DG synapses (n=7 slices per group, \*\* $p < 0.01$ , Mann-Whitney test). (I) Fractional anisotropy in the molecular layer of the dentate gyrus was higher in EAE-MINO mice than in EAE-PBS mice (n=15 per group, \* $p < 0.05$ , t-test). (J and K) Compared to EAE-PBS mice, EAE-MINO mice displayed normal fear memory with enhanced conditioned freezing to the correct predictor of the threat, the conditioning context (J), and reduced conditioned freezing to the non-predictive tone in a familiar and safe box (K) (n=15 per group, \* $p < 0.05$ , t-test).*

Basal excitatory synaptic transmission was preserved at the MPP-DG synapses in EAE-MINO mice as revealed by measuring I/O relationships ( $F=18.81$ ,  $p < 0.0001$ , Fig. 6G). The treatment also prevented LTP impairment in the DG (145.1% in EAE-MINO mice vs 106.3% on EAE-PBS mice,  $p=0.01$ , Fig. 6H). Such protective effect was measurable *in vivo* on MRI metrics as FA was higher in EAE-MINO mice compared to EAE-PBS mice (0.217 vs 0.207,  $p=0.045$ , Fig. 6I). Finally, in the contextual conditioning procedure EAE-MINO mice showed a higher conditioned fear to the predictive conditioning context compared to EAE-PBS mice (freezing rate: 41.6% vs 30.6%,  $p=0.021$ , Fig. 6J) and a lower conditioned fear to the non-predictive tone (freezing ratio: 0.131 vs 0.269,  $p=0.021$ , Fig. 6K), demonstrating that minocycline treatment prevented the early memory impairment observed in EAE-mice.

***Selective inhibition of dentate gyrus microglial activation was sufficient to prevent memory impairment in EAE-mice***

Because we could not exclude that the protection against memory impairment after systemic injections of minocycline could involve additional mechanisms on top of dentate gyrus protection, we selectively infused minocycline in the dentate gyrus of EAE-mice (EAE-MINO-DG) daily from 7 to 20 d.p.i. Intra-dentate gyrus infusions of PBS (EAE-PBS-DG) and intra-CA1 infusions of minocycline (EAE-MINO-CA1) served as controls. Preliminary experiments with blue-dye infusions were used to define the appropriate volume and flow rate to restrict diffusion of drugs to the region of interest (Fig. 7A and B). As expected from intra-hippocampal injections, there was no difference between minocycline and PBS infusions regarding the EAE-scores (which essentially reflect motor symptoms, Fig. 7C). In the contextual fear conditioning procedure, only the EAE-MINO-DG mice were protected against memory impairment as they showed a higher conditioned fear to the predictive conditioning context compared to both EAE-MINO-CA1 mice and EAE-PBS-DG mice (freezing rate: 39.23%, 27.15% and 26.04% respectively,  $F=3.88$ ,  $p=0.028$ , Fig. 7D) and a lower conditioned fear to the non-predictive tone (freezing ratio: 0.099, 0.258 and 0.290 respectively,  $F=8.09$ ,  $p=0.001$ , Fig. 7E). There was no significant behavioral difference between EAE-MINO-CA1 and EAE-PBS-DG mice demonstrating that hippocampal microglial activation outside the dentate gyrus was not involved in early memory impairment in EAE-mice. Taken together, these experiments formally establish a causal link between selective dentate gyrus disruption and memory impairment.

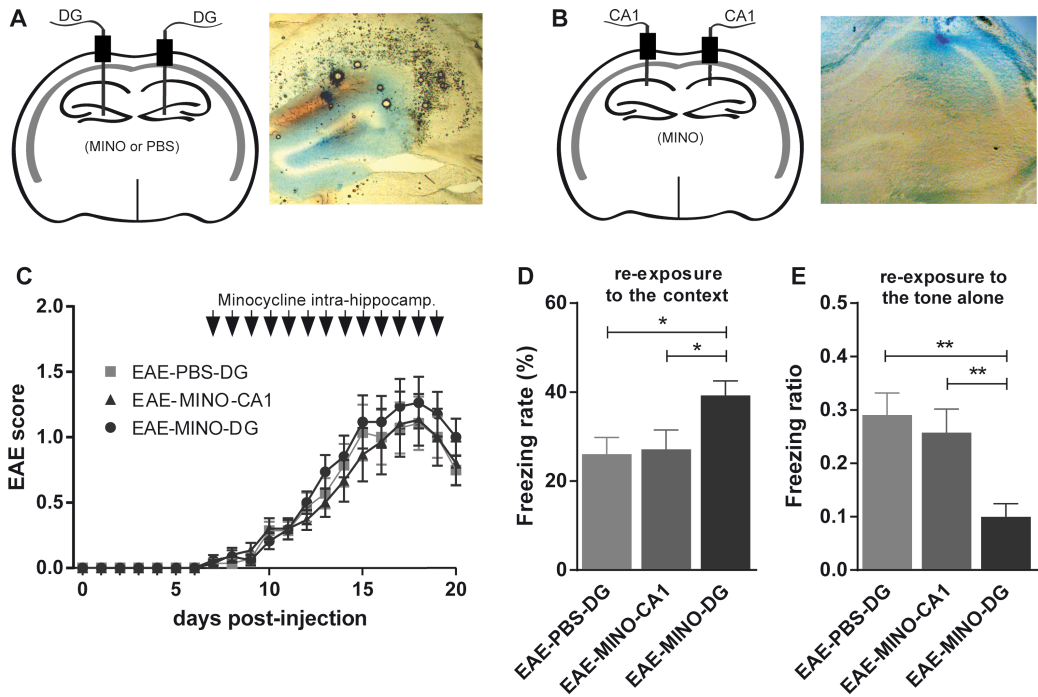


Fig. 7: Selective intra-dentate gyrus infusion of minocycline was sufficient to prevent memory impairment in EAE-mice. (A and B) EAE-mice received bilateral intra-dentate gyrus infusions of minocycline (EAE-MINO-DG,  $n=17$ ) or bilateral intra-dentate gyrus infusions of PBS (EAE-MINO-PBS,  $n=14$ ) or bilateral intra-CA1 infusions of minocycline (EAE-MINO-CA1,  $n=15$ ). In preliminary experiments, Pontamine blue dye was injected to determine optimal volume and flow rate for a local and selective diffusion into the targeted hippocampal subfields. (C) Mice were injected daily through the guide cannulae from 7 d.p.i. to the day of conditioning. There was no difference between groups in disease severity according to EAE-score. (D and E) Compared to EAE-MINO-CA1 mice and EAE-PBS-DG mice, EAE-MINO-DG mice displayed normal fear memory with preserved conditioned freezing to the conditioning context (D), and reduced conditioned freezing to the non-predictive tone in a familiar and safe box (E). (\* $p<0.05$ , \*\* $p<0.01$ , Tukey's multiple comparisons test after ANOVA).

## Discussion

We provided results highlighting the selective vulnerability of the dentate gyrus to microglial activation at the early stage of experimental multiple sclerosis and its involvement in early memory impairment. These data introduce the concept of differential vulnerability of the dentate gyrus in the context of multiple sclerosis; the potential of microglia blockers to maintain the cognitive performances; and the possibility to monitor such effects *in vivo* with high-resolution DTI.

In previous studies on EAE-mice, spatial memory dysfunction was investigated with the Barnes maze, the Morris water maze or object exploration/recognition. Therefore, memory impairment in EAE was reported at later stages, during the recovery of motor symptoms, after selection of animals with mild motor symptoms or during the initial immunization period before EAE onset<sup>37,38,39,40,41,13</sup>. Thus, a reliable and unbiased study of memory impairment, controlling for motor symptoms and slowing of information processing speed, at the early (acute) phase of EAE was still lacking. Our particular contextual conditioning paradigm allowed us to avoid and/or to control several confounding factors linked to EAE specificities such as motor or sensory deficits, amygdala lesion or disconnection. This memory task clearly shows that EAE-mice display an impaired conditioning to complex contextual cues associated with the expression of a maladaptive conditioned fear to a simple, salient, but irrelevant (non-predictive) cue. Furthermore, after local infusions, EAE-MINO-DG mice expressed a normal fear response to contextual conditioning despite sensory-motor extra-hippocampal symptoms. We can therefore conclude that the memory impairment observed in EAE-mice is due to hippocampal dysfunction specifically and not to a hippocampus-independent deficit in fear learning. It can thus be paralleled with deficits in hippocampal-dependent tasks reported in patients with early multiple sclerosis<sup>4</sup>.

In diffuse brain diseases such as EAE and multiple sclerosis, it is usually difficult to understand whether a deficit is due to global brain damage or to more focal alteration and this question is impossible to solve in humans. By using local infusions of minocycline we could demonstrate here that early memory impairment in EAE is selectively due to a microglia-mediated dentate gyrus disruption. Interestingly, a similar memory impairment has been previously associated with deficits in dentate gyrus activation in a mouse model of post-traumatic stress disorder<sup>23</sup>.

The link between dentate gyrus dysfunction and impaired contextual learning has also been described in recent experiments using optogenetic techniques in the mouse brain<sup>26,42</sup>.

This preferential vulnerability of the dentate gyrus results in an impairment of basal synaptic transmission and synaptic plasticity in EAE-mice. Previous studies reported that LTP was preserved at CA3-CA1 synapses at the acute phase of the disease<sup>43,44,45</sup>. One of them<sup>45</sup> showed that, while preserved at the early stage, LTP became impaired in CA1 at the chronic-progressive stage of the disease (40 d.p.i). Then, we can hypothesize that the dysfunction of hippocampal neurons extends beyond the dentate gyrus during the course of EAE. Furthermore, in another study, LTP and long term depression (LTD) were reported to be preserved in CA1 area whereas LTD was disrupted in the superior colliculus and the cerebellum at the same early stage<sup>43</sup>. In terms of synaptic transmission and plasticity, this suggests that some brain regions are more vulnerable than others to the inflammatory mechanisms occurring in EAE. In view of our results, we expand this concept to the hippocampal trisynaptic loop itself where synaptic transmission and plasticity are altered in the dentate gyrus but not in CA1 region. Finally, such synaptic deficits provide a strong cellular and functional explanation to the early memory impairment of EAE-mice.

In humans, the fundamental role of dentate gyrus granule cells compared to CA1 pyramidal neurons in declarative memory acquisition has been suggested<sup>46</sup> but could not be easily demonstrated in the context of early multiple sclerosis. Post-mortem studies have revealed that CA1 and dentate gyrus were the most affected regions in late multiple sclerosis, probably because they are encompassed by CSF, meningeal follicles and cytotoxic factors<sup>5</sup>. Furthermore, the decrease of synaptophysin, a presynaptic protein involved in synaptic vesicle release, has been shown to be more important in demyelinated dentate gyrus than in demyelinated CA1, suggesting that dentate gyrus neurons could be more vulnerable to inflammatory mechanisms<sup>6</sup>. *In vivo* MRI studies of hippocampal subfields in patients with multiple sclerosis described controversial results. In one hand, some authors described that CA1 sub-region is the most atrophic field in the hippocampus of patients with multiple sclerosis<sup>7,19</sup>. In the other hand, a recent study, by using a hippocampal radial mapping analysis, described an expansion of the dentate gyrus related to memory function<sup>20</sup> while another group has correlated the CA2/3-dentate gyrus volume with depressive symptoms and cortisol levels in patients with multiple sclerosis<sup>18</sup>. However, such volumetric analyses might reflect

late modifications that do not presume the early neurodegenerative mechanisms. Furthermore, MRI failed to precisely isolate and measure dentate gyrus itself (the structure being usually confounded with CA2/3 regions on morphological MRI). In this context, our results on EAE provide strong evidence of the vulnerability of the dentate gyrus and focus on its early nature, prior to demyelination, with consistent behavioral, MRI, histological and electrophysiological correlates. Furthermore, we were able to demonstrate a causal link between this vulnerability and microglial activation.

The link between microglial activation, demyelination, neurodegeneration and disability has been suggested in multiple sclerosis by post-mortem histological studies<sup>47</sup>, PET imaging in patients with a progressive form of the disease<sup>48</sup> and EAE induction in transgenic mice<sup>49</sup>. This association is highly complex as noxious effect of activated microglia can be balanced by beneficial role for tissue repair<sup>50</sup>. Here, we suggest a relationship between microglial activation, neurodegeneration and memory impairment, and we extend these data by identifying the particular vulnerability of the dentate gyrus to this process. Indeed, 20 d.p.i., there was neither macrophage nor lymphocytic infiltration in the hippocampus and there was also no demyelination to explain dendrite transection. Furthermore, the inhibition of microglial activation with minocycline protected mice from dendritic damages, synaptic plasticity disruption and memory impairment, demonstrating that microglial activation in EAE dentate gyrus is deleterious for the structure and the function of granular neurons. Because intra-dentate gyrus inhibition of microglial activation prevents memory impairment in EAE-mice, we can exclude that minocycline acts through indirect mechanisms, such as peripheral immune response modulation or matrix metalloproteinase inhibition<sup>51</sup> while direct neuroprotective effect of minocycline might still be possible<sup>52</sup>.

Despite a diffuse microglial proliferation in the hippocampus of EAE-mice, we described here at the transcriptional level a differential pattern of activation within the dentate gyrus, that was absent or less pronounced in CA1. Given that there could be regional differences in microglial phenotype in the brain<sup>50</sup>, we can hypothesize that microglia is already “primed” in the dentate gyrus to control newborn neurons and circuits in physiological conditions, leading to the early aberrant activation that we described here in case of inflammatory disease. Future studies will need to explore the profile of inflammatory markers in each layer. Future studies will also need to address the mechanistic pathways responsible for pathological microglia-

neuron interactions within the dentate gyrus. Recent studies in neuroinflammation suggest that it could involve the complement pathway<sup>53</sup>, the platelet-activating factor receptor<sup>54</sup>, the fractalkine receptor<sup>55</sup>, the interleukin-1 $\beta$ <sup>12</sup>, the NADPH oxidase<sup>13</sup> or indirect mechanisms through astrocytes and the multipartite synapse<sup>14</sup>.

This study highlights the therapeutic potential of minocycline in multiple sclerosis<sup>51</sup>. Its positive effect on myelitis symptoms in EAE has already been described<sup>36</sup> and a small phase II clinical trial in patients with multiple sclerosis demonstrated a trend toward the efficiency of minocycline on usual surrogate MRI criteria<sup>56</sup>. Furthermore, a recent study in another EAE model of the disease, demonstrated that minocycline could prevent memory dysfunction at the chronic phase of the disease, after the recovery of motor symptoms, suggesting that our results are still relevant at later stages<sup>13</sup>. Then, in future human clinical trials, it would be of great interest to evaluate the neuroprotective effect of this drug with cognitive evaluation and advanced MRI techniques such as DTI to assess the microstructure of the hippocampus, particularly the dentate gyrus.

From the translational point of view, this study is a proof-of-concept that early neuritic damage in the dentate gyrus can be monitored *in vivo* by DTI, prior to hippocampal measures of atrophy on T2-weighted images. Indeed, we have shown: (i) the independent correlation between FA/AD and neurofilament staining and (ii) the effect of minocycline treatment on both FA and histological measures. To our knowledge, there is only one previous *in vivo* DTI study of hippocampal subfields with MRI-histological correlations, on an epileptic rat model<sup>57</sup>. Interestingly, several months after status epilepticus, the authors have reported an increased FA in the dentate gyrus, explained by an increased AD and correlated with neuritic sprouting in histological analyses. It represents an external validation of our findings because opposite histological mechanisms (*i.e.* neuritic sprouting vs neuritic loss) lead to opposite DTI parameters changes (*i.e.* FA/AD increased vs FA/AD decreased). This finding opens perspectives to use high resolution hippocampal DTI as a surrogate marker for phase II clinical trial to measure the effects of treatments on memory impairment and neurodegeneration in multiple sclerosis and also to test the selective vulnerability of the dentate gyrus in patients.

To summarize, the present study indicates that early hippocampal-dependent memory impairment in experimental multiple sclerosis is caused by dentate gyrus vulnerability. We

provide compelling results from several complementary techniques converging on this same finding. Accordingly, the concept of differential regional vulnerability within the hippocampal formation must be extended to multiple sclerosis as microglial activation was causing dendritic loss, neuronal death and synaptic plasticity disruption selectively in the dentate gyrus at the early stage of EAE. Furthermore, in order to facilitate future studies in humans, we have demonstrated that these cellular alterations are measurable *in vivo* with DTI and that they can be prevented by minocycline treatment.

### **Acknowledgements:**

This work was supported by Inserm, Université de Bordeaux, and by the Fondation pour la Recherche Médicale (Equipe FRM to SHO). The work was further supported by public grants from the French Agence Nationale de la Recherche within the context of the Investments for the Future program referenced ANR-10-LABX-57 named TRAIL (project IBIO-NI) and ANR-10-LABX-43 named BRAIN (Project MEMO-MS). The microscopy was done in the Bordeaux Imaging Center, a service unit of the CNRS-INSERM and Bordeaux University, member of the national infrastructure France BioImaging. The 4.7 T animal scanner was supported by the FLI (ANR-11-INBS-0006). VP received personal support from Clermont-Ferrand University Hospital and the Inserm MD-PhD program (Ecole de l'Inserm – Liliane Bettencourt).

The microscopy was done in the Bordeaux Imaging Center, a service unit of the CNRS-INSERM and Bordeaux University, member of the national infrastructure France BioImaging. The help of Christel Poujol and Sebastien Marais (Bordeaux Imaging Center) is acknowledged as well as Philippe Ciofi and Lucie Blaszczyk (INSERM U1215) for technical supports regarding histology and microscopy experiments. We thank Laurent Brayda-Bruno (INSERM U1215) for technical support with behavioral experiments and his preliminary experiments for intra-dentate gyrus infusions of drugs.

## References

1. Compston A, Coles A. Multiple sclerosis. *Lancet*. 2008;372:1502–1517.
2. Planche V, Gibelin M, Cregut D, Pereira B, Clavelou P. Cognitive impairment in a population-based study of patients with multiple sclerosis: differences between late relapsing-remitting, secondary progressive and primary progressive multiple sclerosis. *Eur J Neurol*. Epub 2015 Apr 22.
3. Ruet A, Deloire M, Hamel D, Ouallet J-C, Petry K, Brochet B. Cognitive impairment, health-related quality of life and vocational status at early stages of multiple sclerosis: a 7-year longitudinal study. *J Neurol*. 2013;260:776–784.
4. Feuillet L, Reuter F, Audoin B, et al. Early cognitive impairment in patients with clinically isolated syndrome suggestive of multiple sclerosis. *Mult Scler*. 2007;13:124–127.
5. Papadopoulos D, Dukes S, Patel R, Nicholas R, Vora A, Reynolds R. Substantial archaeocortical atrophy and neuronal loss in multiple sclerosis. *Brain Pathol*. 2009;19:238–253.
6. Dutta R, Chang A, Doud MK, et al. Demyelination causes synaptic alterations in hippocampi from multiple sclerosis patients. *Ann Neurol*. 2011;69:445–454.
7. Sicotte NL, Kern KC, Giesser BS, et al. Regional hippocampal atrophy in multiple sclerosis. *Brain*. 2008;131:1134–1141.
8. Koenig KA, Sakaie KE, Lowe MJ, et al. Hippocampal volume is related to cognitive decline and fornical diffusion measures in multiple sclerosis. *Magn Reson Imaging*. 2014;32:354–358.
9. Citri A, Malenka RC. Synaptic plasticity: multiple forms, functions, and mechanisms. *Neuropsychopharmacology*. 2008;33:18–41.
10. 't Hart BA, Gran B, Weissert R. EAE: imperfect but useful models of multiple sclerosis. *Trends Mol Med*. 2011;17:119–125.
11. Centonze D, Muzio L, Rossi S, et al. Inflammation triggers synaptic alteration and degeneration in experimental autoimmune encephalomyelitis. *J Neurosci*. 2009;29:3442–3452.
12. Nisticò R, Mango D, Mandolesi G, et al. Inflammation subverts hippocampal synaptic plasticity in experimental multiple sclerosis. *PLoS ONE*. 2013;8:e54666.
13. Di Filippo M, de Iure A, Giampà C, et al. Persistent activation of microglia and NADPH drive hippocampal dysfunction in experimental multiple sclerosis. *Sci Rep*. 2016;6:20926.
14. Habbas S, Santello M, Becker D, et al. Neuroinflammatory TNF $\alpha$  Impairs

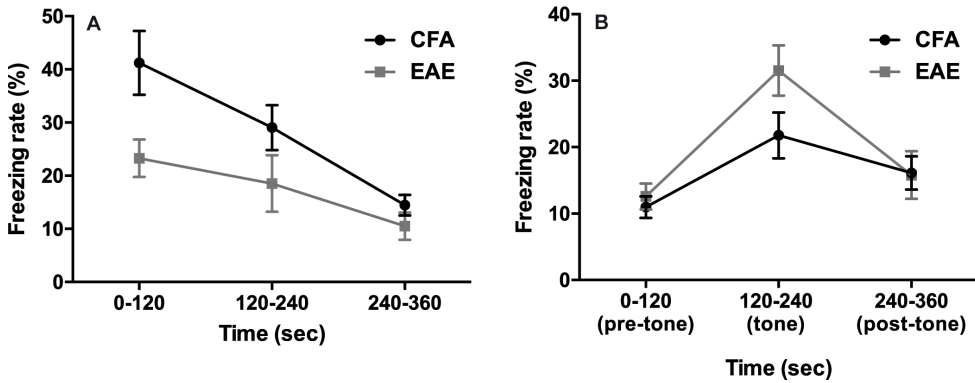
- Memory via Astrocyte Signaling. *Cell*. 2015;163:1730–1741.
15. Mandolesi G, Gentile A, Musella A, et al. Synaptopathy connects inflammation and neurodegeneration in multiple sclerosis. *Nat Rev Neurol*. 2015;11:711–724.
  16. Small SA, Chawla MK, Buonocore M, Rapp PR, Barnes CA. Imaging correlates of brain function in monkeys and rats isolates a hippocampal subregion differentially vulnerable to aging. *Proc Natl Acad Sci USA*. 2004;101:7181–7186.
  17. Small SA. Isolating pathogenic mechanisms embedded within the hippocampal circuit through regional vulnerability. *Neuron*. 2014;84:32–39.
  18. Gold SM, Kern KC, O'Connor M-F, et al. Smaller cornu ammonis 2-3/dentate gyrus volumes and elevated cortisol in multiple sclerosis patients with depressive symptoms. *Biol Psychiatry*. 2010;68:553–559.
  19. Longoni G, Rocca MA, Pagani E, et al. Deficits in memory and visuospatial learning correlate with regional hippocampal atrophy in MS. *Brain Struct Funct*. 2015;220:435–444.
  20. Rocca MA, Longoni G, Pagani E, et al. In vivo evidence of hippocampal dentate gyrus expansion in multiple sclerosis. *Hum Brain Mapp*. 2015;36:4702–4713.
  21. Calandrea L, Trifilieff P, Mons N, et al. Extracellular hippocampal acetylcholine level controls amygdala function and promotes adaptive conditioned emotional response. *J Neurosci*. 2006;26:13556–13566.
  22. Desmedt A, Garcia R, Jaffard R. Vasopressin in the lateral septum promotes elemental conditioning to the detriment of contextual fear conditioning in mice. *Eur J Neurosci*. 1999;11:3913–3921.
  23. Kaouane N, Porte Y, Vallée M, et al. Glucocorticoids can induce PTSD-like memory impairments in mice. *Science*. 2012;335:1510–1513.
  24. Chiaravalloti ND, DeLuca J. Cognitive impairment in multiple sclerosis. *Lancet Neurol*. 2008;7:1139–1151.
  25. Shepherd TM, Ozarslan E, King MA, Mareci TH, Blackband SJ. Structural insights from high-resolution diffusion tensor imaging and tractography of the isolated rat hippocampus. *Neuroimage*. 2006;32:1499–1509.
  26. Kheirbek MA, Drew LJ, Burghardt NS, et al. Differential control of learning and anxiety along the dorsoventral axis of the dentate gyrus. *Neuron*. 2013;77:955–968.
  27. Mikuni N, Babb TL, Chakravarty DN, Chung CK. Postnatal expressions of non-phosphorylated and phosphorylated neurofilament proteins in the rat hippocampus and the Timm-stained mossy fiber pathway. *Brain Res*. 1998;811:1–9.

28. Bustin SA, Benes V, Garson JA, et al. The MIQE guidelines: minimum information for publication of quantitative real-time PCR experiments. *Clin Chem.* 2009;55:611–622.
29. Tikka T, Fiebich BL, Goldsteins G, Keinanen R, Koistinaho J. Minocycline, a tetracycline derivative, is neuroprotective against excitotoxicity by inhibiting activation and proliferation of microglia. *J Neurosci.* 2001;21:2580–2588.
30. Sun S-W, Liang H-F, Schmidt RE, Cross AH, Song S-K. Selective vulnerability of cerebral white matter in a murine model of multiple sclerosis detected using diffusion tensor imaging. *Neurobiol Dis.* 2007;28:30–38.
31. Abiega O, Beccari S, Diaz-Aparicio I, et al. Neuronal Hyperactivity Disturbs ATP Microgradients, Impairs Microglial Motility, and Reduces Phagocytic Receptor Expression Triggering Apoptosis/Microglial Phagocytosis Uncoupling. *PLOS Biol.* 2016;14:e1002466.
32. Giannakopoulou A, Grigoriadis N, Bekiari C, et al. Acute inflammation alters adult hippocampal neurogenesis in a multiple sclerosis mouse model. *J Neurosci Res.* 2013;91:890–900.
33. Bliss TV, Lomo T. Long-lasting potentiation of synaptic transmission in the dentate area of the anaesthetized rabbit following stimulation of the perforant path. *J Physiol (Lond).* 1973;232:331–356.
34. Brosnan CF, Raine CS. The astrocyte in multiple sclerosis revisited. *Glia.* 2013;61:453–465.
35. Kobayashi K, Imagama S, Ohgomori T, et al. Minocycline selectively inhibits M1 polarization of microglia. *Cell Death Dis.* 2013;4:e525.
36. Popovic N, Schubart A, Goetz BD, Zhang S-C, Linington C, Duncan ID. Inhibition of autoimmune encephalomyelitis by a tetracycline. *Ann Neurol.* 2002;51:215–223.
37. Ziehn MO, Avedisian AA, Tiwari-Woodruff S, Voskuhl RR. Hippocampal CA1 atrophy and synaptic loss during experimental autoimmune encephalomyelitis, EAE. *Lab Invest.* 2010;90:774–786.
38. Rahn KA, Watkins CC, Alt J, et al. Inhibition of glutamate carboxypeptidase II (GCP II) activity as a treatment for cognitive impairment in multiple sclerosis. *Proc Natl Acad Sci USA.* 2012;109:20101–20106.
39. D’Intino G, Paradisi M, Fernandez M, et al. Cognitive deficit associated with cholinergic and nerve growth factor down-regulation in experimental allergic encephalomyelitis in rats. *Proc Natl Acad Sci USA.* 2005;102:3070–3075.
40. Kim DY, Hao J, Liu R, Turner G, Shi F-D, Rho JM. Inflammation-mediated memory dysfunction and effects of a

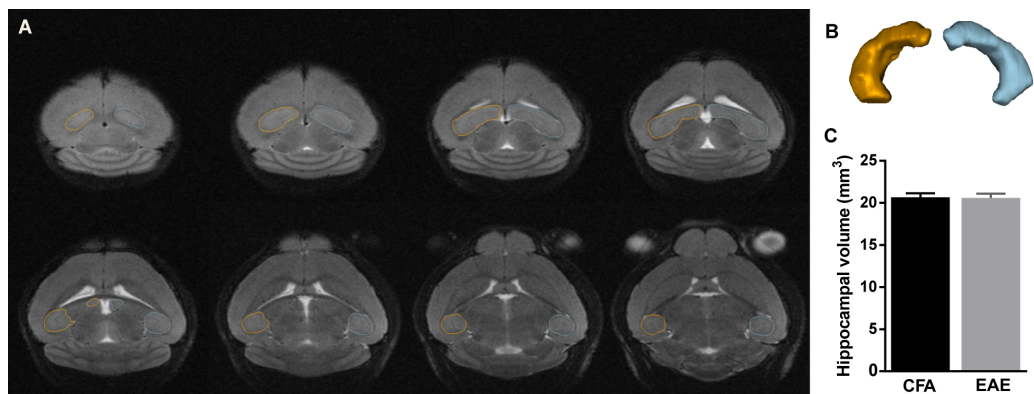
- ketogenic diet in a murine model of multiple sclerosis. *PLoS ONE*. 2012;7:e35476.
41. Dutra RC, Moreira ELG, Alberti TB, Marcon R, Prediger RD, Calixto JB. Spatial reference memory deficits precede motor dysfunction in an experimental autoimmune encephalomyelitis model: the role of kallikrein-kinin system. *Brain Behav Immun*. 2013;33:90–101.
  42. Liu X, Ramirez S, Pang PT, et al. Optogenetic stimulation of a hippocampal engram activates fear memory recall. *Nature*. 2012;484:381–385.
  43. Prochnow N, Gold R, Haghikia A. An electrophysiologic approach to quantify impaired synaptic transmission and plasticity in experimental autoimmune encephalomyelitis. *J Neuroimmunol*. 2013;264:48–53.
  44. Di Filippo M, Chiasserini D, Gardoni F, et al. Effects of central and peripheral inflammation on hippocampal synaptic plasticity. *Neurobiol Dis*. 2013;52:229–236.
  45. Novkovic T, Shchyglo O, Gold R, Manahan-Vaughan D. Hippocampal function is compromised in an animal model of multiple sclerosis. *Neuroscience*. 2015;309:100–112.
  46. Coras R, Pauli E, Li J, et al. Differential influence of hippocampal subfields to memory formation: insights from patients with temporal lobe epilepsy. *Brain*. 2014;137:1945–1957.
  47. Peterson JW, Bö L, Mörk S, Chang A, Trapp BD. Transected neurites, apoptotic neurons, and reduced inflammation in cortical multiple sclerosis lesions. *Ann Neurol*. 2001;50:389–400.
  48. Politis M, Giannetti P, Su P, et al. Increased PK11195 PET binding in the cortex of patients with MS correlates with disability. *Neurology*. 2012;79:523–530.
  49. Heppner FL, Greter M, Marino D, et al. Experimental autoimmune encephalomyelitis repressed by microglial paralysis. *Nat Med*. 2005;11:146–152.
  50. Aguzzi A, Barres BA, Bennett ML. Microglia: scapegoat, saboteur, or something else? *Science*. 2013;339:156–161.
  51. Chen X, Ma X, Jiang Y, Pi R, Liu Y, Ma L. The prospects of minocycline in multiple sclerosis. *J Neuroimmunol*. 2011;235:1–8.
  52. Möller T, Bard F, Bhattacharya A, et al. Critical data-based re-evaluation of minocycline as a putative specific microglia inhibitor. *Glia*. 2016;64:1788–1794.
  53. Michailidou I, Willems JGP, Kooi E-J, et al. Complement C1q-C3-associated synaptic changes in multiple sclerosis hippocampus. *Ann Neurol*. 2015;77:1007–1026.

54. Bellizzi MJ, Geathers JS, Allan KC, Gelbard HA. Platelet-Activating Factor Receptors Mediate Excitatory Postsynaptic Hippocampal Injury in Experimental Autoimmune Encephalomyelitis. *J Neurosci.* 2016;36:1336–1346.
55. Rogers JT, Morganti JM, Bachstetter AD, et al. CX3CR1 deficiency leads to impairment of hippocampal cognitive function and synaptic plasticity. *J Neurosci.* 2011;31:16241–16250.
56. Metz LM, Li D, Traboulsee A, et al. Glatiramer acetate in combination with minocycline in patients with relapsing--remitting multiple sclerosis: results of a Canadian, multicenter, double-blind, placebo-controlled trial. *Mult Scler.* 2009;15:1183–1194.
57. Laitinen T, Sierra A, Pitkänen A, Gröhn O. Diffusion tensor MRI of axonal plasticity in the rat hippocampus. *Neuroimage.* 2010;51:521–530.

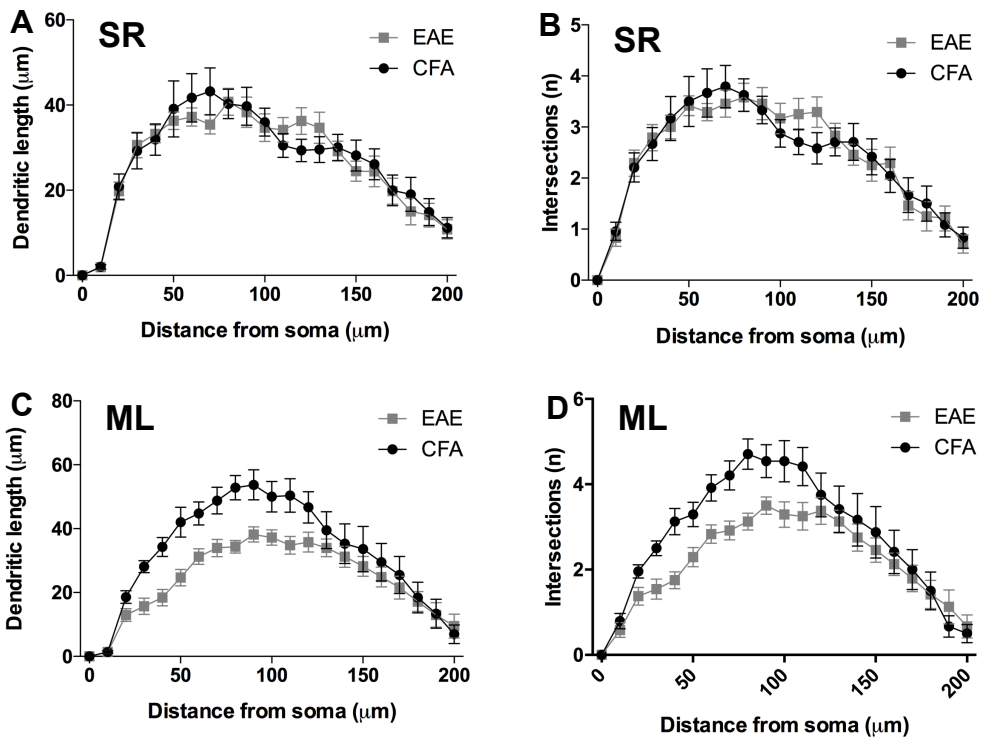
Supplementary figures, table and methods



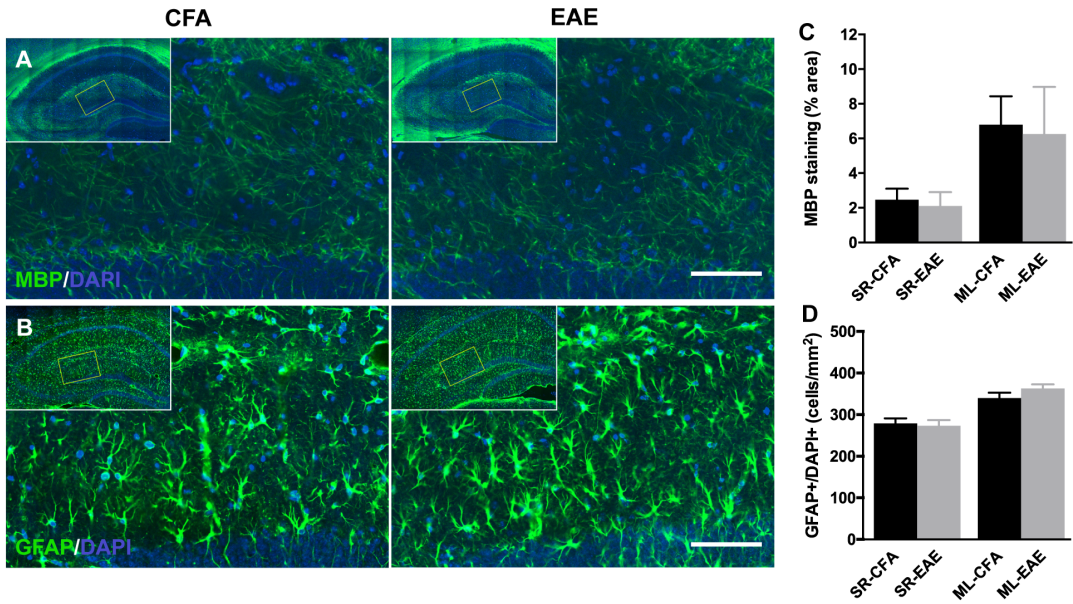
Supplementary fig. A.1: Freezing rate over time when mice were re-exposed to the context (A) and to the tone alone in a safe and familiar environment (B). (A) CFA-mice displayed more conditioned freezing to the predictive conditioning context than EAE-mice and extinction of freezing response was complete and comparable between groups after 6 minutes. (B) EAE-mice exhibited a more important paradoxical freezing behavior to the tone (between 120 and 240 second), compared to pre- and post-exposure period (0-120 and 240-360 seconds respectively). n=12 animals per group.



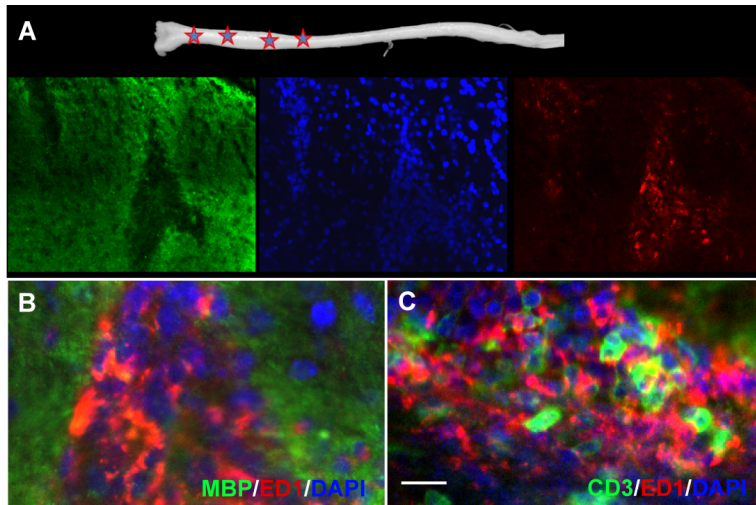
*Supplementary fig. A.2: No early hippocampal atrophy in EAE-mice. (A) Examples of 8 contiguous slices of T2-weighted MRI with manual delineation of right (yellow) and left (blue) hippocampal boundaries. (B) 3D representation of hippocampi after segmentation. (C) EAE and CFA-mice showed the same hippocampal volume at this early stage of the disease (n=12 per group)*



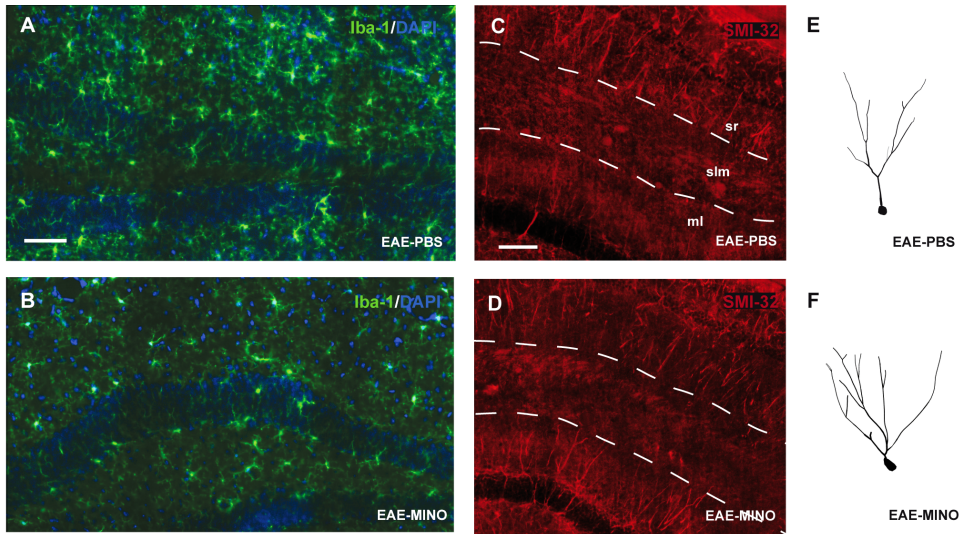
Supplementary fig. A.3: Selective decrease of the dendritic arbor in the molecular layer of the dentate gyrus in EAE-mice compared to CFA-mice (dendritic length between each 10 $\mu\text{m}$  radius and number of intersections at each 10 $\mu\text{m}$  radius from the soma, Sholl analyses). (A and B) There was no significant difference between EAE and CFA-mice regarding the dendrites of CA1 pyramidal neurons in the stratum radiatum (SR) (in both dendritic length and intersections number, respectively  $p=0,84$  and  $p=0,96$ , two-way ANOVA). (C and D) However, the total dendritic length and the complexity of the dendritic arbor were decreased in the molecular layer (ML) of EAE-mice compared to CFA-animals (respectively  $F=4,70$ ,  $p=0,012$  and  $F=3,37$ ,  $p=0,043$ , two-way ANOVA). (see also Fig. 3)



Supplementary fig. A.4 Immunofluorescence and confocal imaging of myelin and astrocytes in the hippocampus of CFA and EAE-mice. (A and C) MBP staining for myelin and quantification of the staining area in the stratum radiatum of CA1 (SR) and the molecular layer of the dentate gyrus (ML). (B and D) GFAP staining for astrocytes and quantification of astrocytes number. Note that there was also no difference between groups after the analysis of GFAP staining area, neither in the stratum radiatum (respectively 6.70% $\pm$ 0.9 in EAE-mice vs 9.11% $\pm$ 0.8 for CFA-mice,  $p=0.063$ ) nor in the molecular layer of the dentate gyrus (7.71% $\pm$ 1.4 vs 11.40% $\pm$ 1.7,  $p=0.11$ ).  $n=12$  animals per group.



Supplementary fig. A.5: Typical inflammatory and demyelinating plaques were detected in the spinal cord but not in the hippocampus of EAE mice. (A and B) Immunofluorescence for myelin (MBP, green), nuclei (DAPI, blue) and macrophages (ED1(CD68), red) illustrating a focal demyelinating lesion with macrophage infiltration within the spinal cord. (C) Immunofluorescence of T lymphocytes (CD3, green), macrophages (ED1(CD68), red) and nuclei (DAPI, blue) with enlarged view illustrating that both T lymphocytes and macrophages were found within the spinal cord inflammatory lesions. No plaque was found within the hippocampus at this stage of the disease. Scale bar: 25µm.

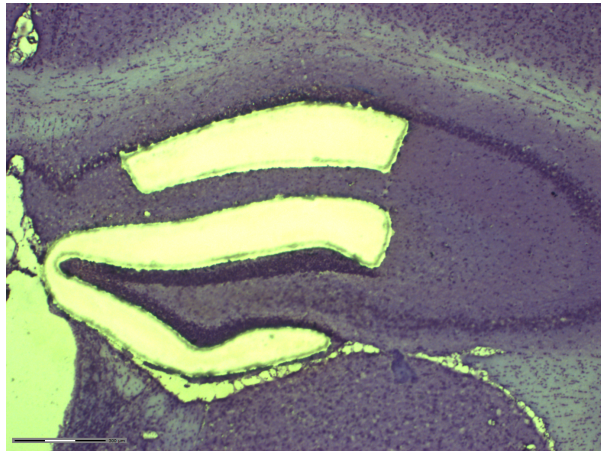


*Supplementary fig. A.6: Systemic injections of EAE-mice with minocycline prevented microglial activation and dendritic loss. (A and B) Representative images of microglial staining with Iba-1 in EAE-PBS and EAE-MINO mice. (C and D) Representative images of dendritic staining with SMI-32 in EAE-PBS and EAE-MINO mice. (E and F) Representative examples of neuroLucida-traced neurons in the granular/molecular layer of the dentate gyrus in EAE-PBS and EAE-MINO mice. Scale bar 100 $\mu$ m. (see also Fig. 6 for quantification)*

	Fractional Anisotropy		Axial Diffusivity	
	Univariate (Pearson's correlation)	Multiple linear regression analysis	Univariate (Pearson's correlation)	Multiple linear regression analysis
<b>Myelin</b>	$r = -0.17, p = 0.4527$	-	$r = 0.069, p = 0.76$	-
<b>Astrocytes</b>	$r = -0.46, p = 0.023$	-	$r = -0.016, p = 0.94$	-
<b>Microglia</b>	$r = -0.44, p = 0.035$	-	$r = -0.38, p = 0.078$	-
<b>Neurogenesis</b>	$r = 0.36, p = 0.089$	-	$r = -0.098, p = 0.66$	-
<b>Dendrites</b>	$r = 0.56, p = 0.0051$	$r^2 = 0.32, p = 0.0051$	$r = 0.47, p = 0.022$	$r^2 = 0.22, p = 0.024$

*Supplementary table A.1: Pearson's correlation and multiple linear regression analyses of the histological predictors of DTI parameters in the molecular layer of the dentate gyrus. Myelin=MBP staining area, Astrocytes=GFAP/DAPI cell counting, Microglia=Iba-1/DAPI cell counting, Neurogenesis=DCX/DAPI cell counting and Dendrites=SMI-32 staining area.*

*There was a strong positive correlation between dendritic content and FA/AD reflecting that water directionality is induced by the dendritic arborisation. There was also a negative correlation between FA values and the number of microglial and astrocytic cells that may reflect decrease directionality of water diffusion by cell hindrance. Nevertheless, this effect was less prominent than the one induced by dendrites. Furthermore, the multiple linear regression statistical model with all potential histological contributors to the reduced FA, including astrocyte proliferation (GFAP), myelin loss (MBP), microglia proliferation (Iba-1), neurogenesis impairment (DCX) and dendrites loss (SMI-32), showed that neuritic loss was the only independent factor correlated with FA and AD in the molecular layer of the dentate gyrus.*



*Supplementary method A.1: Example of laser-microdissection of the hippocampus which allowed us to collect brain tissue in different hippocampal subfields in order to perform region-selective mRNA extractions and quantitative PCR analyses.*

<b>Gene</b>	<b>GenBank ID</b>	<b>Forward Sequence (5'-3')</b>	<b>Reverse Sequence (5'-3')</b>
Aif1 (Iba1)	NM_019467	CAATTCCTCGATGATCCCAAATA	TTCACCTTGAAGGCTTCAAGTTT
Ilgam (Cd11b)	NM_001082960	CTCATCACTGCTGGCCTATACAA	GCAGCTTCATTTCATCATGTCCTT
ED1 (Cd68)	BC021637	ACCCATCCCCACCTGTCTCT	TGATGTAGGTCCTGTTTGAATCCA
Nono	NM_023144	CTGTCTGGTGCATTCTGAACTAT	AGCTCTGAGTTCATTTTCCCATG
Sdha	NM_023281	TACAAAGTGCGGGTCGATGA	TGTTCCCCAAACGGCTTCT

*Supplementary method A.2: Primer sequences for qPCR experiments*



**Loss of pattern separation performances  
in early multiple sclerosis**



## Chapter 4: Loss of pattern separation performances in early multiple sclerosis

### 1. Summary page

**Rationale:** We have demonstrated in chapter 2 that memory impairment occurs early in MS and that it is correlated with hippocampal damages as measured *in vivo* within the whole hippocampus. We have also demonstrated in chapter 3, by using EAE-mice, that the dentate gyrus is the most vulnerable subfields of the hippocampus during the early stage of the disease. Altogether, it suggests that alterations measured within the whole hippocampus in patients could be mainly driven by dentate gyrus disruption at the early stage of the disease. If true, memory tasks mainly dependent on the integrity of the dentate gyrus should be among the first to be altered. Pattern separation is a crucial feature of episodic memory supported by the dentate gyrus, which codes similar memories in a distinct and non-overlapping manner. We hypothesized that pattern separation will be impaired early during the course of MS.

**Summary of the methods:** We tested 19 patients with early MS (less than 18 months after the first relapse) and 19 healthy controls matched on age, gender and education level with a “standard” visuospatial episodic memory test, a test of information processing speed and a new behavioral pattern separation task that has never been used in MS before. This computerized test consisted of 2 phases. The first was an encoding phase in which subjects memorized a series of presented objects. The second phase was a recognition memory test in which another series of objects were presented and patients were asked to determine for each object if it was an old image from the first phase, a novel foil, or a lure that was visually similar to the first studied images. The principle was that participants with poor pattern separation performances failed to recognize lures and answered “old” for similar objects.

**Main results:** Pattern separation scores were significantly lower in the group of patients with early MS compared to healthy controls. However, in this small sample of subjects, no differences among groups could be found for information processing speed performances and “standard” visuospatial episodic memory tests.

**Comments:** This early loss of pattern separation performances argues for an early dentate gyrus dysfunction in MS, in lines with what we have described in the EAE-model.



## 2. Article

### **Decreased pattern separation performances suggest dentate gyrus dysfunction in patients with early multiple sclerosis**

Vincent Planche<sup>1,2,3</sup>, Aurélie Ruet<sup>1,2,4</sup>, Julie Charré-Morin<sup>4</sup>, Mathilde Deloire<sup>4</sup>, Bruno Brochet<sup>1,2,4</sup> and Thomas Tourdias<sup>1,2,4</sup>

<sup>1</sup> Univ. Bordeaux, F-33000 Bordeaux, France;

<sup>2</sup> Inserm U1215 - Neurocentre Magendie, F-33000 Bordeaux, France

<sup>3</sup> CHU de Clermont-Ferrand, F-63000 Clermont-Ferrand, France;

<sup>4</sup> CHU de Bordeaux, F-33000 Bordeaux, France;

**In preparation**

## Abstract

**Background:** Memory impairment related to hippocampal dysfunction is frequent and occurs early during the course of multiple sclerosis (MS). How episodic memory breaks down in patients with MS remains however largely unknown but dentate gyrus structure has been pinpointed to be vulnerable at the early stage of the disease. Then, in this study, we hypothesized that the pattern separation component of episodic memory (a function known to be critically dependent to dentate gyrus function) would be impaired in patients with early MS (PweMS).

**Methods:** Nineteen PweMS (clinically isolated syndrome or clinically definite MS, less than 18 months following their first relapse) and 19 healthy controls matched on age, gender and education level were tested for information processing speed, episodic visuospatial memory and with a mnemonic similarity task.

**Results:** We found no differences among groups for information processing speed performances and “global” visuospatial episodic memory tests regarding learning, long term recall or recognition. However, we reported a significant decrease of pattern separation performances in PweMS compared to healthy controls (27.07 vs 40.01,  $p=0.028$ ) together with a significant higher pattern completion rate (56.11 vs 40.95,  $p=0.0021$ ). Pattern separation performances were not correlated with depression or disability in PweMS.

**Conclusion:** Our results demonstrate that pattern separation performances are impaired early during the course of MS, in a sample of patients where information processing speed and “global” visuospatial episodic memory tests were not significantly modified. It suggests early dentate gyrus vulnerability during the course of the disease.

## Introduction

Memory impairment is frequent in multiple sclerosis (MS)<sup>1,2</sup>. It occurs very early during the course of the disease and correlates with hippocampal microstructural damage<sup>3</sup>. However, the neuropsychological and anatomical mechanisms leading to loss of episodic memory performances remain poorly understood. Recent works support that hippocampal dysfunction mediate memory impairment in MS, both in the human disease<sup>4,5,6</sup> and in animal models (experimental auto-immune encephalomyelitis, EAE)<sup>7,8,9</sup>. Furthermore, recent MRI studies in patients with MS highlighted the vulnerability of specific hippocampal subfields, with a focus either on CA1<sup>4,10</sup> or on dentate gyrus<sup>11,12</sup>. The time course of the disease is probably particularly important for such selective vulnerability of one or another subfield. Our recent work in EAE-mice provided compelling evidence for a dentate gyrus vulnerability to neurodegeneration prior to any other subfield. We indeed demonstrated that dentate gyrus granular neurons are the most vulnerable hippocampal neurons at the early stage of the disease, at the morphological and functional level. This selective neurodegenerative process is responsible for early memory impairment. Whether such early vulnerability of the dentate gyrus is also true in patients with early MS remains to be demonstrated.

A fundamental physiological role of the hippocampus is to allow the formation of new memories as individual representations. The histological and functional “front door” of the hippocampus is the dentate gyrus where the perforant path/dentate granular neurons system eliminates repetitive information, avoiding interference from long term memory and new sensory inputs<sup>13</sup>. This computational view of dentate gyrus function is known as pattern separation, which is the process of establishing independent and non-overlapping new memories<sup>14</sup>. The critical role of the dentate gyrus in pattern separation has been well established with behavioral, gene knock-out and electrophysiological experiments in rodents<sup>15,16</sup> but also with functional MRI in humans<sup>17,18</sup>. The complementary process of pattern separation (*i.e.* the ability to complete a whole memory when just a partial cue for retrieval is presented) is named pattern completion, a function classically attributed to the CA3 subfield of the hippocampus. CA3 (and its projections to CA1) integrate the new pattern of information with previous memories, even when partial or degraded versions of the original inputs are presented<sup>13</sup>.

The investigation of people with early MS (PweMS) provides the opportunity to understand the mechanisms underlying episodic memory deficits before other cognitive impairments and global brain damage emerge. Then, comprehensive neuropsychological evaluations of PweMS has already pointed out deficits in acquisition/encoding of new memories more than storage, retrieval or recognition impairments<sup>19,20,21</sup>. In this context, if dentate gyrus structure and function are more vulnerable than other hippocampal subfields in MS, we hypothesized that pattern separation would be impaired very early during the course of the disease, explaining early deficit in encoding. Then, the aim of this work was to test pattern separation performances in PweMS compared to healthy controls matched on age, gender and educational level.

## **Methods**

### ***Participants***

Nineteen patients with early multiple sclerosis (PweMS) were prospectively recruited from July 2015 to July 2016 at Bordeaux University Hospital. PweMS were included within 6 months to 18 months after their first neurological episode suggestive of MS and presented at least two asymptomatic cerebral lesions on Fast Fluid-Attenuated Inversion-Recovery (FLAIR) images. Patients included in this study could be either patients with clinically isolated syndrome highly suggestive of MS or patients with relapsing-remitting MS according to revised McDonald's criteria<sup>22</sup>. Exclusion criteria were as follows: age under 18 or over 60 years, previous history of other neurological or psychiatric disorder, inability to perform computerized tasks, corticosteroid pulse therapy within two months preceding testing. Clinical assessment and Expanded Disability Status Scale (EDSS) were determined by expert neurologists according to the French standardized version.

Nineteen healthy control (HC) subjects were tightly matched for age, gender and educational level to PweMS. They were free of neurologic, psychiatric, or systemic diseases, and drug or alcohol abuse.

The work described here is an ancillary study of the SCICOG protocol (NCT01865357), which was approved by the local ethics committee. Written informed consent was obtained prior to

participation.

### **Neuropsychological assessment**

All patients and healthy controls performed the Computerized Speed Cognitive Test (CSCT) to assess information processing speed. In order to assess “global” visuospatial episodic memory, all subjects performed the Brief visuospatial memory test revised (BVMT-R). Each participant also completed a standard questionnaire concerning depressive symptoms (Beck Depression Inventory, BDI).

Pattern separation and completion were tested in patients and healthy controls with the Mnemonic similarity test (MST, also known as the Behavioral Pattern Separation Task (BPS-O), <http://faculty.sites.uci.edu/starklab>)<sup>23</sup>. This computerized test consists of two phases. The first phase is an incidental encoding phase where patients and controls were exposed to 128 pictures shown for 2 seconds with an inter-stimulus interval of 0.5 second. During this phase, participants have to identify “indoor” and “outdoor” objects via a button press, in order to maintain their attention. Immediately after this encoding phase, the second phase is an unexpected test phase where participants are exposed to 192 pictures with similar exposition time. One-third of the images are exact repetitions of pictures shown in phase 1 (“targets”), one third of pictures are completely new objects (“foils”) and one third of pictures represented similar but slightly different objects (“lures”). Participants were asked to identify “old”, “new” or “similar” pictures via a button press (Fig. 1).

<b>Presentation (phase 2)</b>	<b>Expected answer</b>
Target	Old
Foil	New
Lure	Similar

Pattern separation = (number of answers “similar” for “lures”) - (number of answers “similar” for “foils”).

Pattern completion = (number of answers “old” for “lures”) – (number of answers “old” for “foils”).

Recognition = (number of answers “old” for “targets”) – (number of answers “old” for “foils”).

Pattern separation score was calculated as the difference between the rates of “similar” responses given to the “lure” items minus “similar” responses given to the “foils” (to correct for response biases). Pattern completion score was the difference between the rates of “old” responses given to the “lure” items minus “old” responses given to the “foils”. Traditional recognition score was the difference between the rate of “old” responses given to the “target” items minus “old” responses given to the “foils”<sup>24</sup>.



*Fig. 1: Design of the Mnemonic separation test (MST) and examples of pictures. During the first phase, participants encoded a series of pictures. The second phase was a surprise recognition memory test in which participants had to respond “old”, “new” or “similar” to a series of pictures that were the exact old images from study, novel foils, or lures that were related but not identical to the studied items. Pattern separation score was the difference between “similar” responses given to the lure items minus the “similar” responses given to the foils*

### **Statistical Analyses**

Statistical analyses were performed with Prism software 6 (Graphpad). Qualitative variables were tested with Chi-square test. The distribution of all continuous data was tested with the Shapiro-Wilk normality test. Then, Student’s t-test or Mann-Whitney test was used as appropriate, to compare the two groups. Relationships between quantitative variables were

assessed using correlation coefficients (Pearson or Spearman according to statistical distribution). All tests were two-sided, with a type I error set at  $\alpha=0.05$

## Results

### ***Demographical and clinical characteristics of patients and controls***

Because patients and controls were matched on age, gender and educational level, no statistically significant difference between groups was reported on these demographical data. According to our inclusion criteria, 12 persons were diagnosed with clinically isolated syndrome at the time of testing and 7 persons had converted to clinically definite multiple sclerosis, less than 18 months after their first clinical relapse. As expected, physical disability and disease duration were very low in our population of PwMS. PwMS were significantly more depressed than healthy controls, as it is usually described<sup>1</sup> (Table 1).

	<b>Early MS</b>	<b>Healthy controls</b>	<b>p-value</b>
<b>Mean age, years (SD)</b>	37.11 (10.24)	34.32 [11.07]	0.43
<b>Sex ratio (F/M)</b>	16/3	15/4	0.68
<b>Education level, years (SD)</b>	13.74 (2.10)	14.42 [2.14]	0.33
<b>Disease duration, months (SD)</b>	11.68 (5.84)	-	
<b>Median EDSS score [range]</b>	1.5 [0 – 3.5]	-	-
<b>Median depression (BDI) score [range]</b>	6 [1 - 34]	1 [0 - 11]	0.0021

*Table 1: Demographical and clinical data of patients and healthy controls. Patients and controls were prospectively included and matched for age, gender and educational level. BDI = Beck Depression Inventory; EDSS = Expanded Disability Status Scale; MS = Multiple Sclerosis; SD = Standard Deviation.*

**Mnemonic similarity task and neuropsychological testing**

There was no difference among groups for information processing speed performances. There was also no difference for “global” visuospatial episodic memory tests regarding learning, long term recall or recognition. However, we found a significant decrease of pattern separation performances in PweMS compared to healthy controls matched on age, gender and education level (27.07 vs 40.01,  $p=0.028$ ). We also found a significant higher pattern completion rate in PweMS than in healthy controls (56.11 vs 40.95,  $p=0.0021$ ) (table2). Because patients and controls were comparable for each demographical or clinical variable except for depression and disability, we looked for potential confusion biases induced by these variables. However, no correlation was found between pattern separation rate and disability (EDSS) or depression (BDI) in PweMS (respectively  $r=-0.17$ ,  $p=0.49$  and  $r=-0.076$ ,  $p=0.75$ ).

	Early MS	Healthy controls	p-value
Information processing speed			
- CSCT, mean (SD)	52.79 (7.87)	52.21 (6.73)	0.81
Visuospatial episodic memory			
- BVMT-R learning, mean (SD)	29.53 (3.20)	28.68 (6.07)	0.60
- BVMT-R delay recall, median [range]	11 [10 - 12]	12 [7 - 12]	0.23
- BVMT-R recognition, median [range]	6 [5 - 6]	6 [5 - 6]	0.61
Mnemonic similarity test			
- pattern separation <sup>#</sup> , mean (SD)	27.07 (17.89)	40.01 (6.90)	<b>0.028</b>
- pattern completion <sup>#</sup> , mean (SD)	56.11 (13.03)	40.95 (15.09)	<b>0.0021</b>
- traditional recognition <sup>#</sup> , mean (SD)	88.89 (4.20)	85.16 (7.14)	0.059

Table 2: Neuropsychological and mnemonic similarity task results of patients and healthy controls. BVMT-R = Brief visuospatial memory test revised; CSCT = Computerized Speed Cognitive Test; SD = Standard Deviation. <sup>#</sup> Bias corrected scores (see method).

## Discussion

Our results demonstrated that pattern separation performances are decreased in a sample of PweMS characterized by absence of detectable information processing speed and visuo-spatial memory impairment, as compared to a sample of healthy controls matched on age, gender and education level. We also found a higher pattern completion rate in PweMS than in healthy controls (the complementary process of pattern separation), potentially explained by impairment in lure discrimination (*i.e.* systematically respond “old” for lure items) or poor initial encoding.

We controlled these results for confounders and sources of variability. First, patients and healthy controls were matched on age because it has been demonstrated that pattern separation performances are negatively correlated with age<sup>25,26</sup>. Second, we demonstrated that patient and controls performed equally in the Computerized Speed Cognitive Test (CSCT), excluding encoding deficit due to impaired attention or slowing of information processing speed. Third, even though PweMS were more depressed than healthy controls (as usually described<sup>1</sup>), BDI score did not correlate with pattern separation performances, potentially excluding bias linked to psychiatric comorbidity, poor motivation or attention deficit.

While verbal or visuospatial episodic memory impairment have been reported from the stage of CIS in previous studies, we did not report here differences between groups in BVMT-R sub-scores. However, previous cross-sectional studies often used larger sample sizes or more severely affected subjects with early MS, and reported differences at the individual level (*i.e.* with calculation of cognitive z-scores and number of impaired subjects) rather than at the group level<sup>27</sup>. Moreover, we can notice that in our study, patients and controls had a high educational level meaning a high cognitive reserve protecting them against memory impairment, as measured with conventional tests. Then, it is important to highlight that behavioural pattern separation tasks can identify subtle memory decline in patients deemed “cognitively intact”<sup>28</sup>.

Loss of pattern separation performances have been described in neurodegenerative disorders such as Alzheimer’s disease<sup>25,29</sup> and neurodevelopmental disorders such as schizophrenia<sup>30</sup>. We extend for the first time this concept to a neuroimmune disorder such as MS. Interestingly, during the course of Alzheimer’s disease, deficit in pattern separation occurred prior to

dementia, from the stage of mild cognitive impairment (MCI)<sup>25</sup>. We also demonstrated here that loss of pattern separation performances occurred early during the course of MS, even in apparently “cognitively intact” patients as measured with CSCT or BVMT-R. Then, the behavioral pattern separation task provides a sensitive measure of episodic memory impairment and may be useful to screen for early hippocampal dysfunction during the course of MS.

Studies on rodents have demonstrated that some hippocampal subfields can be more vulnerable than others to peripheral inflammation and cytokines release or to microglial activation<sup>31</sup>. Given that dentate gyrus morphological abnormalities have been described in MS<sup>11,12</sup>, our results give a neuropsychological support of an early dentate gyrus disruption during the course of MS. The bias towards pattern completion (*i.e.* incorrectly recognized a “similar” item as an “old” studied item) measured in PweMS could be interpreted as the counterpart of pattern separation impairment because these two processes are often considered as working concurrently<sup>29</sup>. In this way, previous rodents and human studies suggested that when dentate gyrus is unable to perform pattern separation, CA3 (and its connections to CA1) could balance this deficit by overwriting previous representations<sup>16,32</sup>.

From a cognitive neuropsychological point of view, because pattern separation can be considered as the preliminary step before encoding, our findings converge to previous conclusions arguing that encoding is impaired early in MS whereas storage, retrieval and recognition are preserved<sup>19,20,21</sup>. However, and contrary to previous conclusions, we can argue that encoding impairment in MS would not be due to attentional deficit or dysexecutive syndrome due to global brain damage or demyelination but to more specific hippocampal damage resulting in loss of pattern separation performances.

The first limitation of this work is its small sample size and our results need to be confirmed in larger studies. Future functional MRI and quantitative imaging experiments (with morphological MRI or diffusion tensor imaging) will need to confirm our hypothesis by demonstrating correlations between loss of pattern separation performances and dentate gyrus dysfunction/degeneration. It will be also interesting to look at functional structural hippocampal connectivity in PweMS with pattern separation impairment, to assess the integrity of the fornix, prefrontal cortex, entorhinal cortex and perforant pathway, that can be

potentially damaged in MS and involved in pattern separation<sup>2,33,34,35</sup>. Furthermore, it will be interesting to perform longitudinal studies in order to demonstrate that pattern separation impairment precedes and predicts larger deficit in episodic memory, as measured with conventional tests.

To conclude, by demonstrating loss of pattern separation performances in PweMS, we provide functional evidence to extend to the human disease the concept of the selective dentate gyrus disruption observed at the early phase of experimental MS in rodents. This work is also the first step toward the development of more sensitive tests to detect early cognitive impairment in MS to better screen patients eligible for neuroprotective clinical trials or neurorehabilitation strategies.

## References

1. Chiaravalloti ND, DeLuca J. Cognitive impairment in multiple sclerosis. *Lancet Neurol.* 2008;7:1139–1151.
2. Rocca MA, Amato MP, De Stefano N, et al. Clinical and imaging assessment of cognitive dysfunction in multiple sclerosis. *Lancet Neurol.* 2015;14:302–317.
3. Feuillet L, Reuter F, Audoin B, et al. Early cognitive impairment in patients with clinically isolated syndrome suggestive of multiple sclerosis. *Mult Scler.* 2007;13:124–127.
4. Sicotte NL, Kern KC, Giesser BS, et al. Regional hippocampal atrophy in multiple sclerosis. *Brain.* 2008;131:1134–1141.
5. Dutta R, Chang A, Doud MK, et al. Demyelination causes synaptic alterations in hippocampi from multiple sclerosis patients. *Ann Neurol.* 2011;69:445–454.
6. Hulst HE, Schoonheim MM, Roosendaal SD, et al. Functional adaptive changes within the hippocampal memory system of patients with multiple sclerosis. *Hum Brain Mapp.* 2012;33:2268–2280.
7. Nisticò R, Mango D, Mandolesi G, et al. Inflammation subverts hippocampal synaptic plasticity in experimental multiple sclerosis. *PLoS One.* 2013;8:e54666.
8. Di Filippo M, de Iure A, Giampà C, et al. Persistent activation of microglia and NADPH drive hippocampal dysfunction in experimental multiple sclerosis. *Sci Rep.* 2016;6:20926.
9. Kim DY, Hao J, Liu R, Turner G, Shi F-D, Rho JM. Inflammation-mediated memory dysfunction and effects of a ketogenic diet in a murine model of multiple sclerosis. *PLoS One.* 2012;7:e35476.
10. Longoni G, Rocca MA, Pagani E, et al. Deficits in memory and visuospatial learning correlate with regional hippocampal atrophy in MS. *Brain Struct Funct.* 2015;220:435–444.
11. Gold SM, Kern KC, O'Connor M-F, et al. Smaller cornu ammonis 2-3/dentate gyrus volumes and elevated cortisol in multiple sclerosis patients with depressive symptoms. *Biol Psychiatry.* 2010;68:553–559.
12. Rocca MA, Longoni G, Pagani E, et al. In vivo evidence of hippocampal dentate gyrus expansion in multiple sclerosis. *Hum Brain Mapp.* 2015;36:4702–4713.
13. Rolls ET. The mechanisms for pattern completion and pattern separation in the hippocampus. *Front Syst Neurosci.* 2013;7:74.
14. Yassa MA, Stark CEL. Pattern separation in the hippocampus. *Trends Neurosci.* 2011;34:515–525.
15. McHugh TJ, Jones MW, Quinn JJ, et al. Dentate gyrus NMDA receptors

- mediate rapid pattern separation in the hippocampal network. *Science*. 2007;317:94–99.
16. Neunuebel JP, Knierim JJ. CA3 retrieves coherent representations from degraded input: direct evidence for CA3 pattern completion and dentate gyrus pattern separation. *Neuron*. 2014;81:416–427.
  17. Bakker A, Kirwan CB, Miller M, Stark CEL. Pattern separation in the human hippocampal CA3 and dentate gyrus. *Science*. 2008;319:1640–1642.
  18. Berron D, Schütze H, Maass A, et al. Strong Evidence for Pattern Separation in Human Dentate Gyrus. *J Neurosci*. 2016;36:7569–7579.
  19. DeLuca J, Gaudino EA, Diamond BJ, Christodoulou C, Engel RA. Acquisition and storage deficits in multiple sclerosis. *J Clin Exp Neuropsychol*. 1998;20:376–390.
  20. Olivares T, Nieto A, Sánchez MP, Wollmann T, Hernández MA, Barroso J. Pattern of neuropsychological impairment in the early phase of relapsing-remitting multiple sclerosis. *Mult Scler*. 2005;11:191–197.
  21. Müller S, Saur R, Greve B, et al. Recognition performance differentiates between elderly patients in the long term course of secondary progressive multiple sclerosis and amnesic mild cognitive impairment. *Mult Scler*. 2013;19:799–805.
  22. Polman CH, Reingold SC, Edan G, et al. Diagnostic criteria for multiple sclerosis: 2005 revisions to the “McDonald Criteria.” *Ann Neurol*. 2005;58:840–846.
  23. Kirwan CB, Stark CEL. Overcoming interference: an fMRI investigation of pattern separation in the medial temporal lobe. *Learn Mem*. 2007;14:625–633.
  24. Liu KY, Gould RL, Coulson MC, Ward EV, Howard RJ. Tests of pattern separation and pattern completion in humans-A systematic review. *Hippocampus*. 2016;26:705–717.
  25. Stark SM, Yassa MA, Lacy JW, Stark CEL. A task to assess behavioral pattern separation (BPS) in humans: Data from healthy aging and mild cognitive impairment. *Neuropsychologia*. 2013;51:2442–2449.
  26. Holden HM, Toner C, Pirogovsky E, Kirwan CB, Gilbert PE. Visual object pattern separation varies in older adults. *Learn Mem*. 2013;20:358–362.
  27. Sumowski JF, Rocca MA, Leavitt VM, et al. Brain reserve and cognitive reserve protect against cognitive decline over 4.5 years in MS. *Neurology*. 2014;82:1776–1783.
  28. Feinstein A, Lapshin H, O’Connor P, Lanctôt KL. Sub-threshold cognitive impairment in multiple sclerosis: the

- association with cognitive reserve. *J Neurol.* 2013;260:2256–2261.
29. Ally BA, Hussey EP, Ko PC, Molitor RJ. Pattern separation and pattern completion in Alzheimer’s disease: evidence of rapid forgetting in amnesic mild cognitive impairment. *Hippocampus.* 2013;23:1246–1258.
30. Das T, Ivleva EI, Wagner AD, Stark CEL, Tammenga CA. Loss of pattern separation performance in schizophrenia suggests dentate gyrus dysfunction. *Schizophr Res.* 2014;159:193–197.
31. Czerniawski J, Guzowski JF. Acute neuroinflammation impairs context discrimination memory and disrupts pattern separation processes in hippocampus. *J Neurosci.* 2014;34:12470–12480.
32. Yassa MA, Stark SM, Bakker A, Albert MS, Gallagher M, Stark CEL. High-resolution structural and functional MRI of hippocampal CA3 and dentate gyrus in patients with amnesic Mild Cognitive Impairment. *NeuroImage.* 2010;51:1242–1252.
33. Pidgeon LM, Morcom AM. Cortical pattern separation and item-specific memory encoding. *Neuropsychologia.* 2016;85:256–271.
34. Bennett IJ, Stark CEL. Mnemonic discrimination relates to perforant path integrity: An ultra-high resolution diffusion tensor imaging study. *Neurobiol Learn Mem.* 2016;129:107–112.
35. Bennett IJ, Huffman DJ, Stark CEL. Limbic Tract Integrity Contributes to Pattern Separation Performance Across the Lifespan. *Cereb Cortex.* 2015;25:2988–2999.

**Conclusion, limitations  
and perspectives**

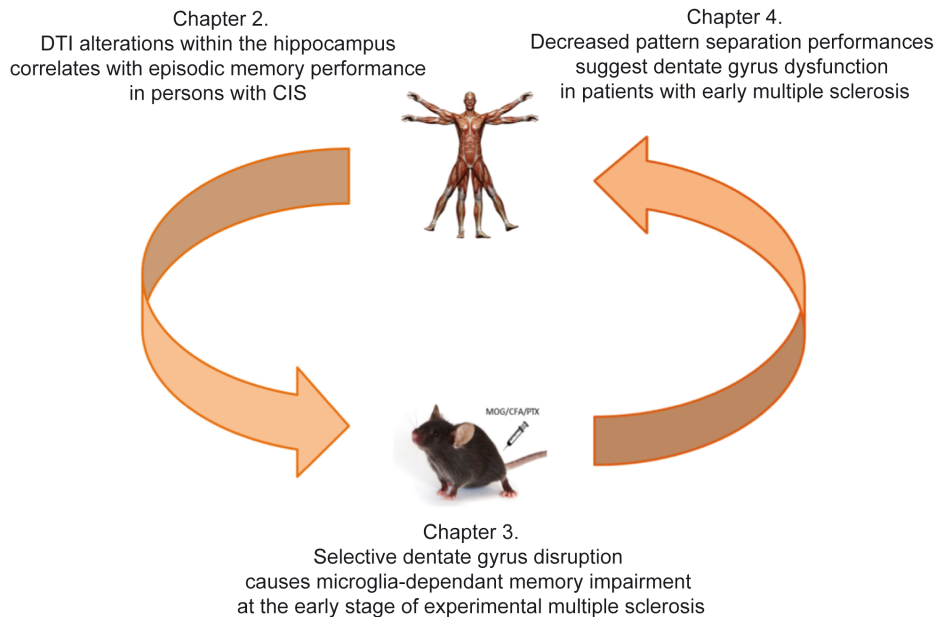


## Chapter 5: Discussion and perspectives

### 1. Bullet points summary of the thesis

- In chapter 2, we demonstrated that:
  - Water diffusivity within the hippocampus is significantly altered in persons with clinically isolated syndrome (PwCIS) compared with healthy controls while there is no global brain atrophy and no hippocampal atrophy.
  - In PwCIS, hippocampal mean diffusivity (MD) strongly and independently correlates with early deficit in episodic memory (adjusted for age, gender, depression and T2-lesion load).
  - Hippocampal MD discriminates between memory-impaired and memory-preserved PwCIS.
  
- In chapter 3, we demonstrated that:
  - Dentate gyrus structure and function are more vulnerable than other hippocampal subfields at the early stage of experimental autoimmune encephalomyelitis (EAE).
  - Selective dentate gyrus disruption causes early memory impairment in EAE-mice.
  - Microglial activation might be an important trigger of the early dentate gyrus disruption.
  - Early memory impairment in EAE-mice can be prevented with minocycline, an agent with microglial inhibitor properties.
  - *In vivo* diffusion tensor imaging can measure early dentate gyrus degeneration and monitor the therapeutic effect of minocycline.
  
- In chapter 4, we demonstrated that:
  - Pattern separation performances are decreased in patients with early MS, suggesting early dentate gyrus dysfunction.

- Behavioral pattern separation task detect neuropsychological impairment while information processing speed or “classical” visuospatial episodic memory tests are not altered.



*Summary figure of the thesis*

## 2. Limitations of the work

The first limitation we have to keep in mind is that a large part of the conclusions from this thesis were made on the EAE-model of multiple sclerosis. Obviously, **EAE is not MS** and we have to be very conscious before translating findings from a mouse model to the human disease. Particularly, the aim of this thesis was to understand *early* pathophysiological mechanisms leading to memory impairment. We have defined this stage in the human disease as patients with clinically isolated syndrome suggestive of MS. However, the exact equivalent in the MOG-EAE model is not easy to define. We chose to study mice 20 days after immunization because it was shortly after the beginning of the remission of the initial relapse,

and before the beginning of the chronic-progressive stage of this model. However, we can question this strategy in a model that usually experience only one single relapse.

In line with this consideration, we do not have strictly demonstrated early selective dentate gyrus disruption in the human disease (as we did in EAE-mice) but we only suggested it. Indeed, we have demonstrated early hippocampal microstructural damage during the course of MS and we have also demonstrated decreased performances on a test that it is dentate-gyrus dependent (but not dentate gyrus specific). Then, we have to be moderate before generalizing our findings.

One other main limitation of our work is the use of minocycline in EAE-mice experiments. We used minocycline in order to inhibit early microglial activation and then to demonstrate that early dentate gyrus disruption is caused by microglial activation. However, **minocycline is not a specific inhibitor of microglial activation**. It has been demonstrated that under inflammatory conditions, minocycline can also inhibit T-cell infiltration, cytokine release, or metalloprotease<sup>1</sup>. To avoid this bias, we used direct infusion of minocycline within the dentate gyrus of EAE-mice, but even in this condition, we can not fully exclude that minocycline could have a direct neuroprotective effect, independently of microglial activation<sup>1</sup>. Then, we have to be cautious on the putative mechanisms underlying early dentate gyrus disruption.

We are currently working on several projects in order to address these limitations, as described bellow.

### **3. Future directions in clinical research:**

#### **a. Hippocampal subfields analyses in patients with early MS**

Our work has pinpointed a differential vulnerability of the dentate gyrus in experimental MS and we believe that these findings might also be true in patients with early MS, regarding their early impairment in pattern separation performances (chapter 3 and 4). Future studies will need to capture directly the corresponding morphological and functional changes within the dentate gyrus of patients with early MS to confirm these results. Indeed, previous studies that looked for **regional vulnerability** within the hippocampus of persons with MS did not investigate the early stages of the disease (*i.e.* clinically isolated syndrome), precluding any

definitive conclusions to early vulnerability<sup>2,3,4,5</sup>. Furthermore, these past studies used morphological MRI acquisition and post-processing technics such as manual segmentation of hippocampal subfields, voxel based morphometry or radial mapping, that are not able to discriminate dentate gyrus from CA2, CA3 and CA4 (Fig. 1). These morphological studies provided contradictory conclusions which are probably due to the different technical approaches and the different cohorts of patients. Finally modifications of morphology and volumes (atrophy) might not be the most appropriate tools to capture early modifications.

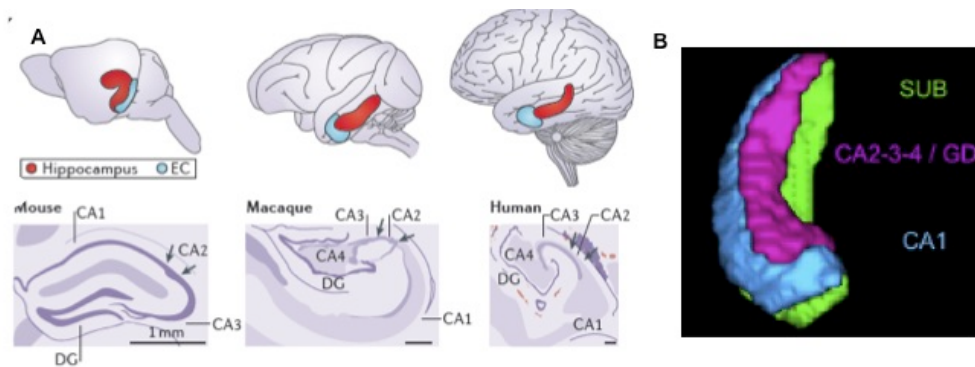


*Fig. 1: Hippocampal subfields organization across mammalian species (A) and MRI segmentation of human hippocampi (B). (A) Differential anatomy of hippocampus (red) and entorhinal cortex (blue) in brains of rats, macaque monkeys and humans (upper panel). Drawings of Nissl cross-sections of mouse, rhesus and human hippocampi. (lower panel). (B) Projection of Voxel Based Morphometry of the right hippocampus. Note that CA2/3/4 and dentate gyrus can not be distinguished. CA: Cornu Ammonis DG: dentate gyrus, EC: Entorhinal Cortex, SUB: Subiculum (Adapted from Strange et al., Nat Rev Neurosci, 2014 and De Flores et al., Neuroscience, 2015)*

Instead of using morphological MRI, **we favored DTI** for its ability to capture early microstructural modifications. Our work in EAE demonstrated that mouse hippocampal subfields can be targeted by DTI technics and that it can measure differential vulnerability of these subfields with histological validations. Basic intrinsic hippocampal anatomy, histology and circuitry are maintained across mammalian species. However, hippocampal folding and compaction are different between rodents and humans (Fig. 1). Then, the direct transposition of our DTI technics from mouse hippocampus to human hippocampus is challenging because dendrites are differentially compacted across species (Fig. 1). Furthermore, scan times can be

long in anesthetized rodents (52 minutes in the technic used in chapter 3) but this is less compatible with clinical research.

Then, we have to deal with **technical challenges** to perform DTI of hippocampal subfields in humans. In the future we aim to develop diffusion MRI methods to assess precise hippocampal alterations, as well as post-processing methods to extract quantitative metrics from the hippocampus of individual subjects. We will advance our diffusion MRI methods by developing new sequences and post-processing pipelines, to improve the precision of our established biomarkers. This should increase the sensitivity of our imaging metrics to changes in cognitive status.

From the methodological development point of view, we will combine effort with partners in MR physics (Dr Bassem Hiba) and in image post-processing (Dr Pierrick Coupé). We will conduct this development on the new 3T magnet (Siemens, Prisma) that has been installed recently in the Bordeaux Institute of Bioimaging. This magnet whose first copy was installed in a US center in May 2014 shows very high performances not found on any other MR system (high performance gradient system of 80 mT/m), which provides the unique opportunity to encode the diffusion with much more resolution.

We plan to improve the acquisition of diffusion MRI by using the “zooming” strategy on the hippocampus: two-dimensional, spatially-selective radiofrequency (RF) excitation pulses will be combined with a reduction in the FOV (i.e. zooming) to decrease the number of k-space acquisition lines in single-shot echo-planar imaging (EPI), therefore shortening the EPI echo train and reducing susceptibility artifacts. We also plan to set up readout-segmented EPI using simultaneous multislice acceleration. Readout-segmented echo-planar imaging can provide high quality diffusion data because it is less prone to distortion and blurring artifacts than single-shot echo-planar imaging. Readout segmentation of k space allows shorter echo-spacing and echo train duration, resulting in reduced image distortion and blurring, respectively, particularly at higher resolution and higher field. However, these benefits come at the expense of longer scan times because the segments are acquired in multiple repetition times. Scan time can be shortened by reducing the TR duration with simultaneous multislice acceleration.

We plan to combine these acquisition strategies with advanced post-processing methods developed by the team of Dr Coupé. This group has pioneered MRI super resolution which

enables to efficiently improve image resolution at the post processing stage<sup>6</sup> and which has been implemented recently for diffusion MRI<sup>7</sup>. This strategy should enable to push up the resolution to submillimetric isotropic from 1 mm resolution acquired data. We will also work on segmentation methods to delineate the hippocampal layers by using the concept of non-local label fusion to perform the segmentation process using a library of manually labeled example cases as already developed by Dr Coupé<sup>8</sup>. Our first results in this direction are encouraging (Fig 2).

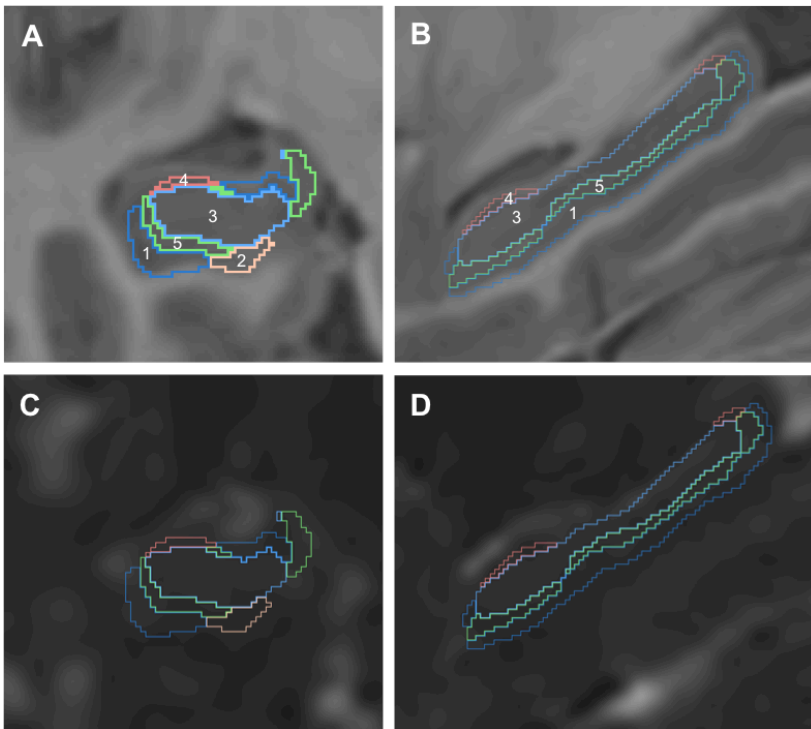


*Fig. 2: Preliminary results showing high-resolution hippocampal segmentation. Hippocampal subfields masks are automatically generated on T1-weighted images (A and B) and can be superimposed to mean diffusivity maps (C and D) in order to measure early microstructural damage in the different hippocampal subfields. 1. CA1; 2. Subiculum; 3. Dentate gyrus; 4. CA2/3; 5. Stratum radiatum/lacunosum/moleculare.*

From the clinical validation point of view, we aim to determine which biomarker shows the greatest difference between MS patients and healthy controls and to determine which **imaging biomarker** or combination of imaging biomarkers accounts for the most variance in cognitive function. In this aim, we will perform measurements of new metrics of hippocampal anatomy in relevant MS patients, and will relate these biomarkers to neuropsychological measures of cognition.

b. Clinical trials: Preventing memory impairment in multiple sclerosis with minocycline

Minocycline is a second-generation tetracycline approved by drug agencies for its antibiotic properties<sup>1</sup>. It has been used for decades, essentially in acne vulgaris, and long term treatment up to 200mg/day is recognized to be **safe and well tolerated**. Furthermore, minocycline is a lipophilic drug that easily cross the blood-brain barrier<sup>9</sup> and that has several anti-inflammatory and immunomodulatory properties. Indeed, it has been demonstrated that during CNS inflammation, minocycline could decrease T-cell proliferation, could prevent blood brain barrier disruption through metalloproteinase inhibition, and could selectively inhibit pro-inflammatory polarization of microglial cells<sup>9,10</sup>.

In this context, pilot studies and phase II clinical trials of minocycline in patients with RRMS have suggested that minocycline can be efficient (alone or in add-on therapy) to prevent demyelination and relapses<sup>11,12</sup>. Metz and collaborators have also reported during the 31<sup>st</sup> congress of theECTRIMS (Barcelona, 2015) that minocycline (200mg/j) reduces conversion of the first clinical demyelinating event to clinically definite MS in a phase III double-blind placebo controlled multicentric clinical trial.

We have demonstrated in chapter 3 that systemic minocycline treatment can **prevent memory impairment** in EAE-mice (20 days post-injection) when administrated daily since the first clinical symptoms of EAE (7 days post-injections). Furthermore, a recent study in another EAE-model demonstrated that minocycline could prevent memory dysfunction at the chronic phase of the disease, after the recovery of motor symptoms, suggesting that our results might still be relevant at later stages<sup>13</sup>. Then, if we extrapolate these findings to the human disease, we can hypothesize that daily treatment with minocycline at the stage of CIS could prevent

memory impairment later on, thanks to inhibition of microglial activation.

Then, it would be now of great interest to evaluate the neuroprotective effect of minocycline in patients with CIS or early MS. We are currently considering the opportunity of a **phase III clinical trial** where memory performances would be the primary outcome measure and hippocampal DTI and morphology would be secondary endpoints, after 2 years of minocycline treatment compared to placebo. Minocycline could be administrated as both monotherapy or as an **add-on therapy** to treatment approved in the treatment of CIS.

#### **4. Future directions in fundamental research:**

- a. Explaining early selective dentate gyrus disruption in multiple sclerosis:  
the complement hypothesis

We have demonstrated in chapter 3 a differential vulnerability of the dentate gyrus to microglial activation at the early stage of EAE. However, we did not identify the molecular mechanisms explaining such a selective degenerative process. We described at the transcriptional level a differential pattern of microglial activation within the dentate gyrus, that was absent or less pronounced in CA1. Given that there could be regional differences in microglial phenotype in the brain<sup>14</sup>, we can hypothesized that microglia is already “primed” in the dentate gyrus to control newborn neurons and circuits in physiological conditions, leading to the early aberrant activation that we described here in case of inflammatory disease.

Adult neurogenesis occurs in the dentate gyrus throughout life and is characterized by **synaptic pruning** mechanisms corresponding to the elimination of immature synapses/circuits by microglia<sup>15</sup>. The physiological process of synaptic pruning, which corresponds to the phagocytosis of supernumerary and improper synapses, is thus particularly important in the dentate gyrus and is **complement-dependent**<sup>16</sup>. Improper synapses accumulate C1q, which leads to downstream activation of C3 (cleaved in C3a and C3b by C3 convertase). Then, C3b covers the membrane of the neurons and provides the signal for phagocytosis by microglia through CR3 receptors. Furthermore, a recent study has demonstrated on post-mortem MS brain that C1q expression and C3 activation were increased in MS hippocampi<sup>17</sup>. Then, we decided to explore the complement pathway as a good candidate molecular pathway to explain the aberrant and selective dendritic pruning observed in the dentate gyrus of EAE-

mice.

We have already started preliminary experiments that support this complement hypothesis (Fig. 3). Indeed, we showed by RT-qPCR experiments after selective microdissection of the stratum radiatum of CA1 and of the molecular layer of the dentate gyrus that there is an **overexpression of C3 gene selectively in the dentate gyrus** (compared to CA1). Furthermore, we were able to **prevent memory impairment** in EAE-mice after a systemic treatment with rosmarinic acid<sup>18</sup> (an **inhibitor of C3 convertase**). These results are the first evidence supporting the role of the complement pathway in the mediation of pathological microglia-neurons interactions selectively in the dentate gyrus of EAE-mice. We have to confirm these preliminary data by using other inhibitors, knock-out gene experiments and histological studies to elucidate how such complement system might play a key role in the microglia-dependant vulnerability of the dentate gyrus. We recently obtained a post doctoral fellow grant from ARSEP (Association pour la Recherche contre la Sclérose en Plaques) for an additional year in the lab, working on this topic.

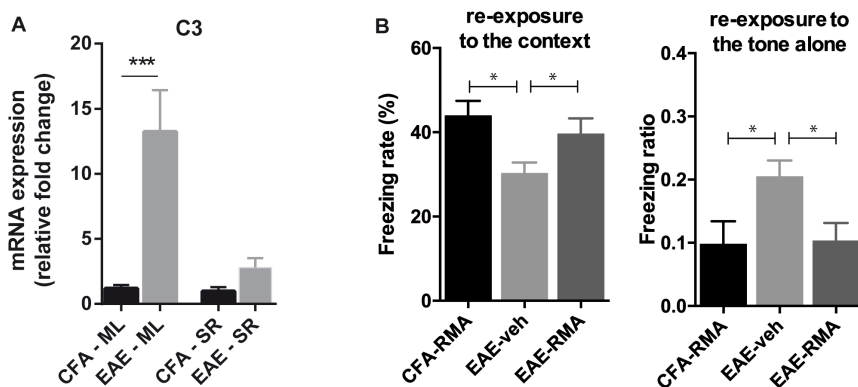


Fig. 3: Preliminary results suggesting a complement-C3 dependant mechanism leading to dentate gyrus vulnerability and memory impairment in EAE (n=4 to n=10 per condition). A. Selective overexpression of C3 gene in the molecular layer (ML) of the dentate gyrus of EAE-mice at 20 d.p.i., compared to CFA-mice while there is no overexpression of C3 gene in the stratum radiatum (SR). B. Compared to EAE-veh (vehicule) mice, EAE-RMA (rosmarinic acid, an inhibitor of C3-convertase activity) mice displayed normal fear memory with enhanced conditioned freezing to the correct predictor of the threat, and reduced conditioned freezing to the non-predictive tone in a familiar and safe box. EAE-RMA mice performed as well as CFA-RMA control mice (n=15 per group).

b. Toward more specific *in vivo* marker of the dentate gyrus vulnerability

By using *in vivo* DTI of the hippocampus in chapter 3, we showed that we can capture non-invasively the vulnerability of the dentate gyrus at the early stage of experimental MS as a decrease of fractional anisotropy (FA) and axial diffusivity (AD). Dendritic alterations were the main factors driving the reduction of FA and AD. Nevertheless, the strength of the relationship between reduced FA (or AD) and dendritic content was not very strong ( $r^2=0.32$  and  $r^2=0.22$  for FA and AD respectively). Then, in order to extrapolate our findings to humans, we expect to identify still more sensitive and specific *in vivo* imaging method to quantify the neurodegenerative process of the dentate gyrus.

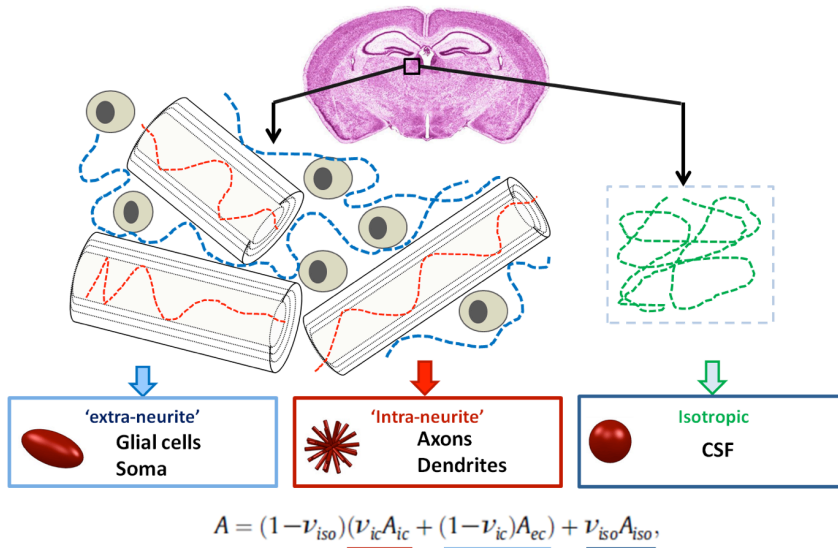
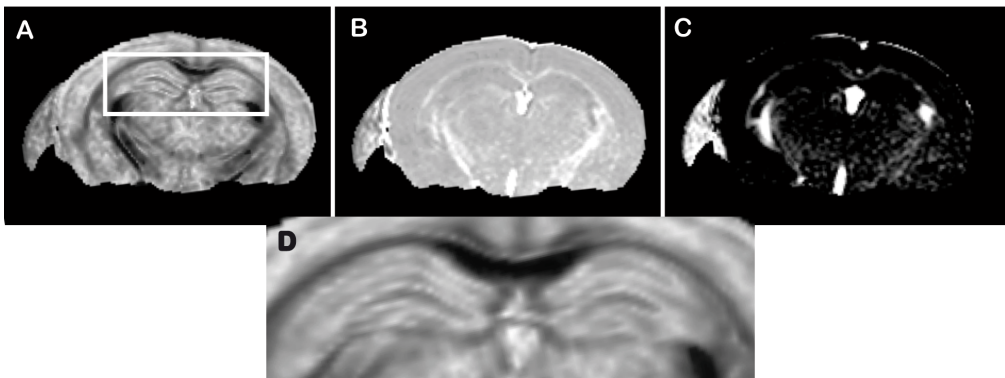


Fig. 4: The NODDI model assumes that water protons in neuronal tissue can be considered as belonging to three different pools: (i) free water, modeling isotropic diffusion such as in areas contaminated by CSF; (ii) restricted water within dispersed sticks, modeling dendrites and axons; and (iii) anisotropically hindered water, modeling diffusion within glial cells, neuronal cell bodies and the extracellular environment. In the NODDI framework, diffusion data are acquired and parametric maps describing the properties of the compartments within which water pools diffuse are obtained fitting the model to the data. Such parametric maps represent indices such as neurite density (ND) and neurite orientation dispersion (OD). ND estimates the fraction of axons and dendrites within tissue. OD quantifies how parallel neurites are to each other. Low OD is indicative of coherent organization, since the orientation of single neurite element does not deviate much from the mean overall orientation. On the other hand, high OD occurs when neurites are dispersed in space and their orientations vary considerably from each other.

DTI is very useful but is a simplistic model of water diffusion. An important research field in diffusion MRI consists in modeling water diffusion more accurately to provide more specific information of the tissue microstructure. Among others, the **NODDI** model (for **neurite orientation dispersion and density imaging**) was introduced in 2012<sup>19</sup> and is appealing for two main reasons. Firstly, this is a three compartments model that provides parametric maps directly related to the neurites (neurite density, neurite orientation dispersion) (Fig. 4). Secondly, the NODDI model can be fitted with the acquisition of only two-shell (2 b values) high-angular-resolution diffusion imaging which can be performed in a clinically feasible time.



*Fig. 5: We have conducted pilot experiments in mice using a 3D sampling of Fourier space (instead of the classical 2D strategy) and echo-navigator to reduce physiological motion effects. Diffusion-weighted images were acquired with two b-values. 22 diffusion directions were encoded for the first shell ( $b=1000s.mm^2$ ) and 43 for the second shell ( $b=2700s.mm^2$ ) according to Tournier et al<sup>20</sup>. Two images without diffusion weighting (called 'b0') were acquired per shell. To obtain the same  $80\mu m \times 80\mu m$  in plane resolution as the one we used before for the layer-by-layer analysis, our protocol currently last 1h and 50 minutes per mouse. NODDI model was fitted and performed on the NODDI data-set using the NODDI Matlab toolbox, ([http://www.nitrc.org/projects/noddi\\_toolbox/](http://www.nitrc.org/projects/noddi_toolbox/)) for reconstruction of orientation dispersion (A, zoom in D), neurite density (B) and CSF maps (C).*

The NODDI model has never been applied to investigate the detailed internal structure of the hippocampus and the parametric maps derived from this mathematical model have not been validated histologically to confirm their specificity. Then, we developed a high-resolution diffusion MRI acquisition method that could reveal hippocampal architecture in live rodents in

acceptable timeframe and we set-up an appropriate post-processing pipeline for the reconstruction of NODDI maps (Fig. 4).

Now, we aim at validating the parametric maps against histological markers in the non-injured hippocampus and finally we aim at testing this method for its ability to detect early microstructural changes in EAE model compared to what DTI can do; and also to monitor the course of the alterations during repeated exams. We have already collected the data for EAE mice (n=18) and CFA mice (n=18) explored at 20 dpi and we are currently analyzing the results. Our final aim is to apply this technics in persons with early MS to understand early cellular alterations in different hippocampal subfields.

## **5. General conclusion.**

Among hippocampal subfields, the dentate gyrus is the most vulnerable to early inflammation in experimental autoimmune encephalomyelitis and its disruption leads to early memory impairment. In humans the same might be true because patients with MS at the early stage of the disease show loss of pattern separation performances. Furthermore, our results demonstrate that early memory impairment can be experimentally prevented in EAE-mice by early microglial inhibition with the FDA-approved drug minocycline and we might envision testing this finding in patient trough a clinical trial. Finally, hippocampal damage can be monitor *in vivo* with diffusion tensor imaging, offering new perspectives as surrogate endpoints in clinical trials. We are currently able to quantify clinically-relevant alterations in patients within the whole hippocampus but our ability to isolate each layer specifically in EAE-mice drive us toward local diffusion analyses in humans too.

We expect that such translational research from rodents to patients and from patients to rodents could still provide new insight into the pathophysiology of memory impairment in multiple sclerosis. Imaging is one of the important method to bridge the clinical and the experimental approaches.

## References

1. Möller, T. *et al.* Critical data-based re-evaluation of minocycline as a putative specific microglia inhibitor. *Glia* **64**, 1788–1794 (2016).
2. Rocca, M. A. *et al.* In vivo evidence of hippocampal dentate gyrus expansion in multiple sclerosis. *Hum. Brain Mapp.* **36**, 4702–4713 (2015).
3. Gold, S. M. *et al.* Smaller cornu ammonis 2-3/dentate gyrus volumes and elevated cortisol in multiple sclerosis patients with depressive symptoms. *Biol. Psychiatry* **68**, 553–559 (2010).
4. Sicotte, N. L. *et al.* Regional hippocampal atrophy in multiple sclerosis. *Brain*. **131**, 1134–1141 (2008).
5. Longoni, G. *et al.* Deficits in memory and visuospatial learning correlate with regional hippocampal atrophy in MS. *Brain Struct. Funct.* **220**, 435–444 (2015).
6. Manjón, J. V., Coupé, P., Buades, A., Collins, D. L. & Robles, M. MRI superresolution using self-similarity and image priors. *Int. J. Biomed. Imaging* **2010**, 425891 (2010).
7. Coupé, P., Manjón, J. V., Chamberland, M., Descoteaux, M. & Hiba, B. Collaborative patch-based super-resolution for diffusion-weighted images. *NeuroImage* **83**, 245–261 (2013).
8. Coupé, P. *et al.* Patch-based segmentation using expert priors: application to hippocampus and ventricle segmentation. *NeuroImage* **54**, 940–954 (2011).
9. Chen, X. *et al.* The prospects of minocycline in multiple sclerosis. *J. Neuroimmunol.* **235**, 1–8 (2011).
10. Kobayashi, K. *et al.* Minocycline selectively inhibits M1 polarization of microglia. *Cell Death Dis.* **4**, e525 (2013).
11. Zhang, Y. *et al.* Pilot study of minocycline in relapsing-remitting multiple sclerosis. *Can. J. Neurol. Sci.* **35**, 185–191 (2008).
12. Metz, L. M. *et al.* Glatiramer acetate in combination with minocycline in patients with relapsing–remitting multiple sclerosis: results of a Canadian, multicenter, double-blind, placebo-controlled trial. *Mult. Scler.* **15**, 1183–1194 (2009).
13. Di Filippo, M. *et al.* Persistent activation of microglia and NADPH oxidase [corrected] drive hippocampal dysfunction in experimental multiple sclerosis. *Sci. Rep.* **6**, 20926 (2016).
14. Aguzzi, A., Barres, B. A. & Bennett, M. L. Microglia: scapegoat, saboteur, or something else? *Science* **339**, 156–161 (2013).
15. Paolicelli, R. C. *et al.* Synaptic pruning by microglia is necessary for normal brain development. *Science* **333**, 1456–1458 (2011).
16. Stevens, B. *et al.* The classical complement cascade mediates CNS synapse elimination. *Cell* **131**, 1164–1178 (2007).
17. Michailidou, I. *et al.* Complement C1q-C3-associated synaptic changes in

multiple sclerosis hippocampus. *Ann. Neurol.* **77**, 1007–1026 (2015).

18. Englberger, W. *et al.* Rosmarinic acid: a new inhibitor of complement C3-convertase with anti-inflammatory activity. *Int. J. Immunopharmacol.* **10**, 729–737 (1988).

19. Zhang, H., Schneider, T., Wheeler-Kingshott, C. A. & Alexander, D. C. NODDI: practical in vivo neurite orientation

dispersion and density imaging of the human brain. *NeuroImage* **61**, 1000–1016 (2012).

20. Tournier, J.-D., Calamante, F. & Connelly, A. Determination of the appropriate b value and number of gradient directions for high-angular-resolution diffusion-weighted imaging. *NMR Biomed.* **26**, 1775–1786 (2013).

*Lady L. savait aujourd'hui qu'il y avait une contradiction entre ce qu'Armand lui enseignait et sa façon d'être, entre cette liberté absolue qu'il invoquait et son propre asservissement à une idée. Il y avait une contradiction même entre l'idée de la liberté absolue et un dévouement absolu à cette idée. Il y avait une contradiction entre la liberté de l'homme dont il se réclamait et sa soumission totale à une pensée, une idéologie. Il lui semblait aujourd'hui que si l'homme devait être vraiment libre, il devait se comporter librement aussi avec ses idées, ne pas se laisser entraîner complètement par la logique, pas même par la vérité, laisser une marge humaine à toute chose, autour de toute pensée. Peut-être même fallait-il savoir s'élever au-dessus de ses idées, de ses convictions, pour demeurer un homme libre. Plus une logique est rigoureuse et plus elle devient une prison, et la vie est faite de contradictions, de compromis, d'arrangements provisoires et les grands principes pouvaient aussi bien éclairer le monde que le brûler.*

Romain Gary, *Lady L.*